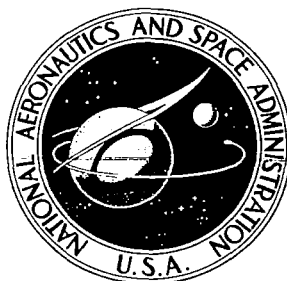


NASA CONTRACTOR REPORT

NASA CR-1442



NASA CR 1442



LOAN COPY: RETURN TO
AFWL (WLQ-2)
KIRTLAND AFB, N MEX

A STUDY OF 2 GHz ELECTROMAGNETIC WAVE PROPAGATION OVER OPTICAL PATHS IN THREE GEOGRAPHICAL REGIONS OF THE UNITED STATES

*by J. O. Hebert, Jr., F. M. Ingels, D. F. Fitzgerald,
E. E. Gross, and S. Y. Lee*

Prepared by
MISSISSIPPI STATE UNIVERSITY
State College, Miss.
for

NATIONAL AERONAUTICS AND SPACE ADMINISTRATION • WASHINGTON, D. C. • OCTOBER 1969

NASA CR-1442
TECH LIBRARY KAFB, NM



0060670

A STUDY OF 2 GHz ELECTROMAGNETIC WAVE
PROPAGATION OVER OPTICAL PATHS IN THREE
GEOGRAPHICAL REGIONS OF THE UNITED STATES

By J. O. Hebert, Jr., F. M. Ingels, D. F. Fitzgerald,
E. E. Gross, and S. Y. Lee

Distribution of this report is provided in the interest of
information exchange. Responsibility for the contents
resides in the author or organization that prepared it.

Prepared under Grant No. NGR 25-001-007 by
Department of Electrical Engineering
MISSISSIPPI STATE UNIVERSITY
State College, Miss.

for

NATIONAL AERONAUTICS AND SPACE ADMINISTRATION

For sale by the Clearinghouse for Federal Scientific and Technical Information
Springfield, Virginia 22151 - CFSTI price \$3.00

ACKNOWLEDGEMENT

The research reported here was supported in part by the National Aeronautics and Space Administration through Research Grant NGR-25-001-007.

The cooperation and assistance of Texas Eastern Transmission Corporation is gratefully acknowledged.

The authors wish to express their personal gratitude to the many individual members of these organizations who contributed so freely of their time and talents, making possible far more significant results than could have been obtained otherwise.



TABLE OF CONTENTS

	PAGE
ACKNOWLEDGEMENT	iii
LIST OF FIGURES	vii
LIST OF TABLES	ix
PART I. PROPAGATION RELIABILITY STUDY	
CHAPTER	
I. INTRODUCTION	1
II. 2 GHz MICROWAVE PROPAGATION WITHIN THE RADIO HORIZON . .	7
Radio Waves	7
Line-of-sight Propagation	8
Effects of the Atmosphere	12
III. DETERMINATION OF THE REQUIRED FADE MARGIN	15
IV. EXPERIMENTAL STUDY OF FADE MARGIN FOR VARIOUS MICROWAVE LINKS	19
V. A THEORETICAL MODEL FOR FADE MARGIN	37
Derivation of the Fade Margin Equation	37
Comparison of Experimental and Theoretical Results .	46
VI. DESIGN OF A TYPICAL 2 GHz LINE-OF-SIGHT MICROWAVE LINK	51
Choosing the Site	51
Calculating the Fade Margin Required	52
Calculating the Antenna Gain Required	54
VII. SUMMARY AND CONCLUSIONS	57

TABLE OF CONTENTS (Continued)

	PAGE
PART II. CROSSCORRELATION STUDY	
CHAPTER	
VIII. INTRODUCTION	59
IX. DISCUSSION OF CROSSCORRELATION FUNCTIONS	60
X. CROSSCORRELATION EXPERIMENTAL PROCEDURE	72
XI. RESULTS AND DISCUSSION	81
PART III. HIGH ELEVATION ANGLE STUDY	
XII. RESULTS AND DISCUSSION	89
APPENDIX I. COMPUTER PROGRAMS	96
APPENDIX II. PATH PROFILES	101
APPENDIX III. DISCUSSION OF EQUIPMENT OPERATION	111
REFERENCES	119
BIBLIOGRAPHY	121

LIST OF FIGURES

FIGURE	PAGE
1. Radio Horizon	2
2. A Typical Fade Margin Curve	4
3. Space Wave Components	9
4. Fresnel Patterns	11
5. Diagram Showing the General Geographical Regions . . .	22
6. Block Diagram of Instrumentation System	25
7. Typical Signal Level Distribution Curve	26
8. Statistical Distribution for Path 1	28
9. Statistical Distribution for Path 2	29
10. Statistical Distribution for Path 3	30
11. Statistical Distribution for Path 4	31
12. Statistical Distribution for Path 5	32
13. Statistical Distribution for Path 6	33
14. Statistical Distribution for Path 7	34
15. Statistical Distribution for Path 8	35
16. Statistical Distribution for Path 9	36
17. Statistical Distribution for Region A	39
18. Statistical Distribution for Region B	40
19. Statistical Distribution for Region C	41
20. Statistical Distribution for 20 Mile Paths	42
21. Statistical Distribution for 30 Mile Paths	43
22. Statistical Distribution for 40 Mile Paths	44
23. Comparison of Experimental Results with the Rayleigh Distribution	49
24. Functions to be Crosscorrelated	73

LIST OF FIGURES (Continued)

FIGURE	PAGE
25. Circuit for Determining the Average Level of the Signal .	78
26. Analog Computer Circuit for Performing Cross-correlation	80
27. Crosscorrelation Curve of Channel 2 (Barton-Coker) and Channel 3 (Bexar-Egypt) with Channel 3 Delayed	85
28. Crosscorrelation Curve of Channel 2 (Barton-Coker) and Channel 4 (Maben-Egypt) with Channel 4 Delayed	86
29. Crosscorrelation Curve of Channel 3 (Bexar-Egypt) and Channel 4 (Maben-Egypt) with Channel 4 Delayed	87
30. Elevation Angle of a Microwave Path	89
31. Statistical Distribution for High Angle Path	94
32. Program for Calculation of Fade Margin	97
33. Program for Fitting a Curve with a Polynominal	99
34. Path Profile for Path 1	102
35. Path Profile for Path 2	103
36. Path Profile for Path 3	104
37. Path Profile for Path 4	105
38. Path Profile for Path 5	106
39. Path Profile for Path 6	107
40. Path Profile for Path 7	108
41. Path Profile for Path 8	109
42. Path Profile for Path 9	110
43. A General AGC Voltage Characteristic Curve	112
44. Photograph Showing Diode Units Mounted on Moseley Recorder	113
45. Photograph Showing the Instrumentation for a Typical Station	116
46. Schematic of the Signal Distribution Analyzer	117
47. Schematic of a Typical Amplifier	118

LIST OF TABLES

TABLE	PAGE
I. Instrumented Paths Grouped Together According to Geographical Region	21
II. Stations Grouped Together According to Path Length . . .	23
III. Comparison of Experimental and Theoretical Data	47
IV. Locations of the Three Transmission Paths	74
V. Data of Crosscorrelation Curve Between Paths of Barton-Coker and Bexar-Egypt	82
VI. Data of Crosscorrelation Curve Between Paths of Barton-Coker and Maben-Egypt	83
VII. Data of Crosscorrelation Curve Between Paths of Bexar-Egypt and Maben-Egypt	84

PART I

PROPAGATION RELIABILITY STUDY

CHAPTER I

INTRODUCTION

The origin of investigation of the effects of the atmosphere upon the propagation of electromagnetic energy was probably a letter written by Lee De Forest to G. W. Pierce in 1912.¹ This letter discussed some very unusual signals received in an experiment by Pierce. Lee De Forest stated his belief that changes in the atmosphere had been responsible.

This interest in atmospheric effects on propagation increased during the 1940's when the use of UHF frequencies gave reason for learning more about these phenomena.

With the advent of radar, operators became aware of detecting targets well below the radio horizon (see Figure 1). Currently accepted theory enabled them to explain this by a mechanism called "surface trapping" or "ducting". This effect occurs when the refractive index of the atmosphere decreases sharply with increasing altitude at a height not far above the earth's surface. Such a region is called a superstandard layer since the reception of signals at a distant station is usually superior for these conditions as compared to that for conditions usually encountered. Another phenomenon often encountered is the loss of signal in a region well above the radio horizon only to have it appear again beyond the radio horizon. Again currently accepted theory provided an explanation based on changes in the atmosphere.

From these experiences investigators saw the importance of studying the atmosphere and its relationship to the index of refraction in an effort to understand these phenomena.

¹Numerical superscripts refer to References.



The radio horizon is a term used to define the borderline between radio optical and non-optical paths. In the figure, receiver A is located above the radio horizon, receiver B is at the radio horizon, and receiver C is below the radio horizon.

Figure 1. Radio Horizon.

One of the main interests of communication system designers is the system reliability. System reliability is defined as the ratio of the time the communication system output is useable to the total time that the system is operated, expressed in percent.

System reliability may be expressed as (Equipment Reliability) times (Propagation Reliability); as a result, the reliability of a communication system can never be greater than the propagation reliability. Propagation reliability is defined as the ratio (expressed in percent) of the time the received signal is detectable to the total time the signal is transmitted. Propagation reliability is related to fade margin, which is defined as the ratio (expressed in decibels) of the median received signal power to the minimum detectable signal power (see Figure 2).

Generally the equipment reliability is known, and is greater than the minimum required. Unfortunately, propagation reliability, which is frequently less than equipment reliability, is often ignored.

Usually there is not enough information about the propagation characteristics of the local geographical region to allow an accurate estimate of the propagation reliability. Experience has proven that the propagation characteristics of one geographical area are, in general, not necessarily the same as those for other areas.

Present theory of the relationship between the propagation of microwave signals and the properties of the atmosphere states that signal fades resulting in loss of communication are often caused by random variations in the atmosphere over the path between two stations.

In the past, research has been conducted in an attempt to relate meteorological conditions along a path to the fading characteristics of

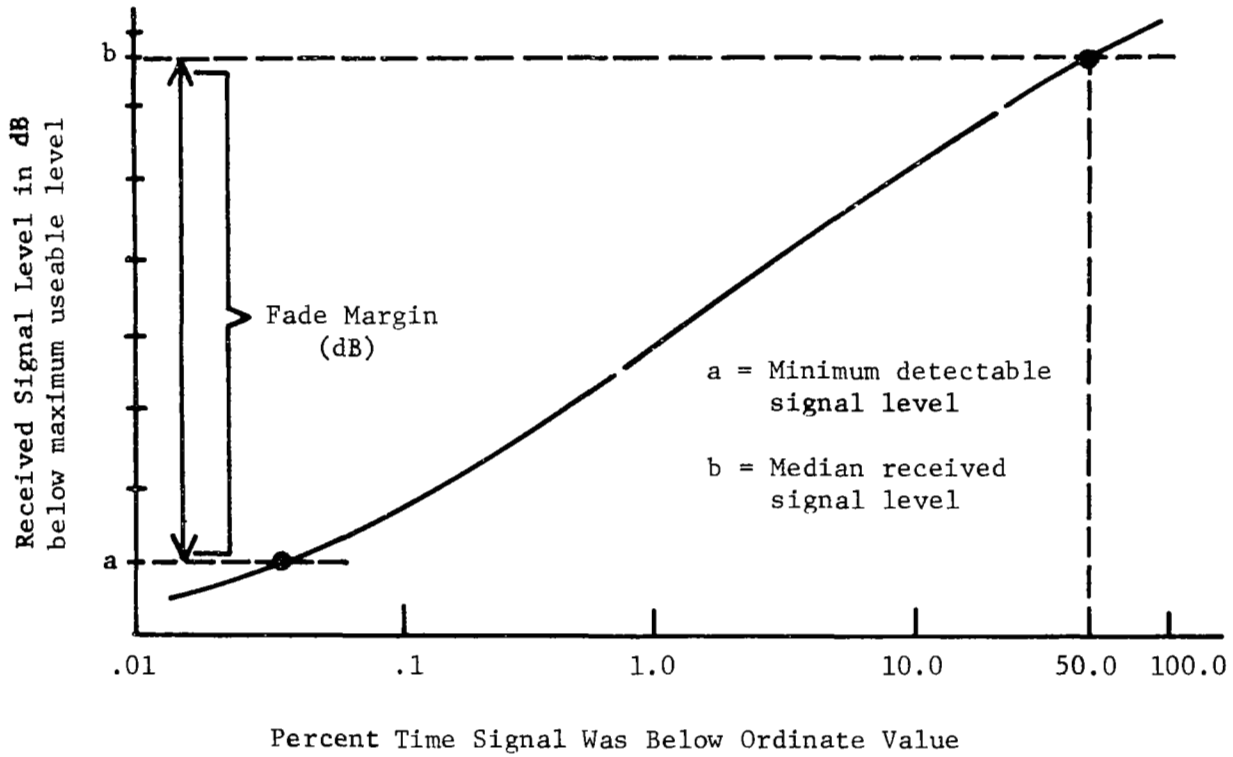


Figure 2. A Typical Fade Margin Curve.

that path. There appears to exist a direct relationship between the two, but it is apparently complicated and involved. As a result, the use of meteorological data by the microwave system designer is very difficult.

In order to properly design an optical microwave link using meteorological data, the designer would have to accumulate statistical records of the meteorological data over the intended path. From these data, which would most probably be temperature, dew point, humidity, and wind conditions, he must derive the statistical distributions of the index of refraction. Using this distribution for the index of refraction he would then derive the expected fading characteristics and subsequently make a plot of fade margin as a function of either the propagation outage time, or the propagation reliability. (Propagation outage time in percent equals $100\% - \text{propagation reliability}$.) It is assumed that for a well designed line-of-sight path the calculated free space signal level is approximately equal to the median received signal level. Previous long term experimental results have shown this to be a reasonable assumption.²

Due to the complexity of the above procedure, meteorological data have not been used by microwave system designers. Instead, the approach has been to use the results from limited propagation experiments as the basis for new system designs. This procedure has two main disadvantages. First, the results obtained from one geographical location are not necessarily valid for another location and second, the results of most of the previous work are not readily applicable to the design of new microwave systems. Consequently, there does not exist a good method for determining the fade margin required for a given path, even though this

is one of the main questions the microwave system designer must answer. It is highly desirable that a good method be available to answer that question since the demand for reliable microwave communication is steadily increasing.

Since propagation reliability is a function of the atmospheric conditions existing between two stations, it appears possible to utilize statistical signal level distributions to derive an empirical relationship between propagation reliability, fade margin, path length, and geographical location.

The principle objective of this research has been the development of a procedure that would allow a microwave system designer to calculate the fade margin required for a particular path and a given reliability for operating frequencies in the 2 GHz region.

Secondary objectives were the study of crosscorrelations of microwave signal fading over selected paths and the study of the fading obtained over a "high elevation angle" path.

CHAPTER II

2 GHz MICROWAVE PROPAGATION WITHIN

THE RADIO HORIZON

Radio Waves

Radio waves propagate from one point to another in three basic ways: sky waves, tropospheric waves, and ground waves.

The sky wave is that portion of the energy that reaches the receiving antenna by reflecting from the ionosphere, which begins about 80 km above the earth's surface. At frequencies below about 100 MHz the change in electron and ion density within the distance of a wavelength is so great that the ionospheric layer appears as an abrupt discontinuity and the wave is reflected as in the case of the reflection of waves at the surface of a dielectric. However, for frequencies above 100 MHz the wavelengths are so short that the ionization density changes only slightly in a wavelength. Under such conditions the radio waves penetrate the ionosphere rather than being reflected earthward. As a result, at 2 GHz the sky wave mode of propagation does not exist.

The tropospheric waves are waves that are reflected at abrupt changes in the effective permittivity of the troposphere, which is that region of the atmosphere from the surface to a height of approximately 10 km.

The ground wave is composed of a space wave and a surface wave. The surface wave is a wave that is guided along the earth's surface. Energy is absorbed from the surface wave to supply energy losses to the ground. This loss factor is dependent upon the frequency and the physical ground constants. For frequencies of 2 GHz the surface wave

attenuation is very high thus making the surface wave unsuitable for communication at 2 GHz.

The space waves are thus the major means of line-of-sight radio wave propagation at 2 GHz. Space waves consist of two types of components--direct waves and ground-reflected waves (see Figure 3). The direct wave travels directly from the transmitter to the receiver. The ground-reflected waves are waves which have been reflected from the surface of the earth and have thus been redirected toward the receiver.

Line-of-sight Propagation

The electric field intensity at a receiving antenna is equal to the vector sum of the waves arriving from all paths. If the transmitter and receiver are located far apart compared to the antenna heights, the grazing angle of the ground-reflected wave is small. The reflection coefficient for the earth's surface for grazing angles less than one degree is approximately unity with a phase shift of approximately 180 degrees.³

The magnitude of the electric field intensity, E_r , resulting from the direct wave and the ground-reflected wave would thus be (see Figure 3)

$$| E_r | = | E_o + kE_o e^{j\phi} | \quad 2-1$$

where E_o = amplitude of the electric field intensity in the direct wave

k = reflection coefficient of the earth

ϕ = phase shift of the ground-reflected wave with respect to the direct wave because of the additional distance traveled by the ground-reflected wave.

$$\text{but } \phi = \frac{2\pi}{\lambda} (r_2 - r_1) \quad 2-2$$

$$\text{and } r_1^2 = d^2 + (h_t - h_r)^2 \quad 2-3$$

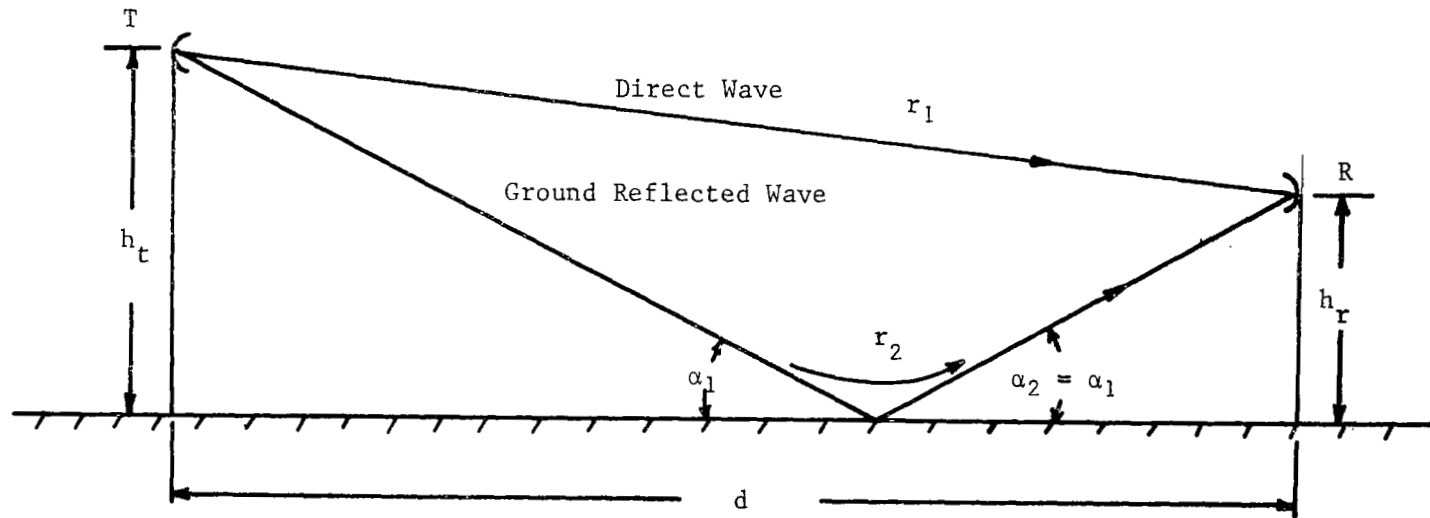


Figure 3. Space Wave Components

$$\text{and } r_2^2 = d^2 + (h_t + h_r)^2 \quad \text{since } \alpha_1 = \alpha_2 \quad 2-4$$

where h_t is the height of the transmitting antenna above the surface and h_r is the height of the receiving antenna above the surface.

$$\text{If } d \gg (h_t + h_r) \geq (h_t - h_r) \quad 2-5$$

$$\text{then } r_1 \approx d + \frac{(h_t + h_r)^2}{2d} ; \quad r_2 \approx d + \frac{(h_t + h_r)^2}{2d} \quad 2-6$$

by the binomial expansion. Hence

$$r_2 - r_1 \approx \frac{2 h_t h_r}{d} \quad \text{and} \quad \phi = \frac{4\pi h_t h_r}{\lambda d} . \quad 2-7$$

If $k \approx e^{j\pi}$ then $|E_r|$ may be expressed as

$$|E_r| = E_o |1 - e^{j\phi}| = E_o |e^{j\phi/2}| |e^{-j\phi/2} - e^{j\phi/2}| \quad 2-8$$

$$|E_r| = 2E_o |\sin \phi/2| = 2E_o \left| \sin \frac{2\pi h_t h_r}{\lambda d} \right| . \quad 2-9$$

Thus, for a perfectly-conducting earth, or for the small grazing angles often encountered in typical microwave systems, the field strength at a receiving point varies with h_r in a sinusoidal fashion. This interference between the direct wave and reflected waves result in maxima and minima patterns called "Fresnel patterns" similar to those shown in Figure 4. The first maximum occurs when the difference in path length, $r_2 - r_1$, is equal to one-half wave-length, remembering that a 180 degree phase reversal occurs at the point of reflection. The vertical height between the first maxima and the first minima for a 2 GHz microwave system with a path length of 30 miles and a transmitting antenna height of 100 feet is 200 feet. Thus if the path is designed so that the

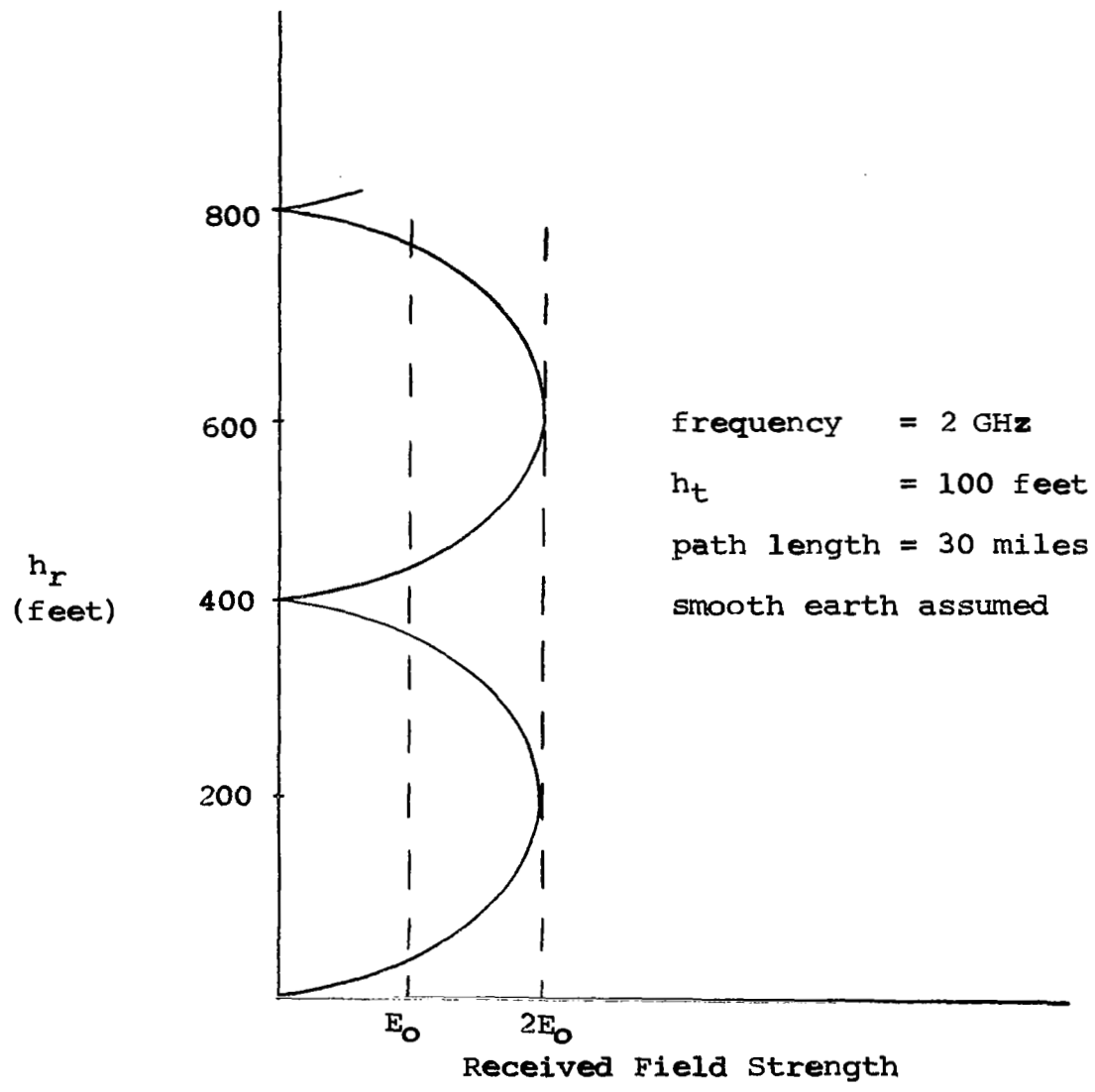


Figure 4. Fresnel Patterns

free space Fresnel clearance for the first maximum is satisfied, there is little danger of locating the receiving antenna in the first minima.

Generally the free space Fresnel clearance required for a microwave relay system is the clearance which at any point in the path results in a direct and reflected path difference of at least $1/6$ of a wavelength.⁴ This results in a received strength of E_0 since $\sin \phi/2$ is .5 for $r_2 - r_1$ equal to $1/6$ of a wave length.

A nomogram method for determining free-space path clearance required for a microwave relay system has been developed.⁴ Using this method it becomes a simple matter to determine the necessary tower heights for a particular path with a known path profile.

Effects of the Atmosphere

The influence of the atmosphere on the radio wave is significant. This is vividly illustrated by the results of many experiments with radar. The presence of molecules of water vapor and other gases of which the atmosphere is composed cause the air in the troposphere to have a relative permittivity greater than unity; but since the density of air varies with height, the density of these molecules decreases, resulting in a decrease of the permittivity of air with height.

A standard atmosphere is defined as one in which the index of refraction decreases linearly with altitude at the rate of 11.8 parts per million per 1000 feet, the index of refraction being the square root of the dielectric constant of air (this is assuming the relative permeability of air is unity).

Since the index of refraction of a standard atmosphere normally decreases linearly with height, the upper portions of a wave front travel with slightly greater velocity than the lower portions of the

wave. This causes the path of the wave to be curved slightly downward. This curvature of the ray path causes the earth's radio horizon to differ from the optical horizon. When drawing the path of a wave from the transmitter to the receiver for standard atmosphere conditions, one must draw a line curved slightly downward rather than a straight line. This becomes a tedious requirement when studying many different paths. If instead the earth's radius were enlarged by the correct amount, then the path of a wave for a standard atmosphere could be drawn as a straight line. For a standard atmosphere the modified earth's radius is $4/3$ the normal earth's radius. For this reason most path profiles of microwave systems are drawn on profile paper with $4/3$ earth's radius.

Unusual conditions of humidity and temperature often cause a non-standard atmosphere; i.e., one in which the index of refraction decreases more than usual, is constant with, or increases with height. A change in the refractive index with height causes a radio wave traveling in the atmosphere to follow a curved path rather than a straight path. As a result, radio waves which normally would be received may be directed away from the receiver and, conversely, waves which are not normally received may be directed towards the receiver. Either condition causes a change in the received signal strength. Decreases in received signal strength are termed fades.

Various changes of the temperature and humidity which affect the path of the radio wave are sometimes peculiar to certain geographical locations. Thus the fading characteristics of a path will in general be a function of its geographical location. How then is a system designed so as to consider the atmospheric effects?

One approach is to calculate the received field strength for free space propagation and then make allowance for the effects of the atmosphere. This is done by designing the system such that the median received signal strength is in excess of the minimum detectable signal strength. This excess signal allowance is defined as the fade margin of the communication system.

The question to be answered then is: What is the fade margin required to achieve a desired propagation reliability for a particular path length and geographical location?

CHAPTER III

DETERMINATION OF THE REQUIRED FADE MARGIN

A simplified procedure for determining the fade margin required for a line-of-sight microwave path has been developed as a result of this research.

This procedure does not require many lengthy calculations to be performed, as is the case when using meteorological data, thus eliminating many sources of possible error and time-consuming work. This procedure was developed by using the following approach.

Consider a typical microwave link that has its terminals located such that the propagation path is line-of-sight. Since the fading characteristics of the signal are a function of the atmosphere between the two terminals, a seasonal variation in the fading activity, corresponding to a seasonal variation in the atmospheric properties along the path, is expected. Since there is generally a yearly cycle in the weather at any location on earth, a yearly cycle in the fading activities of a microwave signal is also expected. Consequently a test microwave system could be designed with the objective of investigating the fading characteristics of the path rather than investigating the meteorological changes of the atmosphere along the path.

After selecting a suitable site and having determined the transmitting and receiving tower heights and location such that proper Fresnel zone clearance is achieved for the path, one could then begin to investigate the fading characteristics of the path caused by changes in the atmosphere.* The objective would be to determine the relationship

*For a nomogram method of calculating path clearances see Reference 4.

between fading characteristics and the propagation reliability of the path.

Instead of monitoring the meteorological changes, the received signal level would be monitored with a level-sensing device. By using a transmitter with a known output power, a receiver with a known minimum detectable signal level for free space propagation and antennas of known gain, the received signal and thus the fade margin could be controlled.

The automatic gain control voltage of the receiver would then indicate the duration and amount of fading of the signal. By monitoring the AGC voltage with the proper instrumentation, a statistical signal level distribution could be obtained. This distribution could be in the form of clock readings indicating the time the received signal was below a certain level.

By recording this information over a given period the outage time of the receiver for various values of fade margin could be determined. If the data were recorded every six hours for one year, this method would also allow determination of the six-hour periods of the day in which the maximum fading activity took place and also the seasons of the year during which the maximum amount of fading activity would be expected.

From the statistical data obtained from the instrumentation, a graph of received signal level versus propagation reliability could be made. This plot could then be used to design microwave systems with the same path length in this geographical area or geographical locations nearby. It would be exceedingly time consuming and expensive if it were necessary to obtain statistical data of this nature for each path used

in a microwave system. However, by performing this type of signal monitoring over a wide geographical region over paths of various lengths, a similar fade graph could be plotted for each path monitored. It should then be possible to determine the relationship between fade margin, propagation reliability, geographical location, and path length from these fade margin graphs. This relationship would be a set of equations which would allow calculation of the required fade margin versus these parameters without requiring any experimental measurements.

Nine links of Texas Eastern Transmission Corporation's microwave system extending from Shreveport, Louisiana, to Linden, New Jersey, have been instrumented in an attempt to derive such a relationship between fade margin, propagation reliability, geographical location, and path length for a 2 GHz signal in the Gulf-South geographical region of the United States. Signal monitoring of each of the nine links instrumented has been performed and a plot of fade margin versus propagation reliability for each path has been plotted. For each path curve, an equation has been derived describing the curve. These equations are logarithmic in form. A relationship has been derived which will predict the equation for each of the paths. This relationship is a function of geographical location and path length as well as the propagation reliability desired. From this relationship it has been possible to write an equation for fade margin as a function of propagation reliability, path length, and geographical location. This equation allows a microwave system designer to calculate the fade margin required to achieve a desired propagation reliability for a path lying within the geographical bounds of Athens, Louisiana (latitude 32° - $40'$, longitude 92° - $37'$), to Garrison, Kentucky (latitude 38° - $33'$, longitude 83° - $06'$), with length

varying from 19 miles to 44 miles, and for propagation reliability varying from 90% to 99.99%. It should be noted that the designer using these equations is not required to make any experimental measurements.

CHAPTER IV

EXPERIMENTAL STUDY OF FADE MARGIN FOR VARIOUS MICROWAVE LINKS

A literature survey was conducted to determine the existing state of knowledge of propagation reliability for microwave signals in the frequency range of 1 GHz through visible light. A summary of the literature survey has been published through the Engineering and Industrial Research Station at Mississippi State University.⁵

Several conclusions concerning microwave transmission occurred repeatedly in the literature and are pertinent to this study. These main points are:

1. Fading activity is at a minimum during cold weather and at a maximum during hot weather and during night hours; that is, fading activity is seasonal.
2. There does not seem to be a great deal of difference in the fading characteristics of horizontally and vertically polarized waves.
3. Signal fluctuations are assumed to be due to atmospheric changes along the propagation path under consideration.
4. The correlation of the yearly statistical fading averages between two paths having the same length and lying within the same geographical area is assumed to be quite high.

From these conclusions it was apparent that the determination of fade margin required as a function of propagation reliability, geographical location, and path length would require additional study of at least two topics. These topics were:

1. The effects of path length on propagation reliability.
2. The effects of geographical location on propagation reliability.

Texas Eastern Transmission Corporation granted the use of their 2 GHz microwave system for the purpose of studying these two topics. This system extends from Shreveport, Louisiana, to Linden, New Jersey, thus covering a large portion of the Gulf-South geographical region of the United States. The system is composed of fifty-four microwave paths varying in length from 3.50 miles to 47.50 miles.

Nine paths of this microwave system were selected to be instrumented. These path locations were selected to satisfy two conditions:

1. Different path lengths in the same geographical area.
2. Similar path lengths in different geographical areas.

Table I gives the location and path length of the nine instrumented paths. These paths are grouped together according to geographical region and thus satisfy condition one. Three geographical regions are indicated with three paths in each region. The sketch in Figure 5 shows the general geographical regions.

Table II shows the path locations grouped together according to the length of the transmission path. Note that a similar path, with respect to length, exists in each geographical region. This satisfies condition two given above.

TABLE I. INSTRUMENTED PATHS GROUPED
TOGETHER ACCORDING TO GEOGRAPHICAL REGION

Path Number	Geographical Region	Nominal Lat.	Long.	Station Location	Path Length (Miles)
1.	A	33°	92°	Dubach, La. to Hurricane, La.	21.50
2.				Holly Ridge, La. to Tallula, Miss.	33.75
3.				Yazoo City, Miss. to Tallula, Miss.	40.75
4.	B	34.50°	88.50°	Maben, Miss. to Egypt, Miss.	30.00
5.				Bexar, Ala. to Egypt, Miss.	37.50
6.				Barton, Ala. to Coker, Ala.	19.50
7.	C	38°	83.50°	Moreland, Ky. to Elkin, Ky.	43.50
8.				Reynoldsville, Ky. to Elkin, Ky.	31.75
9.				Garrison, Ky. to Stricklett, Ky.	21.00

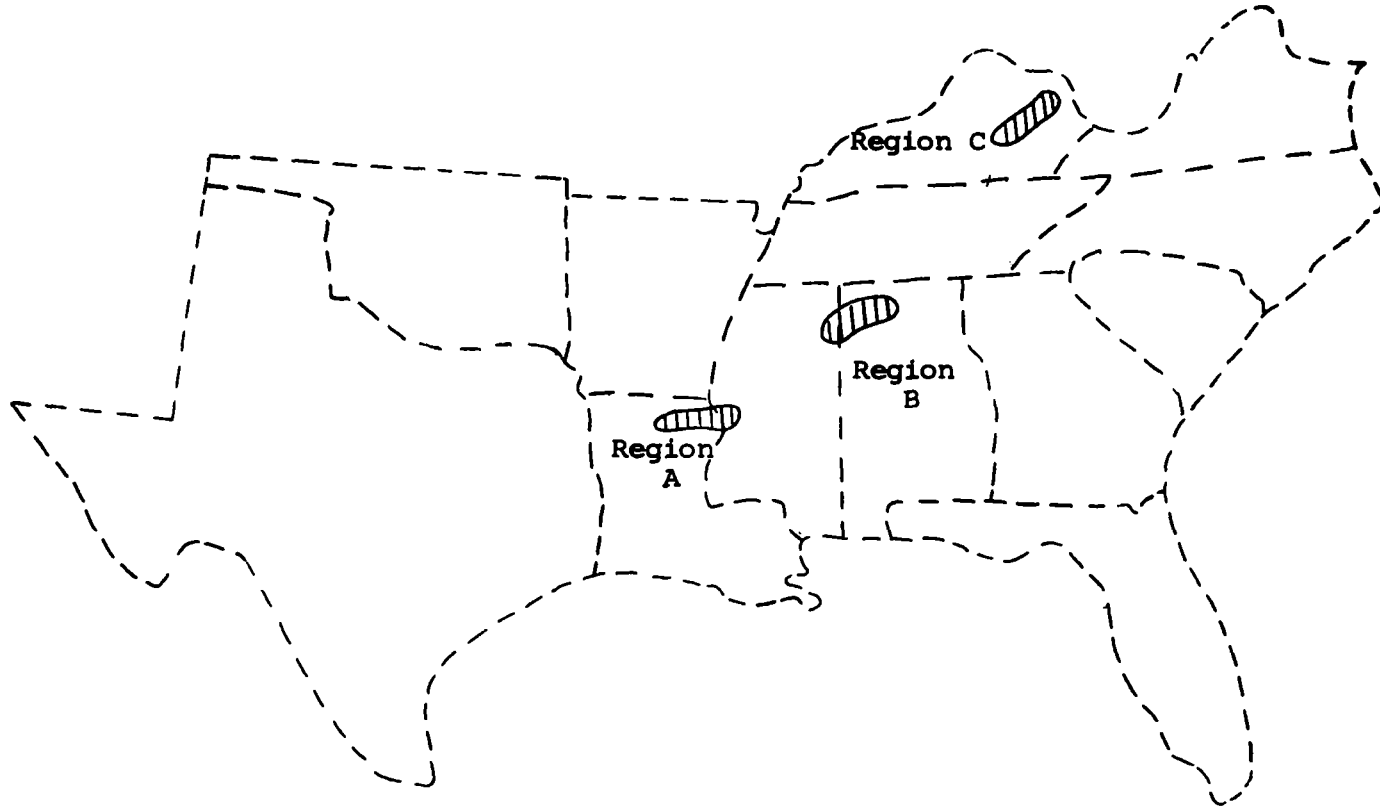


DIAGRAM SHOWING THE GENERAL GEOGRAPHICAL REGIONS

Figure 5. Diagram Showing the General Geographical Regions.

TABLE II. STATIONS GROUPED TOGETHER
 ACCORDING TO PATH LENGTH

Station Location	Path Length (miles)
Dubach, La. to Hurricane, La.	21.50
Barton, Ala. to Coker, Ala.	19.50
Garrison, Ky. to Stricklett, Ky.	21.00
Holly Ridge, La. to Tallula, Miss.	33.75
Maben, Miss. to Egypt, Miss.	30.00
Reynoldsville, Ky. to Elkin, Ky.	31.75
Yazoo City, Miss. to Tallula, Miss.	40.75
Bexar, Ala. to Egypt. Miss.	37.50
Moreland, Ky. to Elkin, Ky.	43.50

A block diagram showing the instrumentation design for each of the nine stations is given in Figure 6. A detailed schematic of the amplifier circuits and the signal distribution analyzer is shown in Appendix III along with a discussion of how the equipment operates.

The data obtained from the signal distribution analyzer were used to plot the signal distribution curves. A typical curve is shown in Figure 7.

The signal distribution curve is normalized with respect to the receiver AGC voltage. From the AGC curve of Figure 43, Appendix III, one can see that there is a particular value of receiver input power for which the AGC voltage drops sharply. This particular value of input power is the maximum useable signal power for the receiver. In normal operation, the received signal never reaches this level. The maximum calibration value is normalized to zero dB for plotting the signal distribution curves. The ordinate of the distribution curve is thus the level (in dB) that the received signal is below the maximum calibration level. The abscissa of the distribution curve is the percent time of the total reporting interval. The time interval considered can be hours, days, weeks, or months. The coordinate points, A and B, shown on the distribution curve of Figure 7 should be interpreted to mean that the received signal level was equal to or less than A dB for B per cent of the time.

Although the data were used to plot curves similar to Figure 7, in order to use the information displayed by these curves it was necessary to renormalize the curves so as to present the ordinate as the fade margin. This was accomplished by relabeling the ordinate value of the curves using the value occurring at the fifty percent points as the zero dB fade margin points.

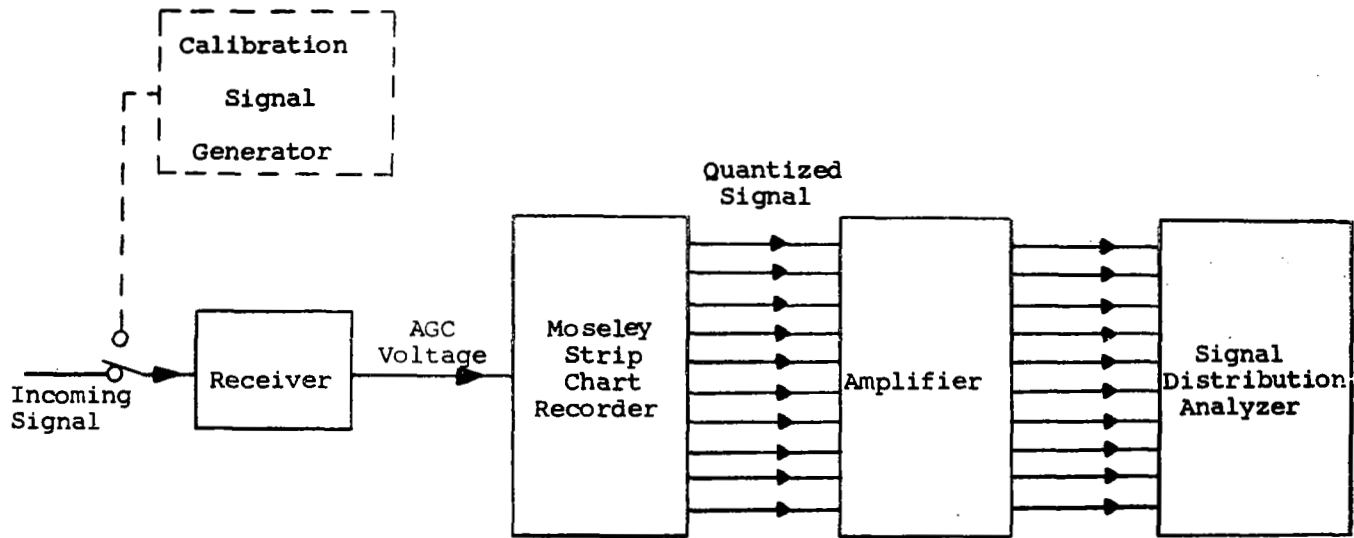


Figure 6. Block Diagram of Instrumentation System.

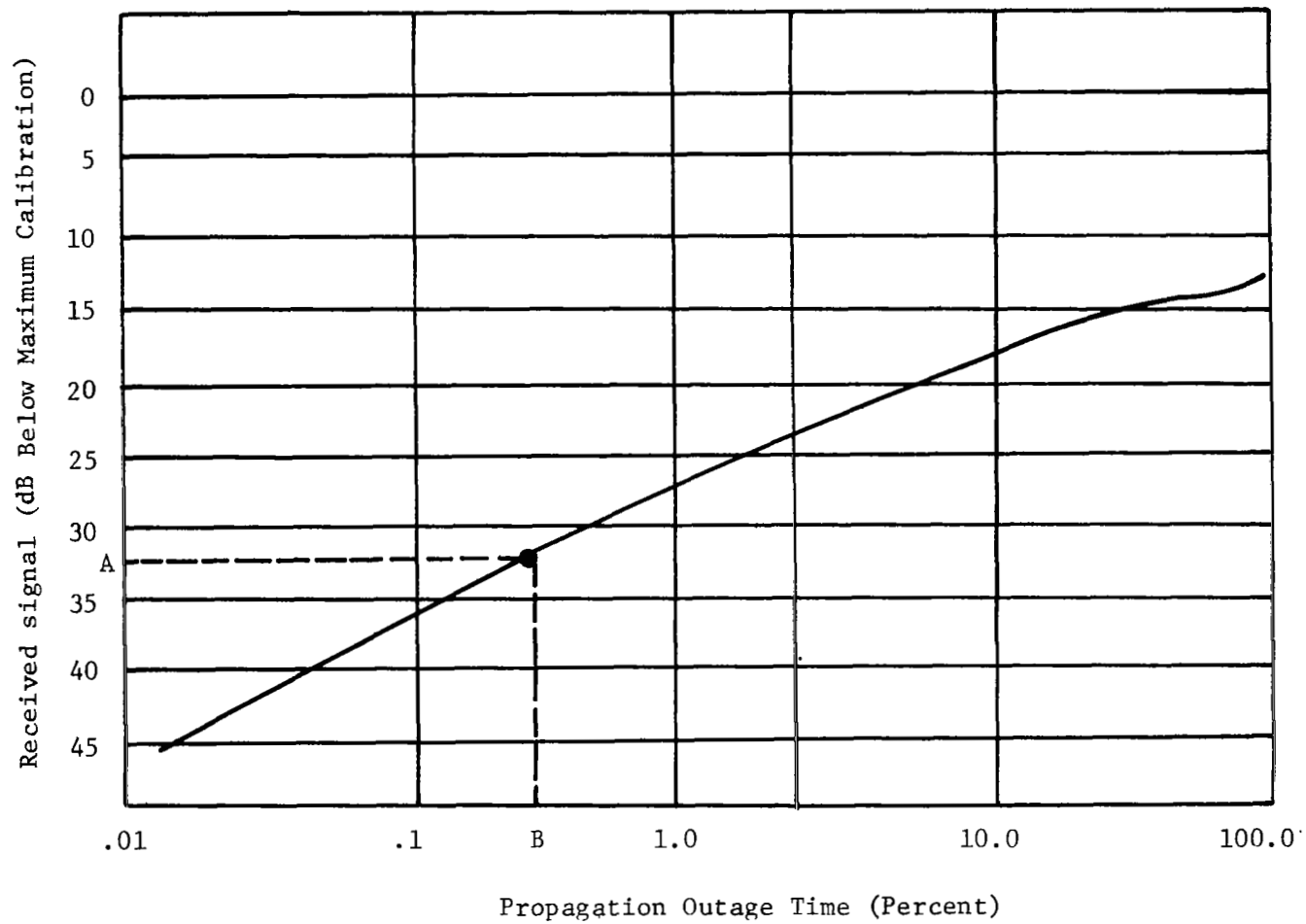


Figure 7. Typical Signal Level Distribution Curve.

A curve for each path showing the statistical distribution of the received signal level was plotted from each of the nine instrumented paths. These are shown in Figures 8-16. These experimental curves are for the nominal ten-month period from January 20, 1966, to November 20, 1966.

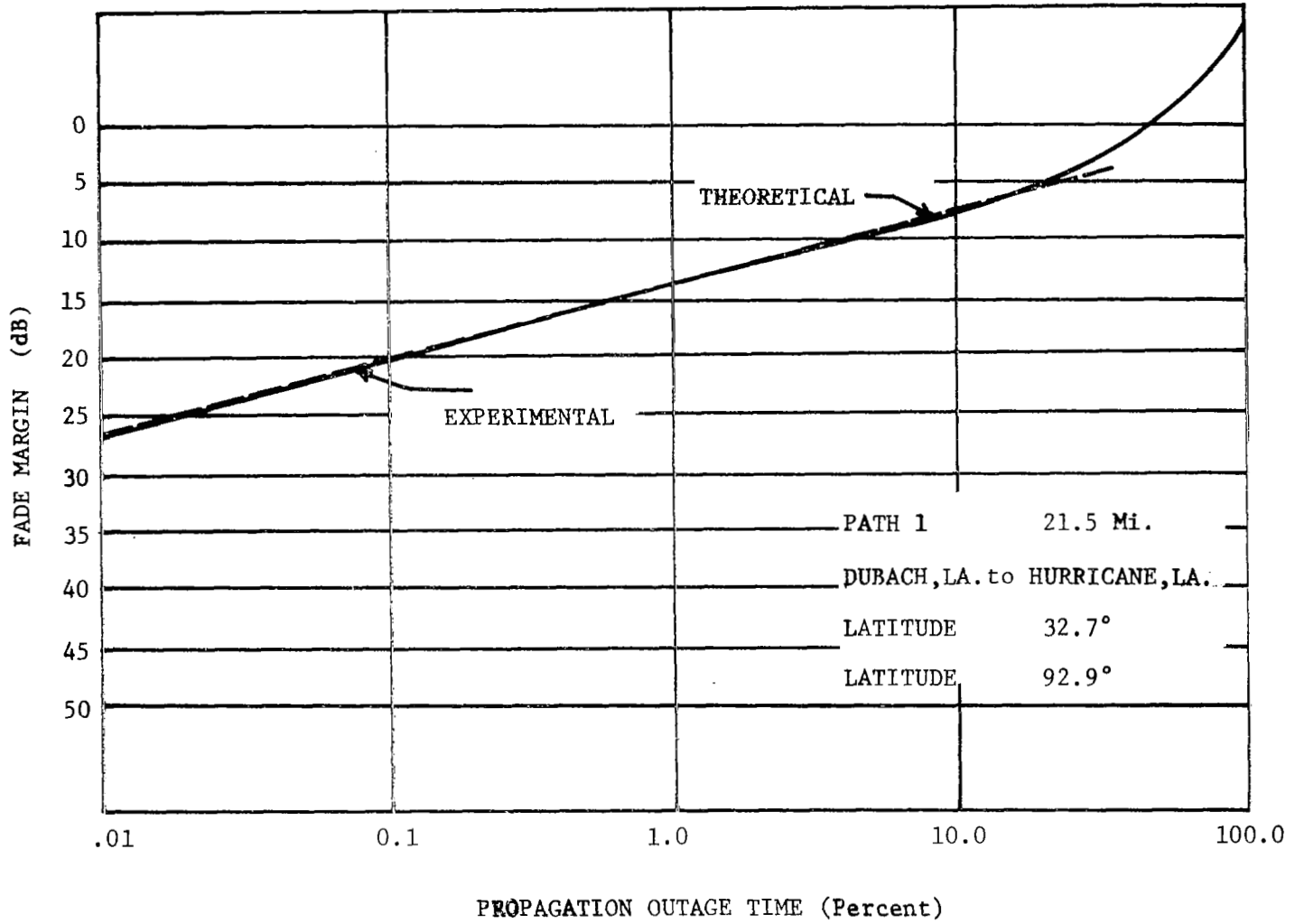


Figure 8. Statistical Distribution for Path 1.

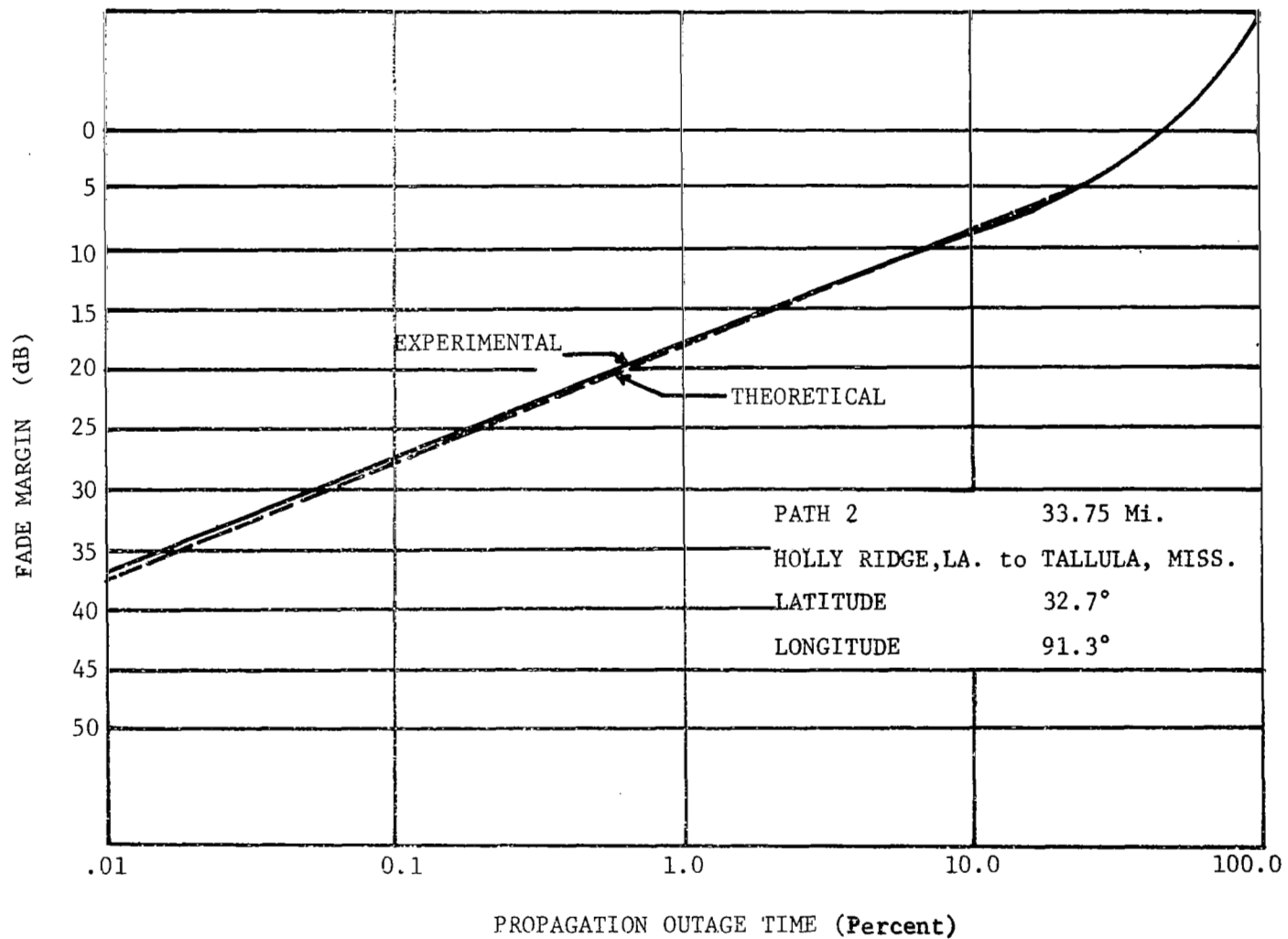


Figure 9. Statistical Distribution for Path 2.

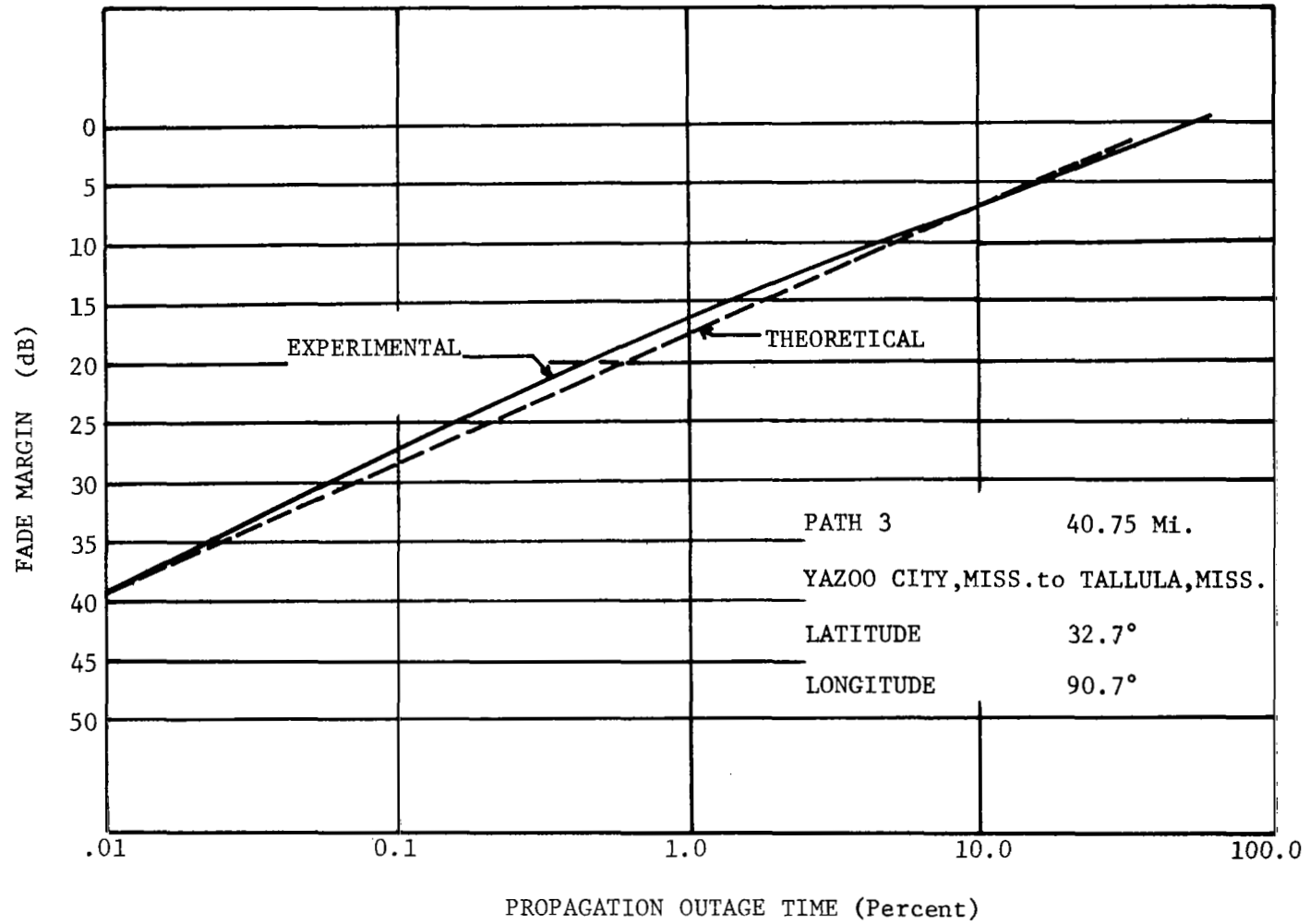


Figure 10. Statistical Distribution for Path 3.

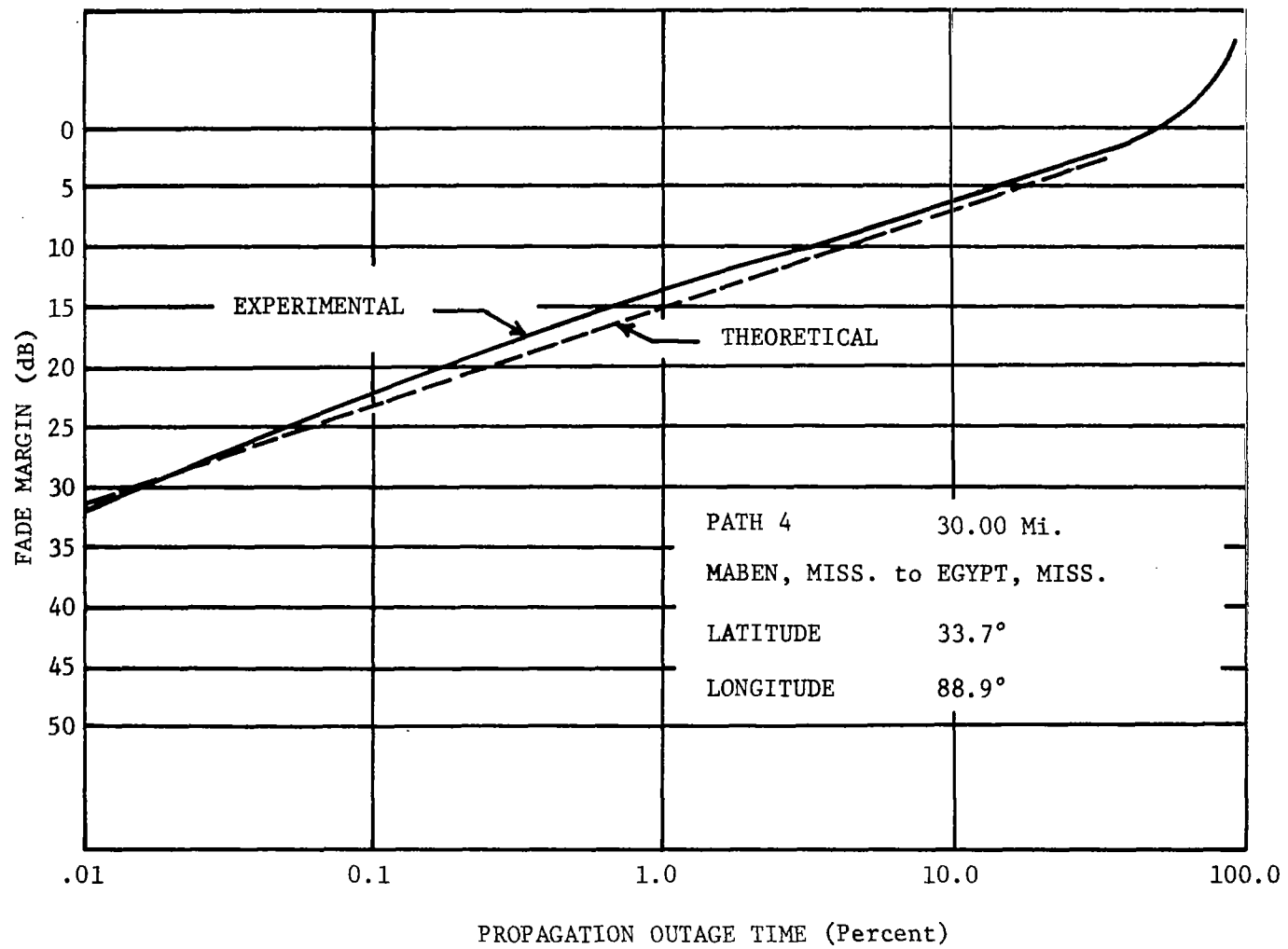


Figure 11. Statistical Distribution for Path 4.

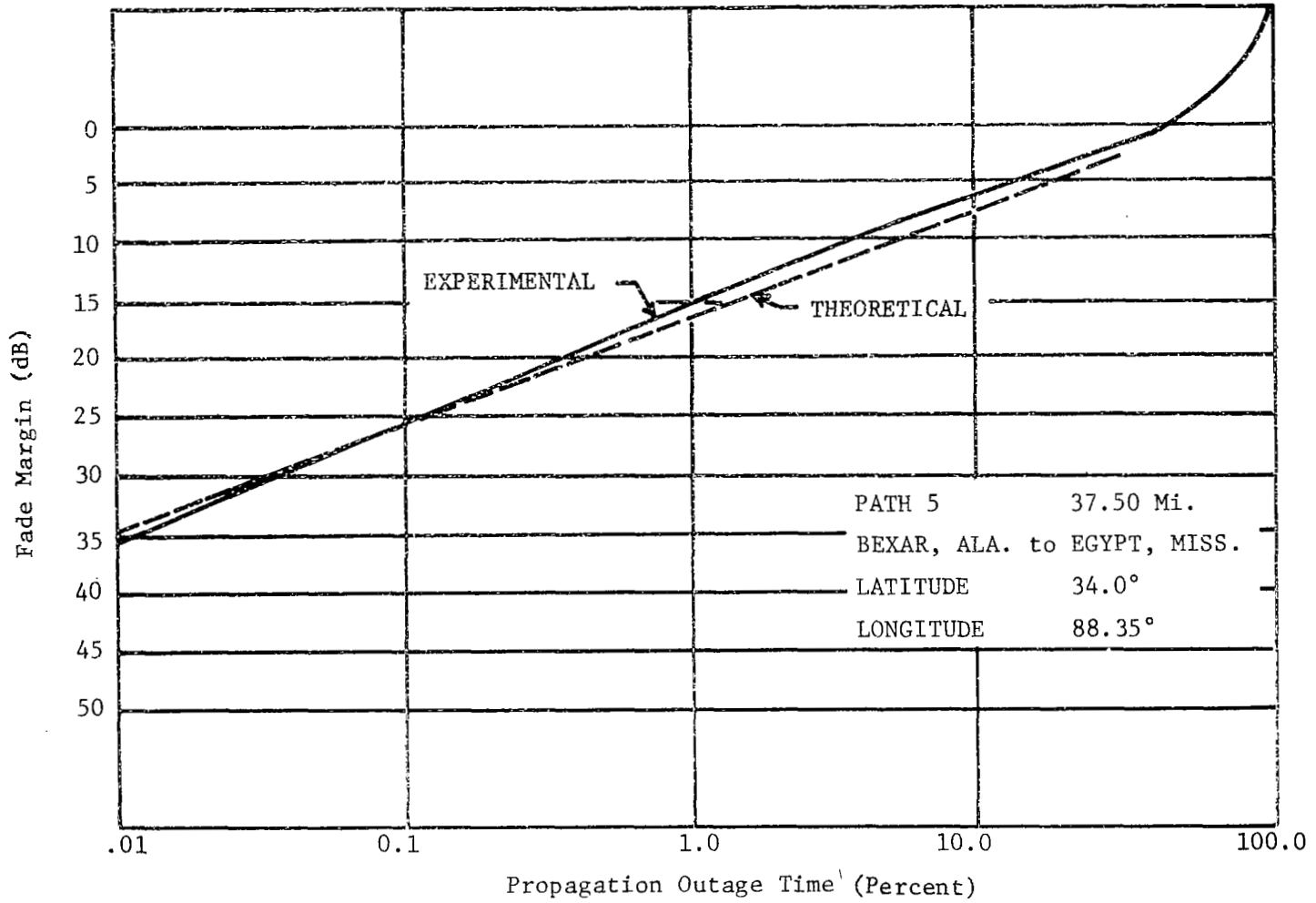


Figure 12. Statistical Distribution for Path 5.

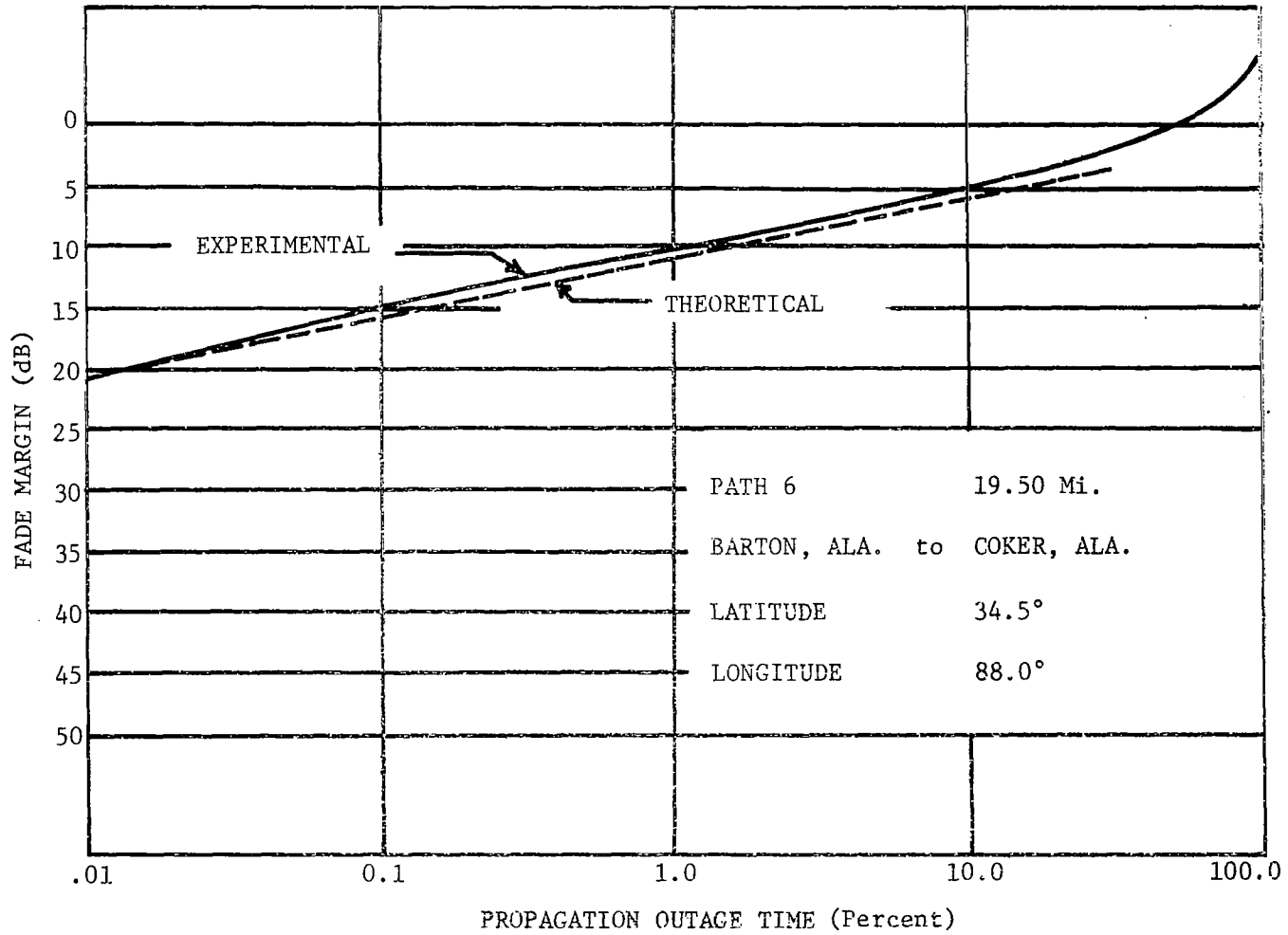


Figure 13. Statistical Distribution for Path 6.

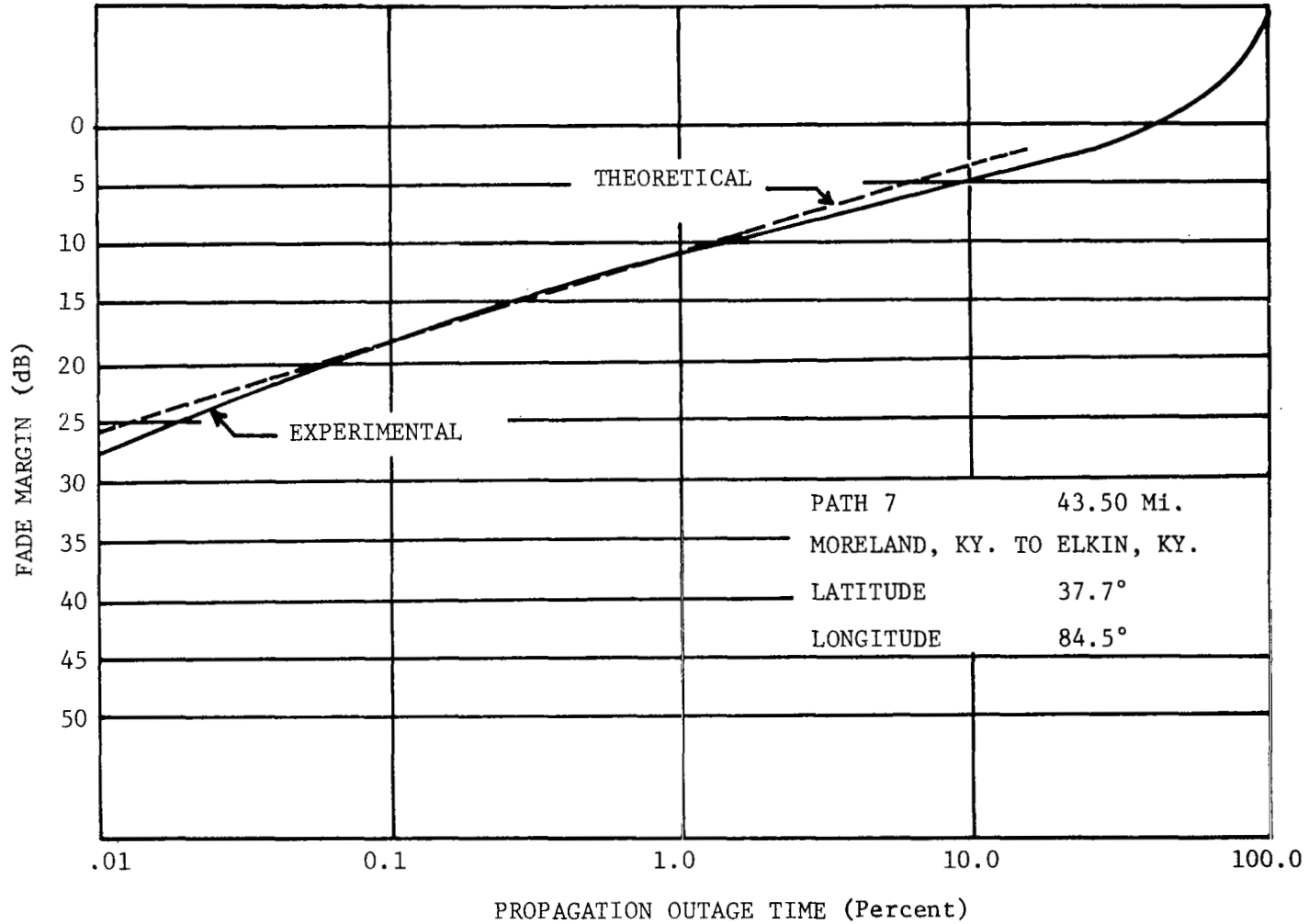


Figure 14. Statistical Distribution for Path 7.

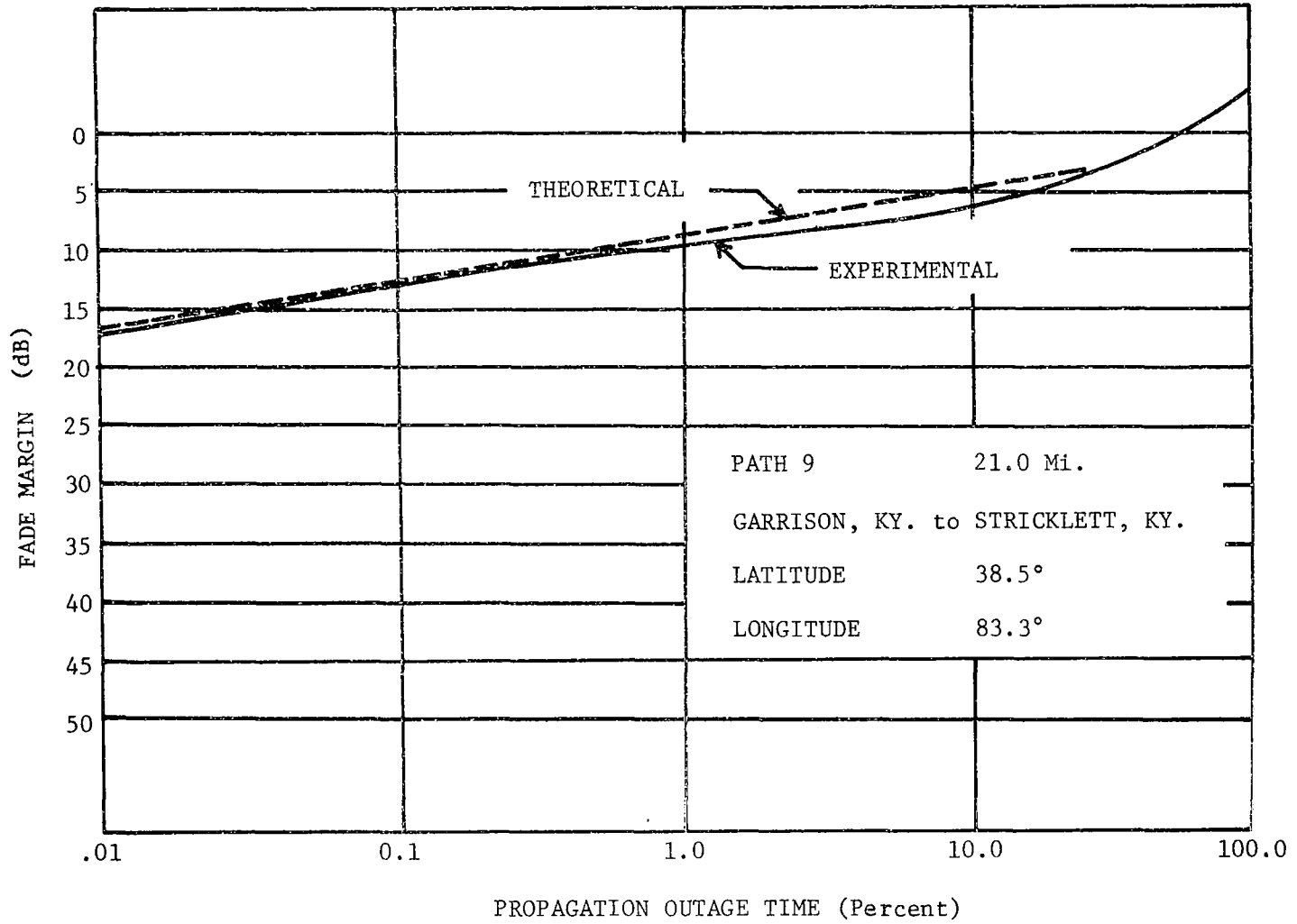


Figure 16. Statistical Distribution for Path 9.

CHAPTER V

A THEORETICAL MODEL FOR FADE MARGIN

Derivation of the Fade Margin Equation

The curves shown in Figures 8-16 were used to derive a general mathematical model describing the fade margin required of any path lying within the geographical bounds of Athens, Louisiana (latitude 32°-40', longitude 92°-37'), to Garrison, Kentucky (latitude 38°-33', longitude 83°-06'), with length varying from 19 miles to 44 miles, and for propagation reliability varying from 90% to 99.99%. The outage time range corresponding to this range of propagation reliability is 10% to .01%. Since outage times greater than 10% are so large as to render any commercial communication system unserviceable, no attempt was made to fit the curve for outage times greater than 10%.

The basic equation for calculation of the required fade margin for a particular path satisfying the above conditions is:

$$\text{Fade Margin} = | K_0 + K_1 \log_{10} [1 + \text{O.T.} (1000)] | \quad 5-1$$

where K_0 and K_1 are constants, and O.T. equals outage time expressed in per cent.

This equation was developed from the general form of the experimental curves which are quite similar to the amplitude plots of simple transfer functions of electrical circuits.⁶ In a sense the atmosphere between the transmitter and the receiver can be represented by a two port transmission device, the transfer characteristics of which determine the relationship between the transmitted signal level and the received signal level.

The transfer characteristics are displayed graphically by the plot of fade margin versus outage time because of the atmosphere. As is the case in system analysis, the equation of the transfer function can then be synthesized from these curves.

Once the fade margin curves are obtained, the dependence upon path length and geographical location can be determined. This dependence of the fade margin upon these variables is analogous to the dependence of the amplitude of the output of a "black box" upon the values of resistors and capacitors that may comprise the circuit in the box. In this case the dependence of K_0 and K_1 upon path length and geographical location needs to be expressed in a set of equations that allow K_0 and K_1 to be calculated for any path satisfying the conditions previously mentioned.

By inspecting the curves plotted for paths of varying length but in the same geographical location, the effects of path length may be derived. Figures 17-19 show plots of the nominal 20, 30, and 40 mile paths in similar geographical locations. The effect of path length is a general increase in the fade margin required for a longer path. Also, the fade margin required decreases as the geographical location moves further north. Figures 20-22 show graphically the effect of geographical location.

The equations used to calculate K_0 and K_1 have been found heuristically. Several approaches were tried and the equations which produced the best fit are the following:

$$K_0 = GF \qquad 5-2$$

where G is a function of path length and F is a function of geographical location. G was determined by writing a polynomial which relates the

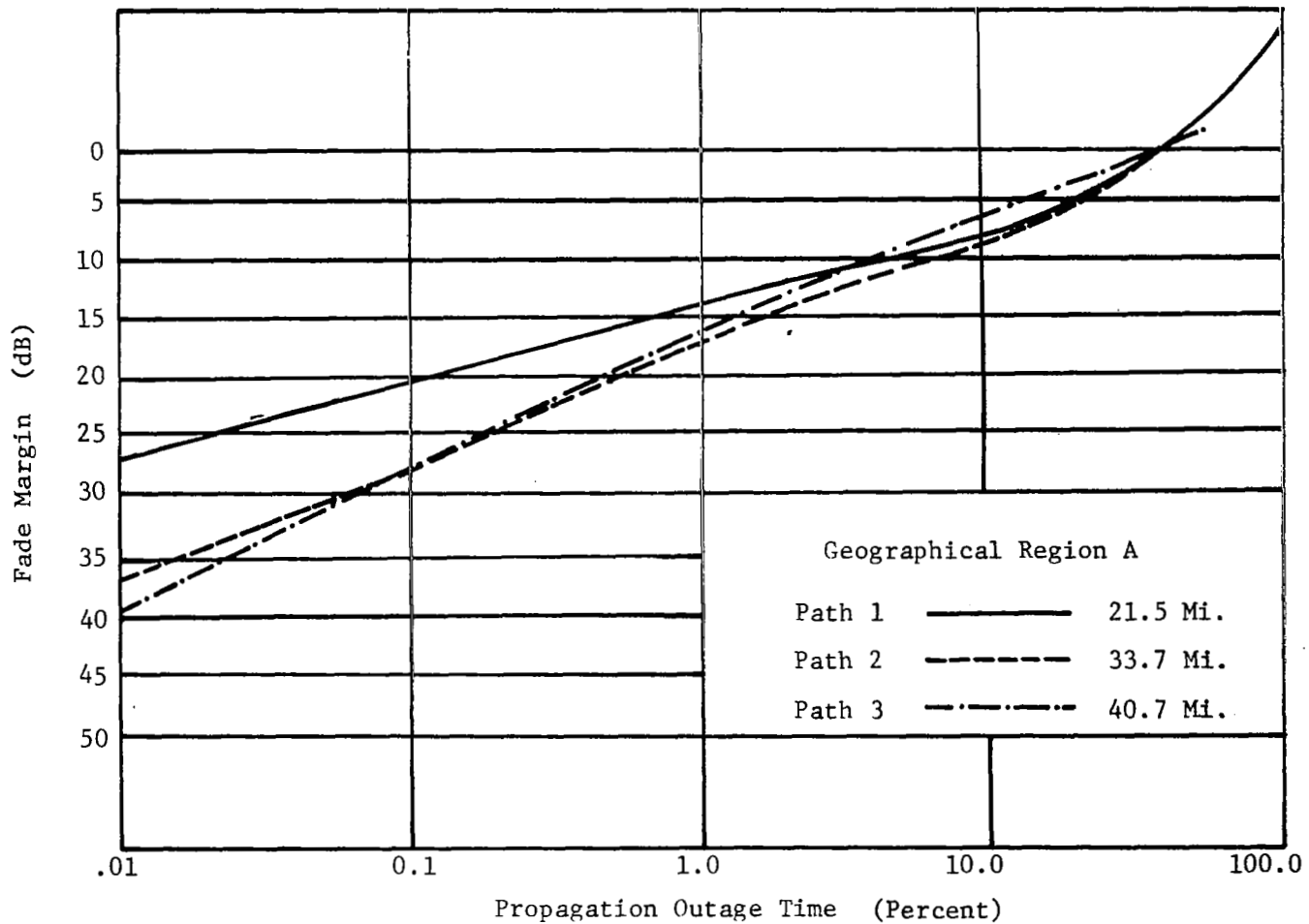


Figure 17. Statistical Distribution for Region A.

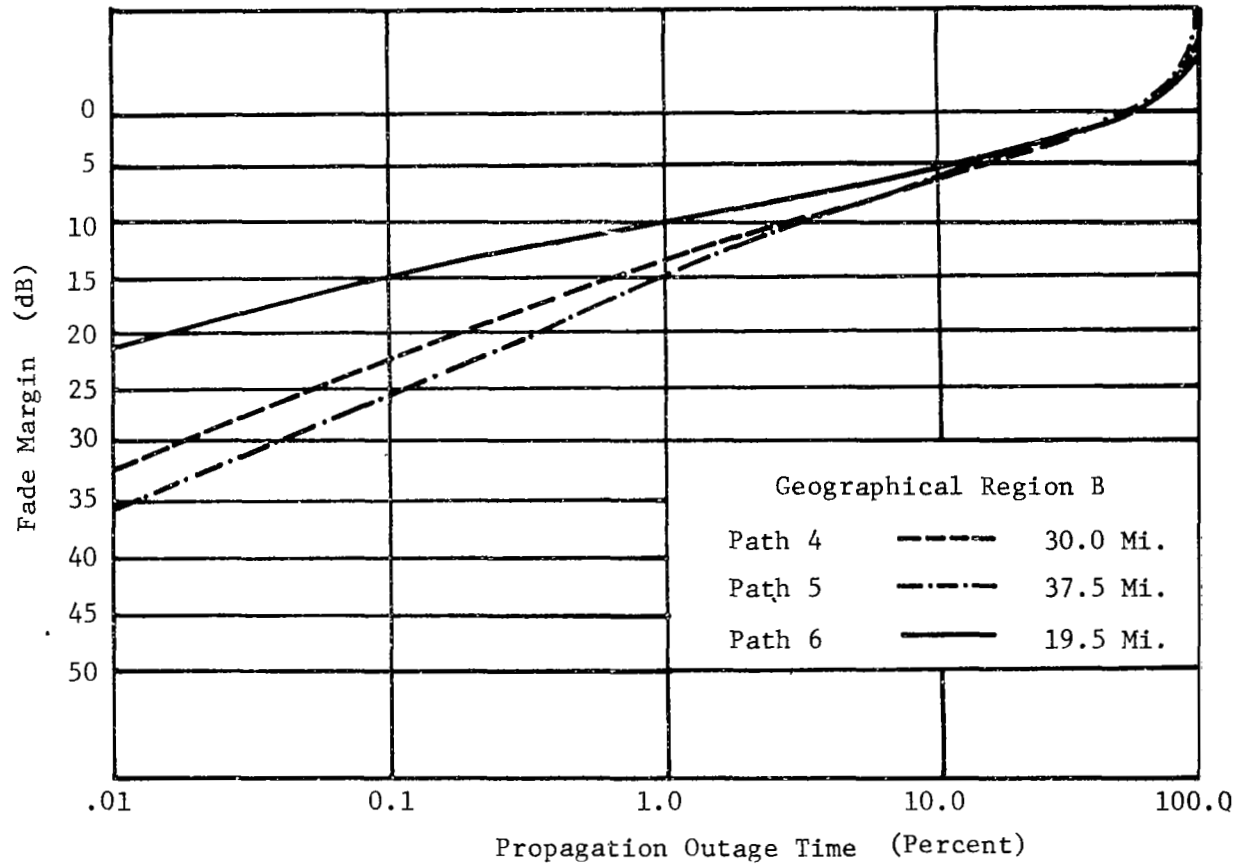


Figure 18. Statistical Distribution for Region B.

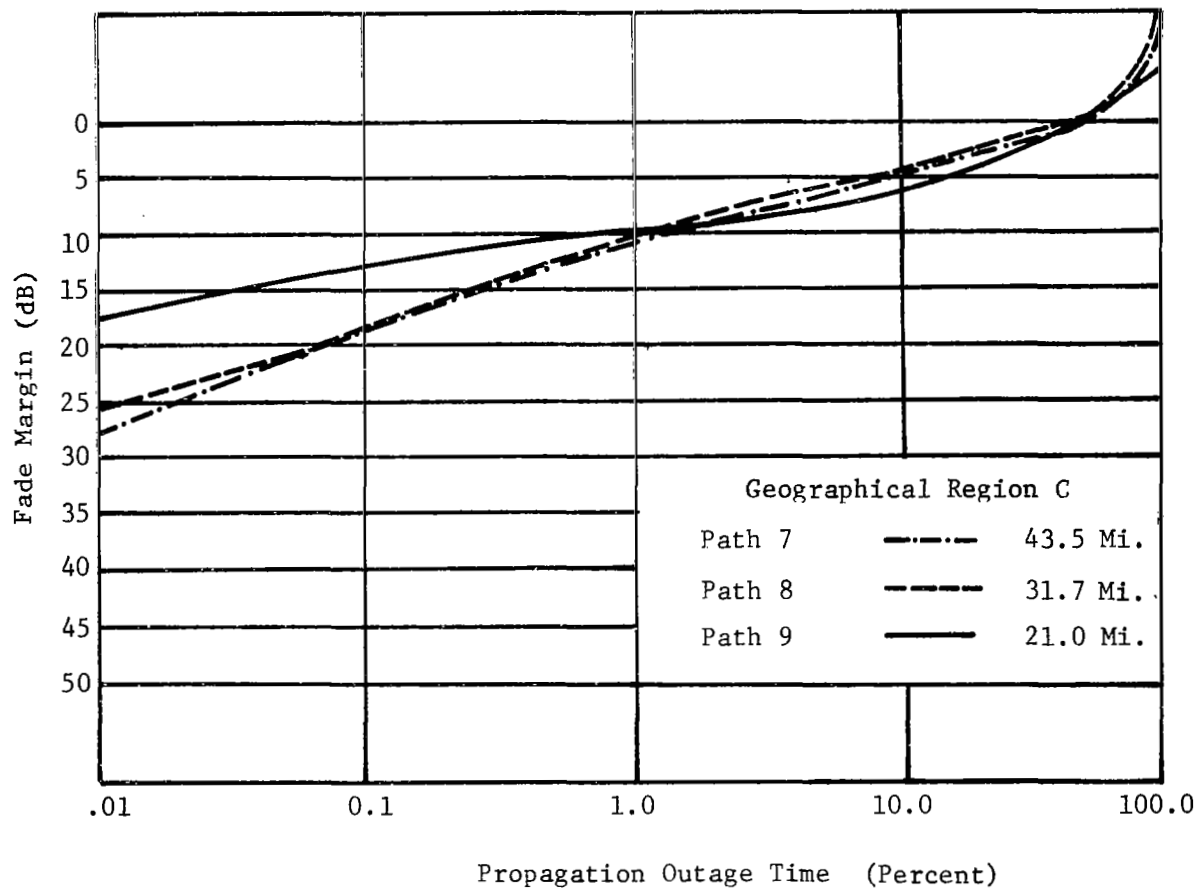


Figure 19. Statistical Distribution for Region C.

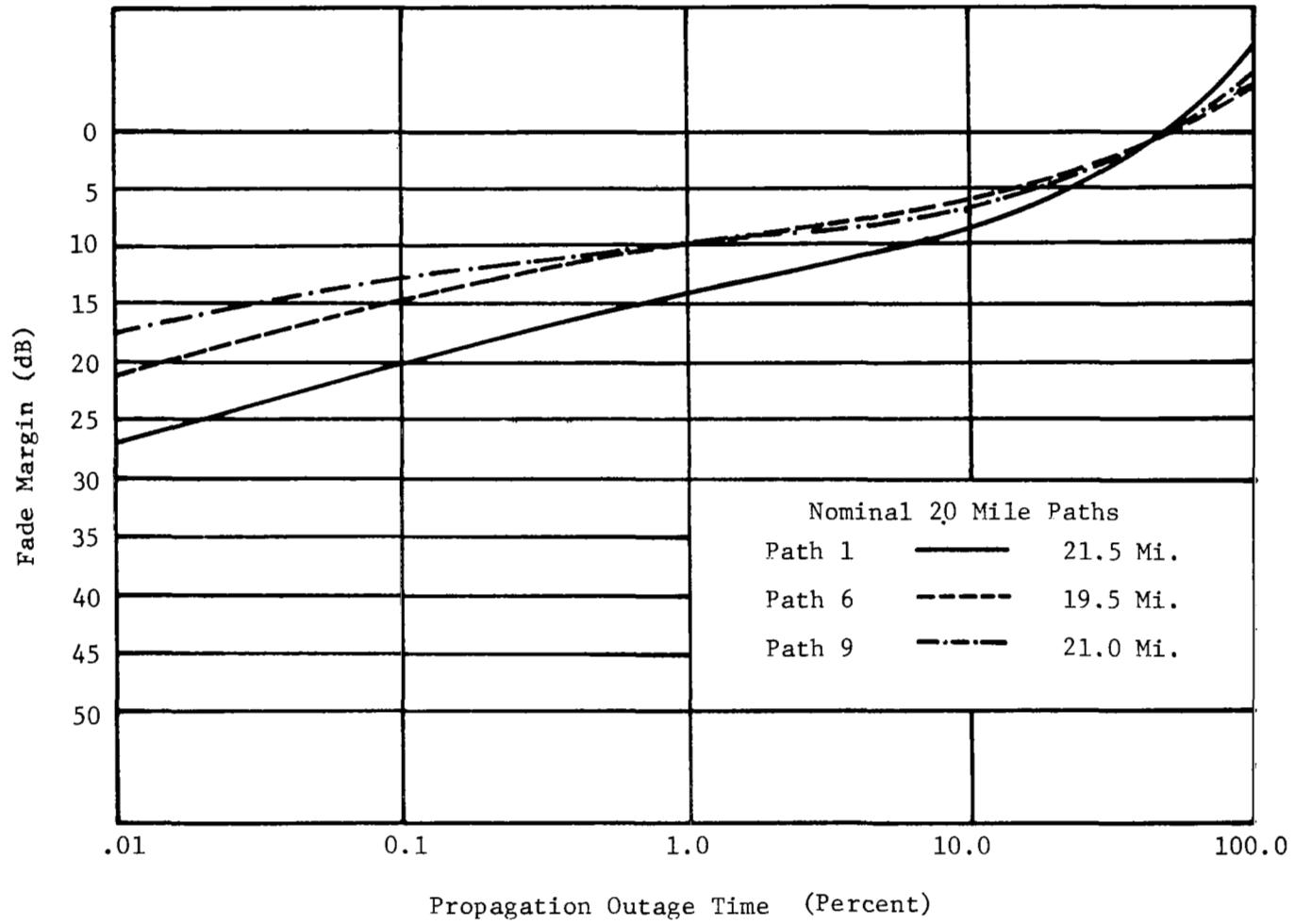


Figure 20. Statistical Distribution for 20 Mile Paths.

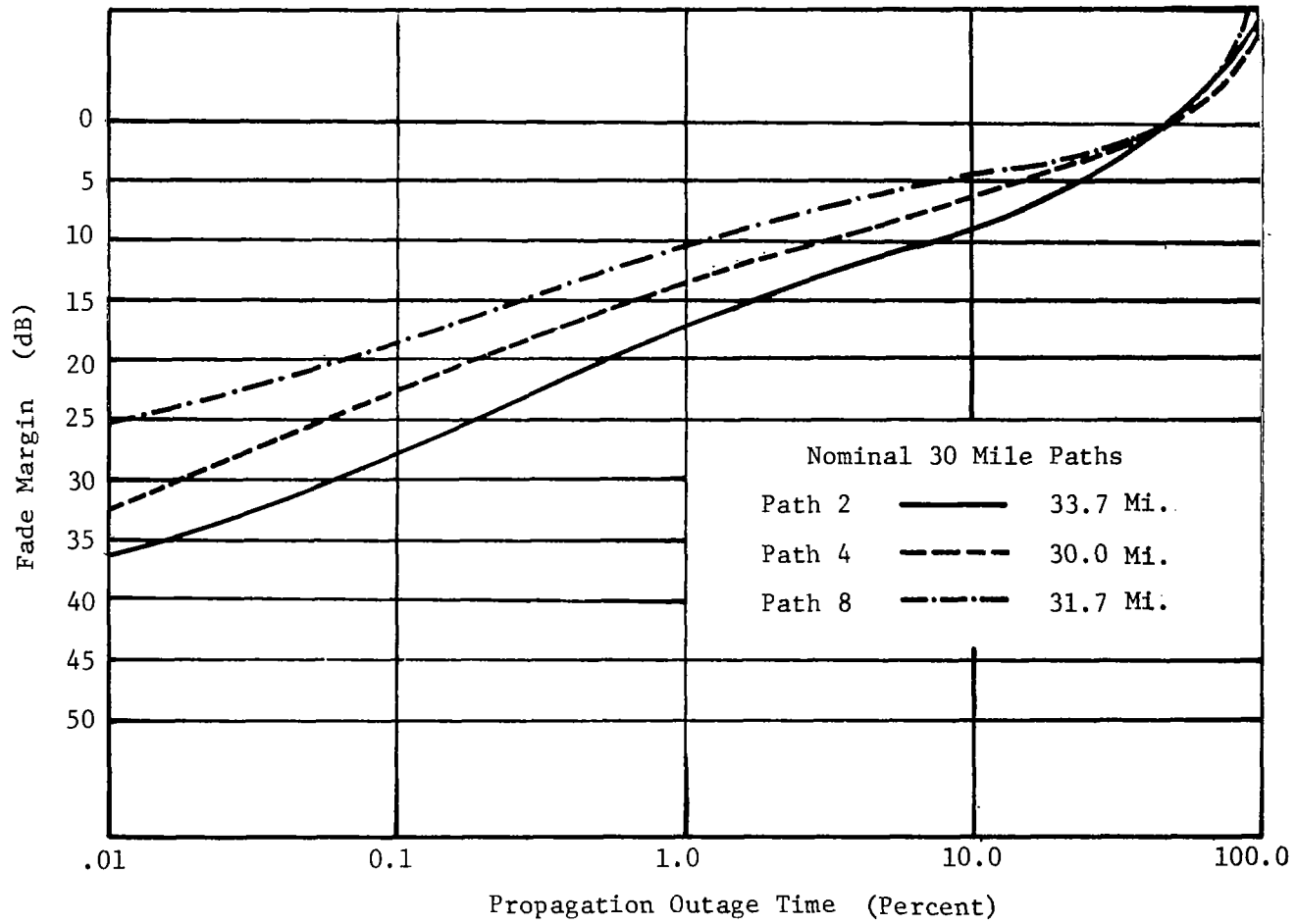


Figure 21. Statistical Distribution for 30 Mile Paths.

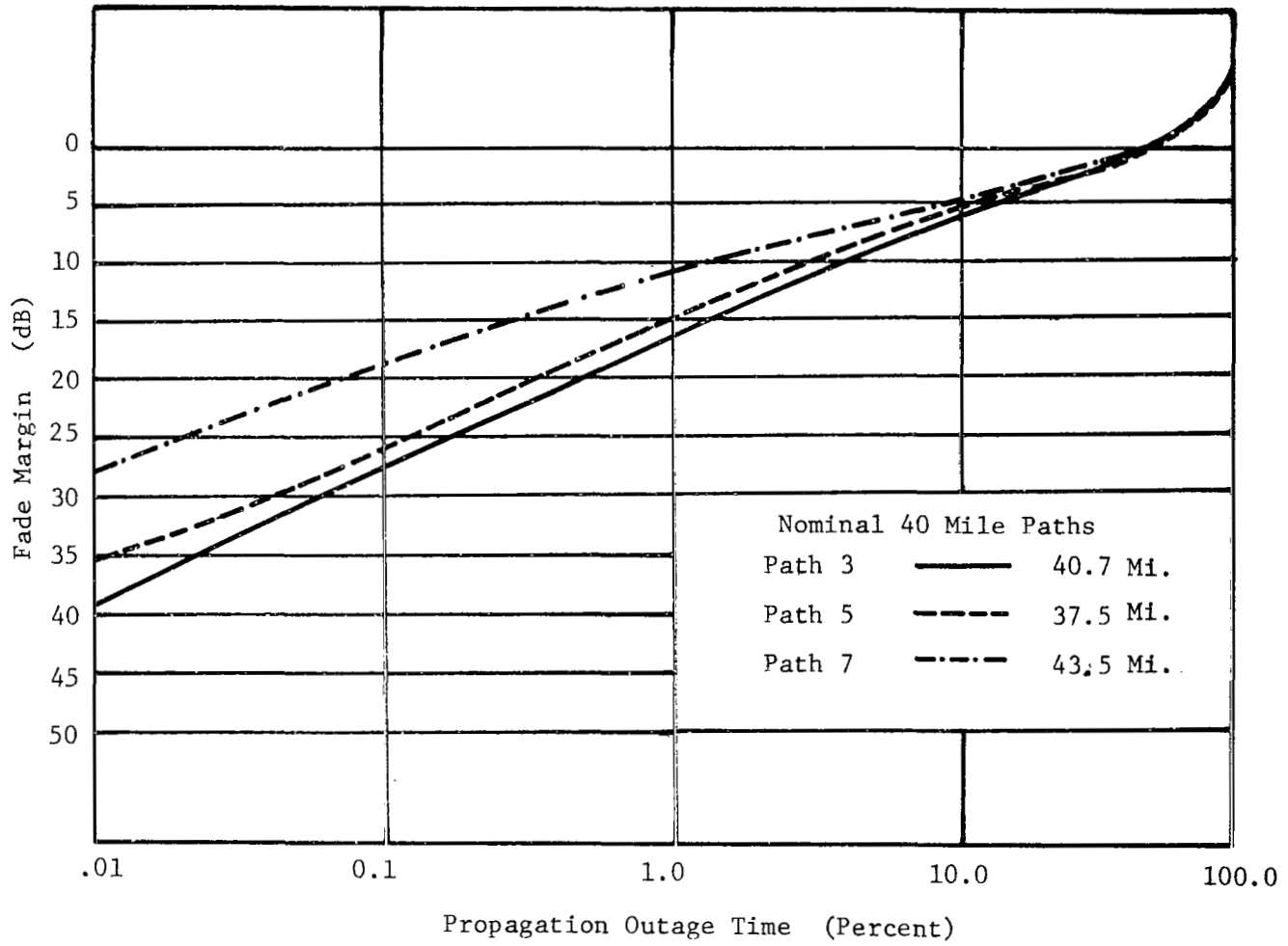


Figure 22. Statistical Distribution for 40 Mile Paths.

change in K_0 to path length for one geographical region. This polynomial was synthesized on a digital computer by a least-squares approximation method. For this research G has been determined to be:

$$G = .052170(\text{path length})^2 - 4.3437(\text{path length}) + 30.074 \quad 5-3$$

Similarly:

$$K_1 = HK \quad 5-4$$

and the polynomial for H is:

$$H = -.0093309(\text{path length})^2 + .86656(\text{path length}) - 6.7179. \quad 5-5$$

Since the geographical location is a function of two coordinates the determination of F and K was more involved than that for G and H. A fairly good approximation of F was found to be $\cos(\text{latitude})$. However, a much better approximation of F was then found by multiplying $\cos(\text{latitude})$ by $\tan(L_1)$ where L_1 is a polynomial in longitude. Thus F may be expressed as:

$$F = \cos(\text{latitude})\tan(L_1) \quad 5-6$$

where

$$L_1 = -.052556(\text{longitude})^2 + 10.341(\text{longitude}) - 461.55, \quad 5-7$$

Similarly K may be expressed as

$$K = \cos(\text{latitude})\tan(L_2) \quad 5-8$$

where

$$L_2 = .000049975(\text{longitude})^2 + .99124(\text{longitude}) - 46.617. \quad 5-9$$

Finally K_0 and K_1 may be expressed as:

$$K_0 = G[\cos(\text{latitude})\tan(L_1)] \quad 5-10$$

$$K_1 = H[\cos(\text{latitude})\tan(L_2)] \quad 5-11$$

where G, H, L_1 , and L_2 are as noted above.

In all of the above equations the path length is expressed in miles, and all arguments of trigonometric functions are expressed in degrees.

In using these equations slide rule accuracy is not sufficient. A small error in squaring a number yields a large error in the result. However, this difficulty is easily overcome by using a digital computer to perform the calculations. For this reason a program to calculate fade margin was written in Forgo language for the IBM 1620 digital computer. Appendix II contains the program which was used to determine the polynomials for G , H , L_1 , and L_2 , as well as the program written to calculate the fade margin directly once the path length, geographical location, and desired propagation reliability are specified.

Comparison of Experimental and Theoretical Results

Table III contains the theoretical values of K_0 and K_1 as calculated for the nine instrumented paths by use of the equations derived above. The theoretical curves plotted using these calculated values match the experimentally determined curves to within plus or minus 2dB or less. Figures 8-16 show the comparison of the theoretical and experimental curves.

Equipment accuracy was limited to plus or minus 2dB because of hysteresis in the switching point of the light-sensitive diodes.

It was postulated several times in the literature that the amplitude distribution of the signals received over a line-of-sight microwave system might follow closely a Rayleigh amplitude distribution.⁷ It should be noted that only two of the nine paths instrumented demonstrated a received signal distribution that was close to the Rayleigh

TABLE III. COMPARISON OF EXPERIMENTAL AND THEORETICAL DATA

Path	Length (miles)	Location Midpoint		K_0 Calculated	K_1 Calculated	Fit of Theoretical Curve to Experi- mental Curve
		Lat.	Long.			
1.	21.50	32.70°	92.90°	-32.862	6.3738	±1.0 dB
2.	33.75	32.70°	91.30°	-47.869	9.9802	±0.5 dB
3.	40.75	32.70°	90.70°	-50.551	10.9860	±1.0 dB
4.	30.00	33.70°	88.90°	-39.535	7.9334	±2.0 dB
5.	37.50	34.00°	88.35	-44.110	9.2279	±2.0 dB
6.	19.50	34.50°	88.00°	-25.813	4.8354	±1.3 dB
7.	43.50	37.70°	84.50	-33.802	7.7675	±1.5 dB
8.	31.75	38.00°	84.00°	-31.043	6.6410	±1.0 dB
9.	21.00	38.50°	83.30°	-21.428	4.2945	±1.5 dB

distribution. These were the Holly Ridge to Tallula path (path 2) and the Yazoo City to Tallula path (path 3) which are the two longest of the most southern paths. These paths required more fade margin for a given outage time than did any of the other paths which were instrumented, and yet they required less than that called for by the Raleigh distribution (see Figure 23). If the Rayleigh distribution were to be used to calculate the required fade margin for 99.99% reliability for the Garrison, Kentucky, to Stricklett, Kentucky, path (path 9) the result would be as much as 25 dB too high. This much error would be very costly in a long microwave system. No attempt was made to explain this difference, but it should be pointed out that the only reported results that show agreement with the Rayleigh distribution are those from short-term studies.

The following chapter illustrates by example the proper use of the mathematical model derived above. The path used is a general path which satisfies the restraints placed on the use of the fade margin equation.

In conclusion, the fade margin required for any general path lying within the geographical bounds of Athens, Louisiana (latitude 32°-40', longitude 92°-37'), to Garrison, Kentucky (latitude 38°-33', longitude 83°-06'), with length varying from 19 miles to 44 miles, and for propagation reliability varying from 90% to 99.99% can be calculated using the following equations:

$$\text{Fade Margin} = \left\{ K_0 + K_1 \log_{10} [1 + 0.T. (1000)] \right\}$$

where O.T. = outage time expressed in percent

$$K_0 = GF; K_1 = HK$$

$$G = .052170 (\text{path length})^2 - 4.3437 (\text{path length}) + 30.074$$

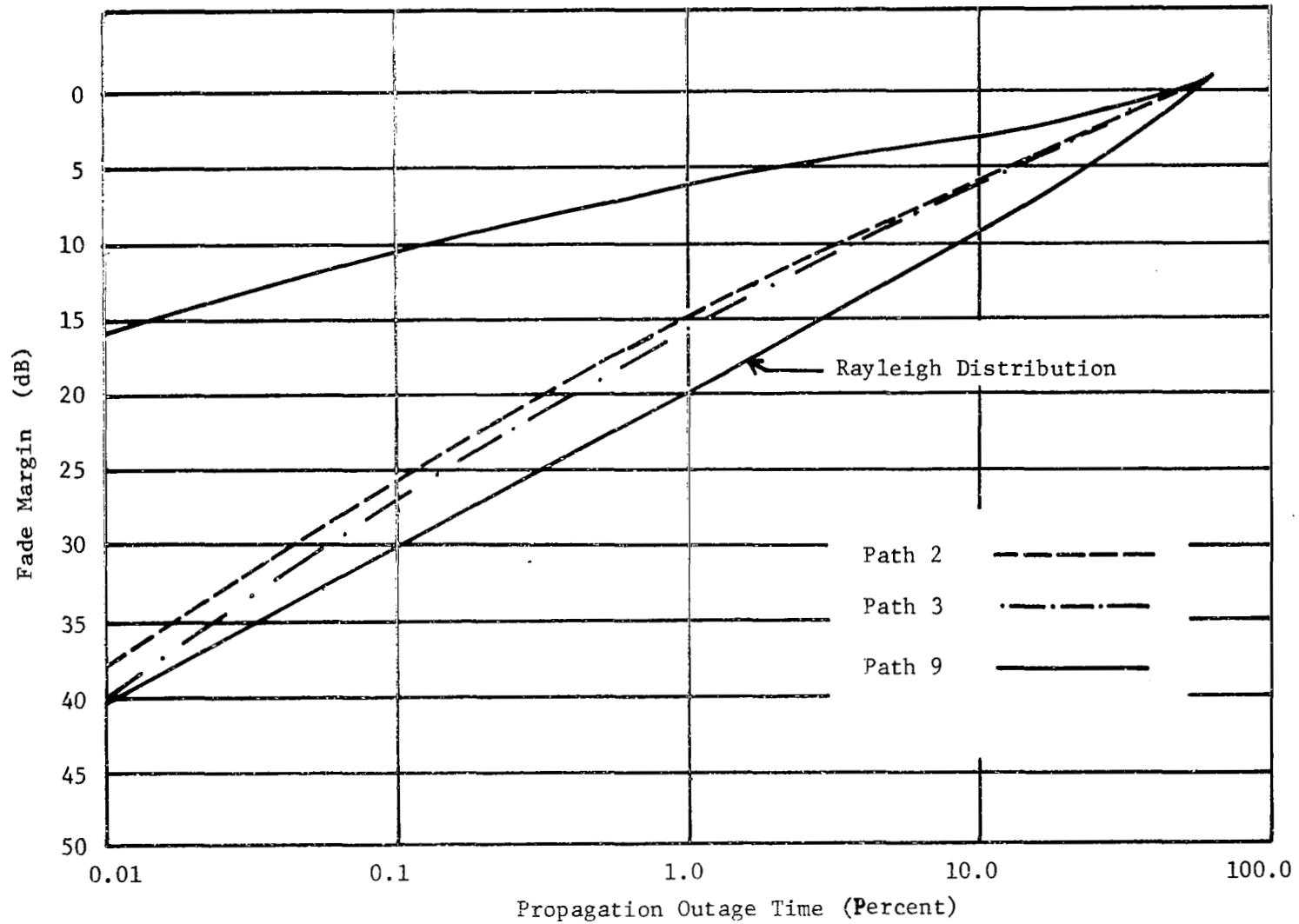


Figure 23. Comparison of Experimental Results with the Rayleigh Distribution.

$$H = -.0093309 (\text{path length})^2 + .86656 (\text{path length}) - 6.7179$$

$$F = \cos (\text{Latitude}) \tan (L_1)$$

$$K = \cos (\text{Latitude}) \tan (L_2)$$

$$L_1 = -.052556 (\text{Longitude})^2 + 10.341 (\text{Longitude}) - 461.55$$

$$L_2 = .000049975 (\text{Longitude})^2 + .99124 (\text{Longitude}) - 46.617$$

To use these equations to design a microwave path only the path length, geographical location, and propagation reliability desired are needed. No experimental propagation measurements are required.

Those familiar with the meteorological approach to the problem of determining the fade margin required will note the ease with which the fade margin is calculated using this mathematical model.

CHAPTER VI

DESIGN OF A TYPICAL 2 GHz LINE-OF-SIGHT MICROWAVE LINK

Choosing the Site

The selection of sites for a microwave relay system must take into account economic factors as well as technical factors. For this reason several alternate sites should be kept in mind when selecting a path location. The path with the most suitable terrain clearance may be a good distance from roads and a main power source. The cost of constructing a service road and bringing in power may outweigh the cost of higher towers at a more convenient site. The removal of all path obstacles, such as trees, power poles, etc., from the transmitter and receiver sites must be kept in mind. Survey of the possible paths by air or vehicle will often disclose obstacles not shown on contour maps.

Once a path is chosen a path profile should be plotted, preferably on profile graph paper which corrects for the slight downward curvature of the microwaves due to a standard atmosphere. Path profiles may be made by electronic airborne profile recorders or by surveying. The completed path profile should now be inspected to see how much clearance there is and what height towers are to be required.

Preferably irregular terrain, such as hills and wash-board countryside, will comprise the propagation path. Smooth terrain, such as large lakes, rivers, flat prairie, etc., should be avoided if possible.

Assuming a path with sufficient clearance is selected, specifications for a typical line-of-sight microwave path might be:

	Tower Heights Above Ground Level	Ground Elevation Above Sea Level
Station A, Transmitter	350 feet	340 feet
Station B, Receiver	350 feet	460 feet
Frequency	2.0 GHz	
Geographical Location: (Midpoint of the Path)	Latitude 33°	Longitude 89.75°
Path Length:	27.75 miles	
Transmitter Power:	26 watts = 14 dBw = 44 dBm	

Where dBw is defined as decibels above a watt and dBm is defined as decibels above a milliwatt.

System Reliability desired is 99.9%.

Equipment Reliability is specified as 99.99%.

Minimum useable signal at input to the receiver is 70 dB below one milliwatt.

Station cable and coupling losses are 10 dB for each station.

From the above specifications the required fade margin and hence the required antenna gains must be determined.

Calculating the Fade Margin Required

The fade margin required may be calculated from the equations derived in Chapter V as follows:

$$\text{System Reliability} = (\text{Equipment Reliability}) \text{ times} \\ (\text{Propagation Reliability})$$

therefore:

$$\text{Propagation Reliability required} = \frac{99.9\%}{99.99\%} \approx 99.909\% \approx 99.91\%$$

$$\text{Fade Margin} = \left| K_0 + K_1 \log_{10} [1 + \text{O.T. (1000)}] \right| .$$

Calculation of K_0 :

From page 45, G is given by equation 5-3, thus

$$\begin{aligned} G &= .052170 (\text{path length})^2 - 4.3437(\text{path length}) + 30.074 \\ &= .052170 (27.75)^2 - 4.3437 (27.75) + 30.074 \\ G &= -50.29 \end{aligned}$$

$$\text{and } \cos (\text{Latitude}) = \cos (33^\circ) = .83867$$

and from Page 45, L_1 is given by equation 5-7, thus

$$\begin{aligned} L_1 &= -.052556 (\text{Longitude})^2 + 10.341 (\text{Longitude}) - 461.55 \\ &= -.052556 (89.75)^2 + 10.341 (89.75) - 461.55 \\ L_1 &= .74521 \text{ radians} \\ \tan (L_1) &= .93949 . \end{aligned}$$

K_0 is found from equation 5-10 ,

$$\text{then } K_0 = G \cos (\text{Latitude}) \tan (L_1)$$

$$\text{or } K_0 = (-50.29) (.83867) (.93949) = - 39.624 .$$

$$\text{Thus } K_0 = -39.624 .$$

Calculation of K_1 :

From page 45, H is given by equation 5-5 . Thus

$$\begin{aligned} H &= -.0093309 (\text{path length})^2 + .86656 (\text{path length}) - 6.7179 \\ &= -.0093309 (27.75)^2 + .86656 (27.75) - 6.7179 \\ H &= 10.144 \end{aligned}$$

and from page 45, L_2 is given by equation 5-9, thus

$$\begin{aligned}L_2 &= .000049975 (\text{Longitude})^2 + .99124 (\text{Longitude}) - 46.617 \\ &= .000049975 (89.75)^2 + .99124 (89.75) - 46.617\end{aligned}$$

$$L_2 = .74612 \text{ radians} ,$$

$$\tan (L_2) = .92437$$

K_1 is found from equation 5-11, then

$$K_1 = H \cos (\text{Latitude}) \tan (L_2)$$

$$\text{or } K_1 = (10.144) (.83867) (.92437) = 7.8638$$

$$\text{Thus } K_1 = 7.8638$$

For a propagation reliability = 99.91%

$$\text{O.T.} = 100\% - 99.91\% = .09\% .$$

Hence fade margin =

$$\left| -39.624 + 7.8638 \log_{10}[1 + .09 (1000)] \right| = 24.2 \text{ dB}$$

Thus the required fade margin is found to be 24.2 dB.

Calculating the Antenna Gain Required

The fade margin may be expressed in terms of the system losses and gains as:

$$\begin{aligned}\text{Fade Margin (dB)} &= \text{Transmitted Power (dBm)} \\ &- \text{Minimum Useable Power (dBm)} - \text{path loss (dB)} \\ &+ \text{antenna gains (dB)}\end{aligned}$$

where the path loss is equal to free space attenuation of an isotropic source plus cabling and coaxial losses.

The free space attenuation loss is calculated by⁸

$$\text{Free space loss} = 10 \log_{10} \frac{(4\pi \text{ path length})^2}{(\lambda)^2}$$

$$\begin{aligned} \text{or free space loss} &= 10 \log_{10} (4\pi)^2 + 10 \log_{10} (\text{path length})^2 \\ &\quad - 10 \log_{10} (\lambda)^2 \end{aligned}$$

$$= 22 + 64 + 10 \log_{10} (\text{path length})^2 - 10 \log_{10} (\lambda)^2$$

$$= 86 + 20 \log_{10} (\text{path length}) - 20 \log_{10} (\lambda)$$

where path length is in miles and λ is the frequency wavelength in meters.

$$\begin{aligned} \text{Thus free space loss} &= 86 + 20 \log_{10} (27.75) - 20 \log_{10} (.15) \\ &= 86 + 28.84 + 16.5 \\ &= 132 \text{ dB.} \end{aligned}$$

Therefore total path loss (dB) is equal to:

Free space loss	132 dB
Cable and coupling loss	<u>20 dB</u>
Total path loss	152 dB

The antenna gains may now be calculated from:

$$\begin{aligned} \text{Antenna Gains (dB)} &= \text{Fade Margin (dB)} + \text{Path loss (dB)} \\ &\quad + \text{Minimum Useable Power (dBm)} - \text{Transmitter} \\ &\quad \text{Power (dBm)} . \end{aligned}$$

Therefore, the antenna gain required to obtain sufficient fade margin to achieve 99.91% propagation reliability is:

$$\text{Antenna Gains (dB)} = 24.2 + 152 + (-70) - (44) = 62.2 \text{ dB} .$$

The required antenna gains may be achieved by use of parabolic dish antennas with diameters as follows:

Station A: Six-foot	29	dB Gain
Station B: Ten-foot	33.5	dB Gain
	<hr/>	
Total Antenna Gain	=	62.5 dB

CHAPTER VII

SUMMARY AND CONCLUSIONS

The research reported here consisted of three main phases, a comprehensive literature survey, an experimental study, and a theoretical study.

The literature survey was conducted to determine what, if any, research had been conducted towards determining the propagation reliability of microwave signals over line-of-sight paths on earth. The most pertinent books and articles reviewed are tabulated in the bibliography. The result of the survey was the conclusion that virtually no work had been conducted with the determination of propagation reliability as the main objective. Most of the work reported had been directed towards the relationship between the meteorological changes in the atmosphere and the resulting signal fading which took place. Only a very few of the articles and books reviewed discussed the depth of fades encountered versus the percentage of time these fades are present. This, however, is one of the main problems the microwave system engineer must consider since the propagation reliability is a direct function of this phenomenon. Without the solution to this problem the systems engineer is at a loss to accurately determine the path gain required to achieve a desired system reliability. This research was directed toward a useable solution to this problem in the most direct manner apparent at the time.

The approach used was to derive a set of equations which would allow calculation of the fade margin required for a given propagation

reliability, path length, and geographical location. These empirical equations were determined using experimentally obtained data as the basis for the model. An example was given to illustrate the use of these equations. These equations are valid for path lengths of approximately 19 miles to 44 miles, located in the geographical region between 32° and 39° latitude and 83° and 93° longitude, and for a propagation reliability varying from 90% to 99.99%. These equations match the experimental data to within ± 2 dB.

It is felt that this research could be extended in several ways which would make further contributions to the knowledge of microwave propagation. First, by making experimental studies at 2 GHz in other parts of the United States, a more comprehensive picture of the relationship between fade margin, propagation reliability, geographical location, and path length could be obtained. Secondly, it would be highly advantageous to know the effects of transmitting frequency on the required fade margin for a given value of propagation reliability.

With the results obtained from studying these two topics, it should be possible to expand the equations developed in this research to include all the variables a microwave system engineer would normally encounter in calculating the proper fade margin for a given value of propagation reliability.

With the increasing use of microwave systems with their large bandwidth capabilities, expanded knowledge of microwave propagation is more important than ever before.

PART II

CROSSCORRELATION STUDY

CHAPTER VIII

INTRODUCTION

The generally accepted theory concerning propagation reliability is that variations in the received level of a signal transmitted over a given propagation path are caused by changes in local meteorological conditions along that path. If there is any major degree of correlation between the fluctuations of the received levels of signals transmitted over two or more different paths during periods of fading activity, as determined by the present study, then this theory should be reconsidered. A search of published literature revealed no investigation of possible crosscorrelation of signal fading over different propagation paths, other than visual observation of strip chart records.

CHAPTER IX

DISCUSSION OF CROSSCORRELATION FUNCTIONS

In the analysis of natural and man-made physical systems, one may deal with amplitude-time variations. These may be the level of vibration, the strength of a communication signal from an unknown transmitter, or countless other phenomena that vary as a function of time. Usually, a representation of the particular phenomenon can be obtained in the form of voltage amplitude versus time through the use of appropriate transducers. In many cases suitable analyses can be carried out by simply recording the transducer output on a strip chart, photographic film, or magnetic tape, and studying the resulting amplitude-time variations. As the system under investigation becomes more complex, the visual analysis of simple amplitude-time variations fails to provide the necessary information. For example the transmitted signal may be obscured in random noise, or the wave shape may be so complex that no significant pattern can be detected visually. Under such circumstances other data analysis or reduction methods must be employed to assist the scientists or engineers in analyzing the basic process and making some predictions regarding future events. Time correlation is one of the most basic of these methods. This includes the autocorrelation function, employed with a single amplitude-time function; and the crosscorrelation function, employed with pairs of amplitude-time functions.

The primary concern in a communication problem is the flow of messages. Associated with the flow of messages is noise which may be generalized to include any unwanted message in the presence of a wanted

message, and fading caused by many factors if wave propagation is of concern. The fluctuations of these messages with noise or fading as functions of time are extremely complex. Furthermore, frequently the underlying causes of the fluctuations are not completely understood. Hence these functions are called random functions or random processes. Because of their complexity the future of these functions cannot be precisely predicted.

A recent advance in communication engineering which has attracted considerable attention is the development of statistical communication theory. According to this theory, communication problems may be considered statistically and described in accordance with the concept of probability theory. The theory of correlation and its application to a large class of problems is one phase of the development of statistical communication theory. The concept of correlation is quite important and effective in handling a random phenomenon or one in which periodic, transient, and random functions are intermixed.

Before considering correlation functions as an application in the communication area, it would be interesting and helpful to have a brief discussion of correlation. Correlation is an expression of relationship which implies common causes with respect to two or more phenomena, but does not provide the interpretation of cause and effect. A correlation analysis can only establish the "facts" of the relation. For the meaning of these facts, the investigator must look elsewhere. Simple correlation may indicate the existence of a relationship between two variables, say X and Y. There is a measure which is used to indicate the degree of the relationship that exists between two variables. This

measure is known as the correlation coefficient, and is an attempt to summarize in one number the degree of relationship existing between two functions. Given N pairs of values as $X_1Y_1, X_2Y_2, \dots, X_nY_n$, it is defined mathematically, by notation r , as^{9,10}

$$r = \frac{\overline{XY} - \bar{X} \bar{Y}}{x y}$$

where \overline{XY} = the average or mean of the products of the pairs,

$\bar{X} \bar{Y}$ = the average of the X 's times the average of Y 's,

x = the standard deviation of the X 's,

y = the standard deviation of the Y 's.

Some other useful formulas which can be derived from the above equation are

$$r = \frac{\frac{1}{N} \sum_{i=1}^N (X_i - \bar{X})(Y_i - \bar{Y})}{x y} ,$$

$$r = \frac{\frac{1}{N} \sum_{i=1}^N X_i Y_i - \bar{X} \bar{Y}}{\left[\frac{1}{N} \sum_{i=1}^N X_i^2 - \bar{X}^2 \quad \frac{1}{N} \sum_{i=1}^N Y_i^2 - \bar{Y}^2 \right]^{1/2}} ,$$

and

$$r = \frac{\text{co-variance}}{(\text{variance of } X)^{1/2} (\text{variance of } Y)^{1/2}} .$$

If the variables X and Y are independent, i.e., not correlated, the co-variance is zero.¹¹ The simple correlation coefficient is a quantitative estimate of the direction and magnitude of the relationship between two variables when the observations are randomly drawn. It is symmetrical with respect to X and Y , and can vary between $+1$ and -1 , i.e., r must lie

in the range $0 \leq |r| \leq 1$, but in practice, because of random error, $0 < |r| < 1$. An increase in the degree of relationship is indicated by an increase in the absolute value of r , the sign indicates the direction of the correlation. The sign of r tells the investigator whether Y increases with an increase in X (r is positive) or whether Y decreases with an increase in X (r is negative). If there is no correlation between two variables, the value of r is zero; if there is a perfect correlation, the value of r is unity, i.e., either $+1$ or -1 . It is realized that if some common factors affect two variables, the correlation coefficient may be high. A higher correlation coefficient proves the existence of a closer relation between the variables, but does not necessarily imply causes.

The observation of a moderate degree of correlation does not necessarily mean that common causes exist. The observation may be due to chance. Likewise, the observation of zero correlation does not necessarily mean that no correlation exists.¹² Thus, correlation analysis assists in determining the significance of a relationship between two variables. Reasons why the relationship exists (whether spurious, casual, or effect of some unknown variables) cannot be determined from the mathematics. It involves a scientific study of the subject, possibly using additional experimental data.

If there is an attempt to make a statement of results of the correlation analysis, the investigator should carefully compare the results with the original hypothesis. If hypothesis and statistical results do not agree, the hypothesis must be carefully examined to see if it may logically be restated so as to be consistent with the facts as found; and the

analysis must be carefully studied to see if there are any loopholes and misinterpretation. If the hypothesis and results are found to be consistent, the project may be regarded as completed; however, statistical analysis is not a substitute for logical analysis, careful thinking, and full knowledge of a problem. It is merely an aid which may be employed in arriving at the right answer.

The effect of correlation with respect to statistics has been shown. It is also advantageous to discuss the correlation function and its applications in communications. Correlation functions are related in a quite natural way to time functions (or time series) which carry information. They refer to those in which the variations of the quantity under observation as a function of time cannot be precisely predicted. No mathematical expression that uniquely relates the effect to the cause is available. In order to establish a simple basic method of analysis which is suitable for application to physical problems, unnecessary complication and refinement are avoided. Certain restrictions and idealizations are introduced.

First, it is assumed that random functions theoretically have a duration extending from the infinite past to the infinite future. In practical problems it is impossible to meet this assumption, but the time functions used as experimental data should be physically of considerable duration. Second, the observation of time functions and the measurement of correlation functions are based on statistical theory. Since a random function does not repeat in repeated experiments, the interest in communication problems concerns not just a single random time function but rather an aggregate of random functions which are produced by similarly prepared sources. The infinite aggregate of

random time functions is called the ensemble. Each function in the ensemble is called a member function of the ensemble. Third, it is assumed that the statistical properties of these functions are invariant under a shift in time origin. That is, the complete set of probability densities describing an ensemble of random functions are independent of the origin from which time is measured. In other words, those properties are stationary in time. These assumptions are easily justified for a large number of practical situations.

The concept of an average is of basic importance in scientific analysis, particularly in the study of random phenomena. Since correlation functions are a special type of average, they play a central role in the harmonic analysis of random processes. In statistical communication theory there are two kinds of averages; namely, time average and ensemble (statistical) average. Since, for the general case, a random process is described in terms of statistics and probability densities; the ensemble average can be evaluated if the necessary probability density is known. On the other hand, without necessary information, the time average can be estimated only from the past behavior of the random time functions. Since its future cannot be predicted exactly, most of the probability densities or distribution functions are difficult to determine, either theoretically or experimentally. Fortunately, in most practical applications, direct measurements of probability densities or distribution functions are unnecessary. Other desired properties such as time averages and correlation functions may be obtained experimentally. In this study of the crosscorrelation, time functions rather than joint probability

densities are used and time averages are estimated. It may be shown in the practical sense that the time average of an ensemble member, over the infinite past and future, is equal to the ensemble average for a stationary random process.¹³ The expression may be written as

$$\lim_{T \rightarrow \infty} \frac{1}{2T} \int_{-T}^T f(t) dt = \int_{-\infty}^{\infty} x P_{\xi}(x) dx$$

where $P_{\xi}(x)$ is the probability density, or simply as $\overline{f(t)} = \bar{\xi}$. However, as a mathematical problem, the equivalence deserves rigorous consideration.

The crosscorrelation is an important expression of the relationships between two random functions which are related to each other in some way. In discussing the crosscorrelation of two random functions, one considers the functions as individual members of two separate ensembles. The members of one ensemble are produced quite similarly in every respect. For the definition of crosscorrelation, let $f_1(t)$ and $f_2(t)$ be the two random functions. The crosscorrelation function of the random time functions is then theoretically defined as

$$\phi_{12}(\tau) = \lim_{T \rightarrow \infty} \frac{1}{2T} \int_{-T}^T f_1(t) f_2(t+\tau) dt$$

where τ is a displacement along the time axis and $2T$ is the length of time over which averaging of the product $f_1(t) f_2(t+\tau)$ is done. It is a time average. The subscript 12 indicates that the crosscorrelation involves $f_1(t)$ and $f_2(t)$ with the second numeral 2 referring to the fact that $f_2(t)$ has been shifted in time by an amount of τ seconds. The order of the subscripts should be kept properly, for when they are interchanged, the definition refers to

$$\phi_{21}(\tau) = \lim_{T \rightarrow \infty} \frac{1}{2T} \int_{-T}^T f_2(t) f_1(t+\tau) dt \quad .$$

This function is assumed to exist for every value of the time delay, that is, the crosscorrelation function is continuous with respect to the displacement τ . The ensemble average is defined as¹⁴

$$\phi_{21}(\tau) = \int_{-\infty}^{\infty} \int_{-\infty}^{\infty} x_1 y_2 P_{\xi_1 \xi_2}(x_1, y_2; \tau) dx_1 dy_2$$

where x_1 and y_2 are variables and $P_{\xi_1 \xi_2}(x_1, y_2; \tau)$ is the first joint probability density.

In a similar manner, the autocorrelation for a random function $f_1(t)$ is defined as a time average as

$$\phi_{11}(\tau) = \lim_{T \rightarrow \infty} \frac{1}{2T} \int_{-T}^T f_1(t) f_1(t+\tau) dt \quad .$$

The ensemble average of the autocorrelation function of $f_1(t)$ is defined as

$$\phi_{11}(\tau) = \int_{-\infty}^{\infty} \int_{-\infty}^{\infty} x_1 x_2 P_{\xi_1 \xi_2}(x_1, x_2; \tau) dx_1 dx_2 \quad .$$

It is sufficient to point out that the two expressions, time and ensemble average, are equivalent for stationary random processes, according to an important theorem in random processes known as the Ergodic Theorem.¹⁵

In a general sense, the correlation function shows the degree of dependence of one value in a time series to another at a different time. In the computation of both crosscorrelation and autocorrelation functions three operations are involved: (1) One time function has to be delayed or shifted in time with respect to the other for a value of $\tau = \tau_1$ (in

autocorrelation, the time function is delayed with reference to itself). Then $f_2(t+\tau_1)$ is obtained for all values of t . (2) The delayed function is multiplied by the other to produce a continuous instantaneous product. Then $f_1(t)f_2(t+\tau_1)$ is formed for all t . (3) The instantaneous product is averaged by integration over the entire duration of the function, $2T$, which is theoretically infinite. However, practically, a sufficiently long duration is considered and the resulting integral is divided by the overlapped duration of the two functions for the mean value which is represented by $\phi_{12}(\tau)$ or $\phi_{11}(\tau)$.

Since the autocorrelation function has very useful characteristics which are applied to a large number of physical problems, some of its important properties should be examined. The autocorrelation function is even, that is, $\phi_{11}(\tau) = \phi_{11}(-\tau)$. For $\tau = 0$, the expression of autocorrelation is

$$\phi_{11}(0) = \lim_{T \rightarrow \infty} \frac{1}{2T} \int_{-T}^T f_1^2(t) dt$$

which is the mean square of $f_1(t)$, or mean power if $f_1(t)$ represents a voltage or a current for a 1-ohm load. The very extreme value $\phi_{11}(\tau)$, when τ tends to infinity, tends to zero if $f_1(t)$ contains no d.c. or periodic components. The autocorrelation is continuous everywhere if it is continuous at the origin.¹⁶ Its value at the origin is maximum in magnitude and is positive. The autocorrelation function of a periodic function is also periodic.

The crosscorrelation of random functions also applies to communication problems in various ways. Its properties are somewhat different from that of autocorrelation. The function $\phi_{12}(\tau)$ is not necessarily even and in general, it is neither even nor odd. However, it is easy

to see $\phi_{12}(-\tau) = \phi_{21}(+\tau)$. Graphically this means, with respect to the vertical axis, the function $\phi_{12}(-\tau)$ is the mirror image of $\phi_{21}(\tau)$, and vice versa. Furthermore, in contrast to autocorrelation, the value of $\phi_{12}(\tau)$ at the origin, $\tau = 0$, need not be the maximum; but, similar to autocorrelation, the crosscorrelation tends to zero as the displacement tends to infinity in either direction, that is, $\phi_{12}(\pm\infty) = 0$. This is true provided there are no d.c. or periodic components contained in either one or both of the random functions. Concerning the upper and lower bounds of the crosscorrelation function, it has been shown that¹⁷

$$\phi_{12}(\tau) < 1/2 [\phi_{11}(0) + \phi_{22}(0)] \text{ for } -\infty < \tau < \infty .$$

This inequality indicates that the crosscorrelation of two random functions $f_1(t)$ and $f_2(t)$, provided that $f_1(t) = f_2(t+\tau)$ for all values of τ , is always less in magnitude than the average of the two mean square values of the random functions.

After considering correlation in both statistics and communications, it is clear that the correlation coefficient, or the covariance, of the statistics and the correlation function of communication theory bear a close resemblance to each other. Both of them are essentially mean values of the product of two random variables. Nevertheless, one important difference between them is that the correlation function, as the name implies, is a function of time, while the correlation coefficient is a single mean value or just a number. Since, in communication problems, time is a primarily important variable, while in statistical problems it is not necessarily a relevant parameter, such a difference is to be expected.

The crosscorrelation function has been shown to serve as a measure of similarity between two statistical time functions $f_1(t)$ and $f_2(t)$. Since it is expressed as the mean value of the product of $f_1(t)f_2(t+\tau)$, the same crosscorrelation for every value of displacement τ is expected if the functions $f_1(t)$ and $f_2(t)$ are originated from statistically independent sources. It is noted that the crosscorrelation function is a function of time displacement τ , not the instantaneous time t in the time functions of the ensemble. When the crosscorrelation function for two functions is a constant or zero for all τ , that is, a horizontal line on the plot of the crosscorrelation versus time displacement, the functions are said to be incoherent or have no correlation between them. If two functions are dependent upon each other, though not identical, the crosscorrelation function should be a curve with peaks at some specific values of τ . The places where the peaks of the crosscorrelation function occur are of greatest interest to the investigator. The values of τ where peaks occur will give some information concerning the similarity between two functions with respect to time. If both functions $f_1(t)$ and $f_2(t)$ follow each other very closely, or there are some causes which have the same effects on both functions at the same time, they are both simultaneously large (or small) in variation. If some causes have the same effect upon two functions, but the effect upon one is delayed by some time τ with respect to the other, then the variations of one function will follow those of the other, except that they are delayed by a time shift τ . The product of these two functions is also a function of time. In this case, when the variations of both functions are of the same sign, the product would be a positive function and the average will

tend to accumulate positively. Similarly, if they are both large (or small), even with one delayed to the other, and always of opposite sign, the product would be a negative function and the average will again accumulate, although negatively. Thus the magnitude of the crosscorrelation function is more significant than its algebraic sign. If two functions are independent of each other, or no common causes exist between them, they would tend to cancel each other on the average.

Since the crosscorrelation is a function of τ , it is interesting to examine the meaning of the time delay τ . When the amplitude variations of $f_1(t)$ follow those of $f_2(t)$ exactly, that is, the peaks and dips of $f_1(t)$ coincide with those of $f_2(t)$ without any shift of time, it is expected that the maximum in amplitude of their crosscorrelation function occurs at the origin, $\tau = 0$. Similarly, when the peaks of the crosscorrelation function occur at some specific values of τ rather than at the origin, the indication is that some unknown factors have the same influence on both functions, making them vary in the same way, but with one variation delayed with respect to the other by a time displacement τ . By observing the crosscorrelation curve, one obtains information concerning similar effects occurring on both functions, and the separation in time of occurrence of these effects.

In radio wave propagation, the fading in signal strength due to atmospheric conditions or other possible causes is a common occurrence. Crosscorrelation of the recorded AGC signals of different selected paths, the objective of this study, may help determine if the variations in signal strength are due only to changes in local meteorological conditions along the propagation path, as is assumed in currently accepted theories of microwave propagation over optical paths.

CHAPTER X

CROSSCORRELATION EXPERIMENTAL PROCEDURE

The purpose of this portion of the study was to determine experimentally, by use of an analog computer, if any time correlation existed between the fading of microwave signals over two different paths.

The crosscorrelation equation has been defined as

$$\phi_{12}(\tau) = \lim_{T \rightarrow \infty} \frac{1}{2T} \int_{-T}^T f_1(t) f_2(t+\tau) dt$$

where the entire duration, $2T$, over which the average is taken, is theoretically infinite. In actual situations the time of observation is finite; however, this introduces little error so long as the period of integration is long compared with the longest period of variation in either function.

The following example illustrates the practical measurement of a crosscorrelation function. Let $f_1(t)$ and $f_2(t)$, shown in Figure 24 with an arbitrary reference point $t = 0$ as indicated, represent two recorded random voltage waves for the duration T . Here a modification is made in the definition of the crosscorrelation function, in that the duration of observation is from 0 to T_k seconds instead of being from $-T$ to $+T$. The approximate expression for the crosscorrelation function is thus given by

$$\phi_{12}(\tau_k) = \frac{1}{T_k} \int_0^{T_k} f_1(t) f_2(t+\tau_k) dt$$

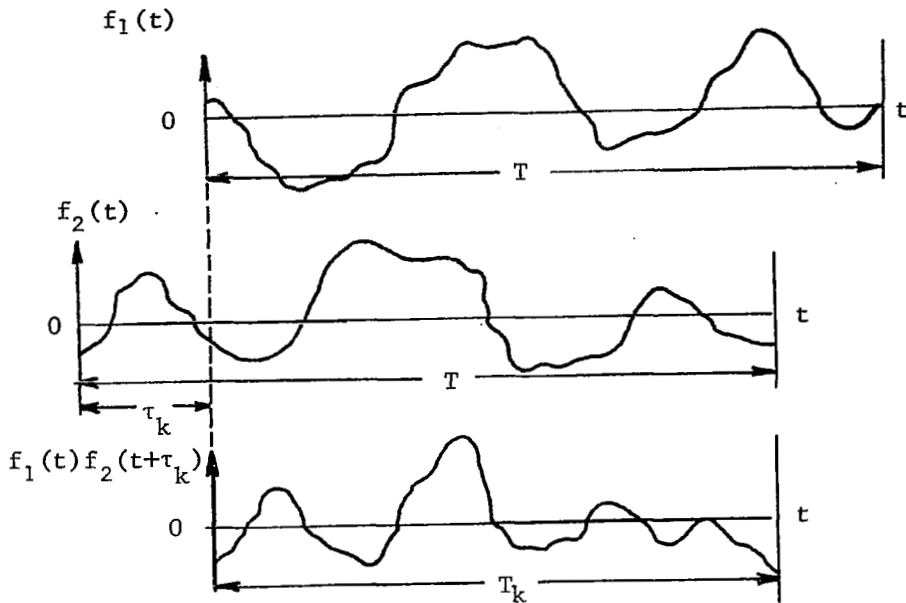


Figure 24. Functions to be crosscorrelated.

where τ is positive if $f_2(t)$ is displaced in the negative direction on the time axis by the amount τ , and τ is negative if $f_2(t)$ is displaced in the positive direction on the time axis by τ . To evaluate this function graphically, the first step is to form the function $f_2(t+\tau_k)$ by displacing $f_2(t)$ to the left by the amount $\tau = \tau_k$ as indicated in Figure 24. Then the product $f_1(t) f_2(t+\tau_k)$, represented by the lower curve, is obtained. Finally, the average of the product curve is found by performing the integration and dividing by T_k , the length of the common interval. The value thus obtained is a point on the crosscorrelation curve at $\tau = \tau_k$. This method results in discrete values of $\phi_{12}(\tau)$ instead of a continuous curve of the crosscorrelation function. The averaging procedure is repeated for a series of values of τ until sufficient points are obtained to determine the entire curve. Since

$f_1(t)$, $f_2(t)$, and $f_1(t)f_2(t+\tau_k)$ are continuous functions, the multiplication and integration can be accomplished by using an analog computer.

As indicated previously, this study was performed over three selected optical paths which are part of the Texas Eastern Transmission Corporation's 2 GHz microwave system. They are located in the northeastern portion of Mississippi and the extreme northwestern portion of Alabama. The stations, their path lengths, and operating frequencies are listed in Table IV. These three paths are in similar geographic areas, but have different lengths.

TABLE IV

Locations of the three transmission paths

Station Location	Path Length (miles)	Operating Frequency (GHz)
1. Maben, Miss. to Egypt, Miss.	30.00	1.98
2. Bexar, Ala. to Egypt, Miss.	37.50	1.98
3. Barton, Ala. to Coker, Ala.	19.50	1.98

The experimental data for this work were obtained by recording the AGC voltages of the three receivers simultaneously on an Ampex SP-300 magnetic tape data recorder (hereafter referred to as recorder A) located at the Egypt terminal. The AGC signal from the Barton to Coker path was transmitted to Egypt, Mississippi, via a pulse modulated telemetering channel utilizing equipment which was specifically designed for this experiment. WWV standard timing pulses were recorded simultaneously on the magnetic tape, together with the three AGC signals.

Since fading activity is at a maximum during night hours, recordings were obtained during darkness. These experimental data were recorded on the early morning of July 8, 1966. The data were recorded at a speed of $1\frac{7}{8}$ inches per second, the lowest speed of the recorder, for a period of approximately three hours. There are four available channels on the magnetic tape. The channels 1, 2, 3, and 4 are WWV timing pulses, Barton to Coker path, Bexar to Egypt path, and Maben to Egypt path, respectively. The maximum frequency of the variations in amplitude of the received signals is 5 Hz, due to the time constant of the AGC circuit of the receivers.

The next step of this experiment was to obtain the three cross-correlation curves between any two out of these three received signals (they are called channel 2, 3, or 4, in the following discussion for simplicity), utilizing the analog computer facility of Mississippi State University. It is incidental that the voltage polarity of channel 2 is reversed with respect to the other two channels; and, as would be expected, the crosscorrelation functions of channel 2 with each of the other two channels are of opposite sign to that of channel 3 with channel 4. Since time displacement of one channel with respect to the other is necessary for performing the crosscorrelation a duplicate tape was recorded, and two recorders were utilized to run the tapes simultaneously. The second recorder was an Ampex FR-1100 multichannel magnetic tape recorder (hereafter referred to as recorder B) with half-inch tape.

For saving time in performing the crosscorrelation with the analog computer, the two recorders were run at a speed of 15 inches per second, which is the maximum speed of recorder A. In this case, the time scale of the output of the recorders is 8 times the actual time. The maximum

frequency of the signal variations is increased by 8 times to about 40 Hz which is still within the frequency limit (100 Hz) of the multipliers of the analog computer. The total period recorded and used in performing the crosscorrelation was two hours of actual time. Because of the increased speed of the tape recorders, only 15 minutes was required to run the whole period of tape in the analog computer.

Since it is difficult to obtain the continuous time displacement for a crosscorrelation curve, discrete values of τ were chosen; then by connecting the discrete points, an approximate crosscorrelation curve was obtained. The time shift, $\Delta\tau$, chosen for each performance of the crosscorrelation was one-half minute, which corresponds to 4 minutes of actual time. It was decided that the greatest total time displacement in either the positive or the negative direction would be about 6 minutes, which represents 40% of the actual recording time. In this case, a finite number of points on the curve were obtained. The main interest is in investigating the peaks of the correlation curve. Thus, in the neighborhood of every peak, more values of τ separated from each other by 10 seconds were chosen in order to reveal possible sharp peaks occurring between the 30 second intervals of displacement. For any specific value of τ , the period over which the average was taken was only the overlapping period of the two tapes, i. e.,

$$T = (15 \times 60) - \tau = 900 - \tau \text{ seconds.}$$

The variation in signal level of the output of the recorder was generally below 1 volt; but the average d.c. level was about 3 or 4 volts. The first step was to determine the d.c. level for each channel and remove it; otherwise the d.c. level would have a dominant effect on

the curve, since the output of the integrator of the computer with a d.c. input is a ramp function. The actual fluctuations of the signal would have very little effect on this ramp function and could not be examined; therefore, the resulting curves would be meaningless. The method of determining the d.c. level of each channel was to average each channel through the analog computer, utilizing the circuit shown in Figure 25. The positive voltage necessary to cancel the d.c. level was estimated and obtained from the +100 volts supply of the computer through a potentiometer, then added to the tape signal by a summing amplifier. A potentiometer with a gain setting of 0.1 was inserted before the integrator in order to keep the variation of the integral, i.e., $\int_0^T [f(t)+\text{d.c. voltage}] dt$, within the limits of the computer, ± 100 volts. If the output of the integrator was significantly different from zero, the positive d.c. voltage was adjusted by trial and error until negligible output was obtained.

The time displacement τ also had to be considered before performing the crosscorrelation. Since the two recorders are driven by synchronous motors, the speeds were assumed to be the same. The time displacement τ was accomplished by winding enough tape for τ seconds of running time on the take-up reel before starting to run the problem. The tape on recorder A was wound for positive τ , and the tape on recorder B for negative τ . For example, if channel 3 was shifted by $\tau = +30$ seconds from channel 2 for $\phi_{23}(30)$, the recorder A was run 30 seconds in advance, then the other recorder and the computer were started simultaneously. For $\tau = -30$ seconds, recorder A was started first, since $\phi_{23}(\tau) = \phi_{32}(-\tau)$.

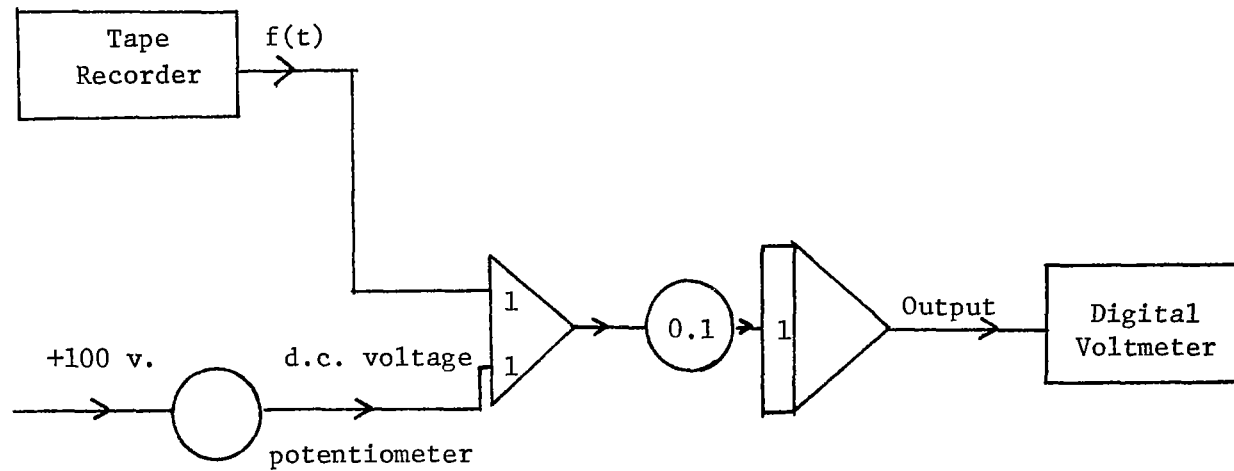


Figure 25. Circuit for Determining the Average Level of the Signal.

The analog computer circuit used for performing the crosscorrelation between any two out of these three channels is shown in Figure 26. The only difference is in the d.c. voltage added to each channel. Because the output of the multiplier is just one hundredth of its real value and the multiplier has a small d.c. level, two amplifiers with a gain of 5 each were placed before the multiplier in order to make the output of the multiplier more meaningful. Each channel signal strength level is increased by about 6 times. This amplification made the variations of the product more pronounced and minimized the effect of the d.c. offset at the output of the multiplier which would otherwise have resulted in a ramp function. Potentiometer C was selected with a gain value of 0.016 for simplicity in calculation; and, as indicated in Figure 26, it makes the output of the integrator be

$$-\frac{1}{10} \int_0^T f_1(t) f_2(t+\tau) dt = -\frac{T}{10} \phi_{12}(\tau)$$

where

$$\phi_{12}(\tau) = \frac{1}{T} \int_0^T f_1(t) f_2(t+\tau) dt .$$

The value of the crosscorrelation function, measured in volts, for some τ is obtained by multiplying the output reading of the digital voltmeter by a factor of $-\frac{10}{T}$ where T is the overlapped period for two tapes.

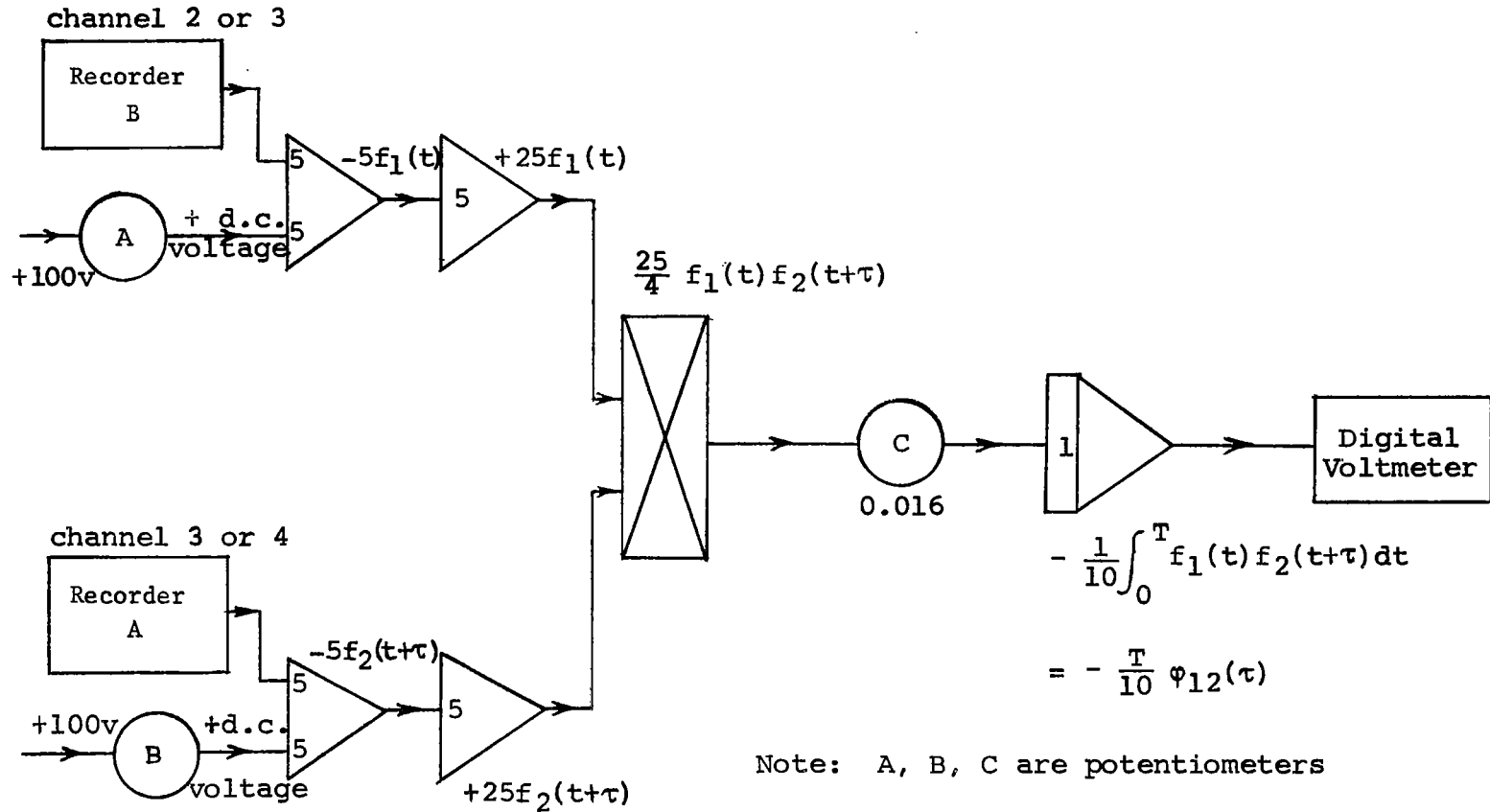


Figure 26. Analog computer circuit for performing crosscorrelation.

CHAPTER XI

RESULTS AND DISCUSSION

According to the procedures described in the previous chapter, the crosscorrelation curves of channel 2 and channel 3 [$\phi_{23}(\tau)$], channel 2 and channel 4 [$\phi_{24}(\tau)$], and channel 3 and channel 4 [$\phi_{34}(\tau)$] were obtained by the analog computer. The data for these three curves are listed in Tables 5, 6, and 7; and the three crosscorrelation curves are shown in Figures 27, 28, and 29. The sign of the curves which include channel 2 are reversed in order to take care of the reverse polarity of the signal recorded on channel 2.

Since every point of a crosscorrelation curve should represent the result of a large number of observations made on the random function so as to ensure its close approximation to the true value, many sets of data need to be processed. Consequently, it is impossible to make a definite conclusion just by processing one set of data. Nevertheless some information about the crosscorrelation between different selected optical paths was obtained.

The crosscorrelation curve of channel 2 (Barton-Coker) and channel 4 (Maben-Egypt) in Figure 28 indicates a definite correlation between these two paths which have no common station. Since the peak occurs at the origin, there is reason to believe that there are some common effects on both paths simultaneously from some unknown causes. Examining the crosscorrelation curves of $\phi_{23}(\tau)$ and $\phi_{34}(\tau)$ in Figures 27 and 29, the general

TABLE 5

Data of crosscorrelation curve between paths of Barton-Coker and Bexar-Egypt. (Time of this table should be multiplied by 8 for actual time).

Time Shift τ (seconds)	Overlapped Period T (seconds)	Reading of Digital Voltmeter V (volts)	Crosscorrelation Value $\phi_{23}(\tau)$ (volts)
-360	540	1.07	-0.0198
-330	570	1.44	-0.0253
-320	580	1.71	-0.0294
-310	590	1.82	-0.0308
-300	600	1.69	-0.0281
-290	610	1.56	-0.0256
-280	620	1.53	-0.0248
-270	630	1.74	-0.0276
-260	640	1.55	-0.0242
-250	650	1.45	-0.0223
-240	660	1.27	-0.0192
-210	690	0.52	-0.0075
-180	720	0.15	-0.0021
-150	750	-0.07	0.0009
-120	780	-1.02	0.0131
- 90	810	-1.58	0.0195
- 60	840	-2.23	0.0265
- 30	870	-2.45	0.0282
- 5	895	-2.40	0.0268
- 0	900	-1.96	0.0218
5	895	-2.42	0.0271
30	870	-2.82	0.0324
60	840	-2.28	0.0271
80	820	-1.98	0.0241
85	815	-1.95	0.0239
90	810	-1.88	0.0232
95	805	-1.80	0.0224
100	800	-1.78	0.0223
110	790	-1.83	0.0232
120	780	-2.43	0.0311
130	770	-2.15	0.0280
140	760	-2.13	0.0280
150	750	-1.72	0.0230
160	740	-1.75	0.0236
180	720	-1.95	0.0271
190	710	-1.29	0.0182
200	700	-1.21	0.0173
205	695	-1.26	0.0181
210	690	-1.22	0.0177
220	680	-1.20	0.0176
230	670	-1.52	0.0227
240	660	-1.50	0.0227

Table 5. (Continued)

Time Shift τ (seconds)	Overlapped Period T (seconds)	Reading of Digital Voltmeter V (volts)	Crosscorrelation Value $\phi_{23}(\tau)$ (volts)
270	630	-1.48	0.0219
300	600	-0.60	0.0100
330	570	-0.04	0.0007
360	540	0.88	-0.0163
390	510	1.59	-0.0312

TABLE 6

Data of crosscorrelation curve between paths of Barton-Coker and Maben-Egypt. (Time of this table should be multiplied by 8 for actual time).

Time Shift τ (seconds)	Overlapped Period T (seconds)	Reading of Digital Voltmeter V (volts)	Crosscorrelation Value $\phi_{24}(\tau)$ (volts)
-360	540	3.73	-0.0691
-330	570	2.71	-0.0475
-320	580	2.55	-0.0440
-310	590	2.14	-0.0360
-300	600	2.13	-0.0355
-270	630	2.18	-0.0346
-240	660	1.49	-0.0226
-210	690	-1.20	0.0174
-180	720	-4.60	0.0640
-150	750	-5.85	0.0780
-120	780	-8.71	0.1220
- 90	810	-10.34	0.1280
- 60	840	-11.99	0.1430
- 50	850	-13.41	0.1577
- 40	860	-13.62	0.1580
- 35	865	-12.39	0.1430
- 30	870	-13.40	0.1540
- 25	875	-13.49	0.1560
- 0	900	-14.82	0.1650
30	870	-12.49	0.1436
60	840	-11.40	0.1360
90	810	-10.84	0.1320
120	780	-9.87	0.1265
150	750	-8.20	0.1090
180	720	-7.64	0.1060
210	690	-5.89	0.0854
220	680	-5.11	0.0751
230	670	-4.60	0.0687
240	660	-4.17	0.0632
270	630	-3.28	0.0521
300	600	-0.93	0.0155
330	570	0.50	-0.0088
360	540	3.07	-0.0569
390	510	3.81	-0.0747

TABLE 7

Data of Crosscorrelation curve between paths of Bexar-Egypt and Maben-Egypt. (Time of this table should be multiplied by 8 for actual time).

Time Shift τ (seconds)	Overlapped Period T (seconds)	Reading of Digital Voltmeter V (volts)	Crosscorrelation Value $\phi_{34}(\tau)$ (volts)
-540	360	0.10	-0.0028
-510	390	-0.17	0.0044
-480	420	-0.14	0.0033
-450	450	-0.35	0.0078
-420	480	-1.51	0.0296
-390	510	-1.53	0.0300
-360	540	-1.77	0.0328
-340	560	-2.44	0.0436
-330	570	-2.96	0.0519
-320	580	-2.74	0.0472
-300	600	-2.47	0.0412
-270	630	-1.70	0.0270
-250	650	-1.92	0.0295
-240	660	-1.91	0.0289
-230	670	-1.92	0.0278
-210	690	-1.50	0.0220
-180	720	-1.67	0.0232
-150	750	-1.55	0.0207
-120	780	-2.30	0.0295
-100	800	-2.93	0.0366
- 90	810	-3.02	0.0373
- 80	820	-2.87	0.0350
- 60	840	-2.38	0.0283
- 30	870	-3.30	0.0379
- 10	890	-3.77	0.0424
0	900	-4.05	0.0450
10	890	-3.67	0.0412
30	870	-3.57	0.0410
60	840	-2.78	0.0331
90	810	-2.25	0.0278
120	780	-1.38	0.0177
150	750	-0.61	0.0081
180	720	0.15	-0.0021
210	690	1.19	-0.0172
240	660	1.48	-0.0224
270	630	2.01	-0.0319
300	600	1.68	-0.0280
310	590	1.68	-0.0285
330	570	2.07	-0.0363
360	540	1.95	-0.0361

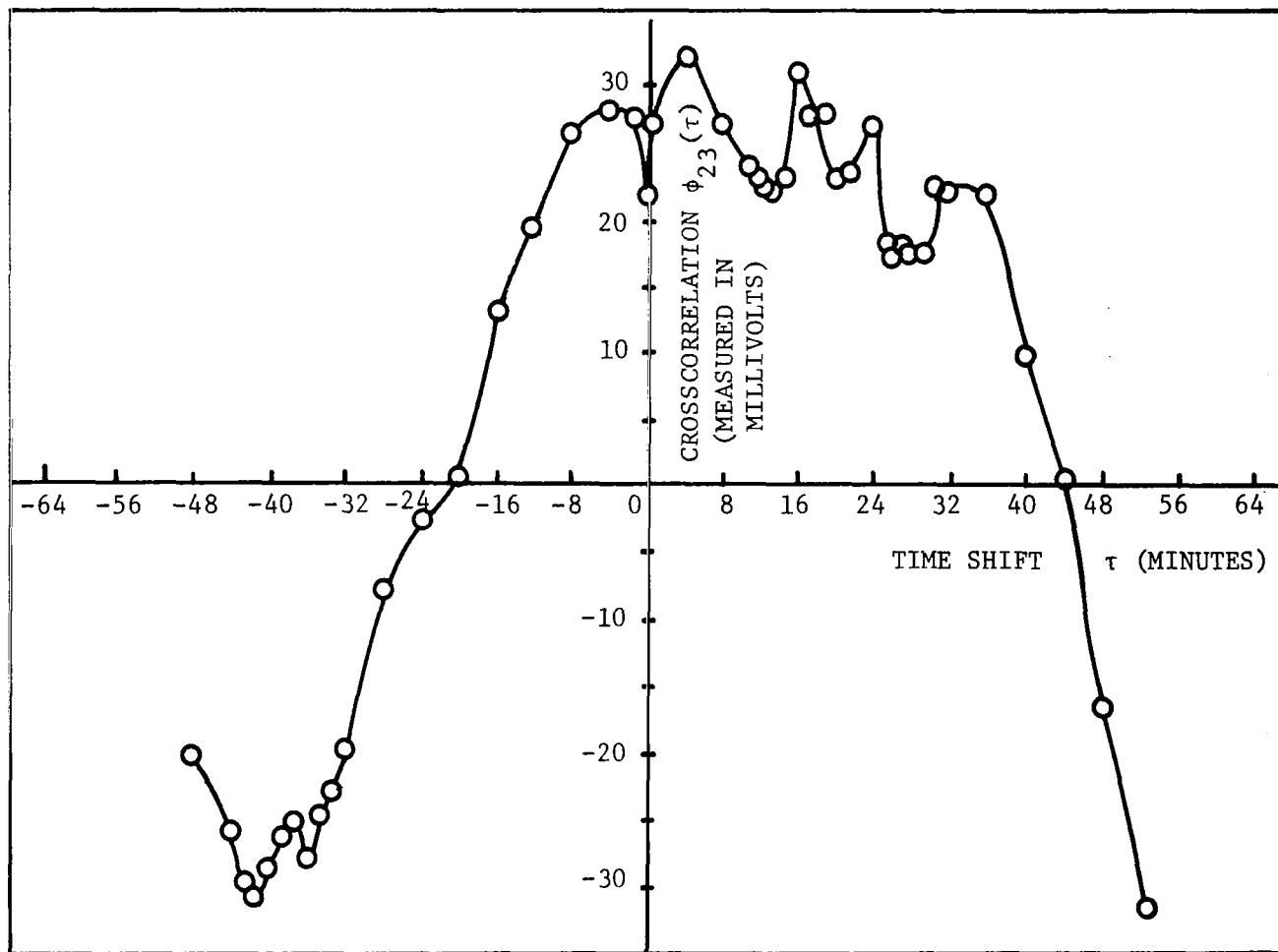


Figure 27. Cross correlation curve of channel 2 (Barton-Coker) and channel 3 (Bexar-Egypt) with channel 3 delayed.

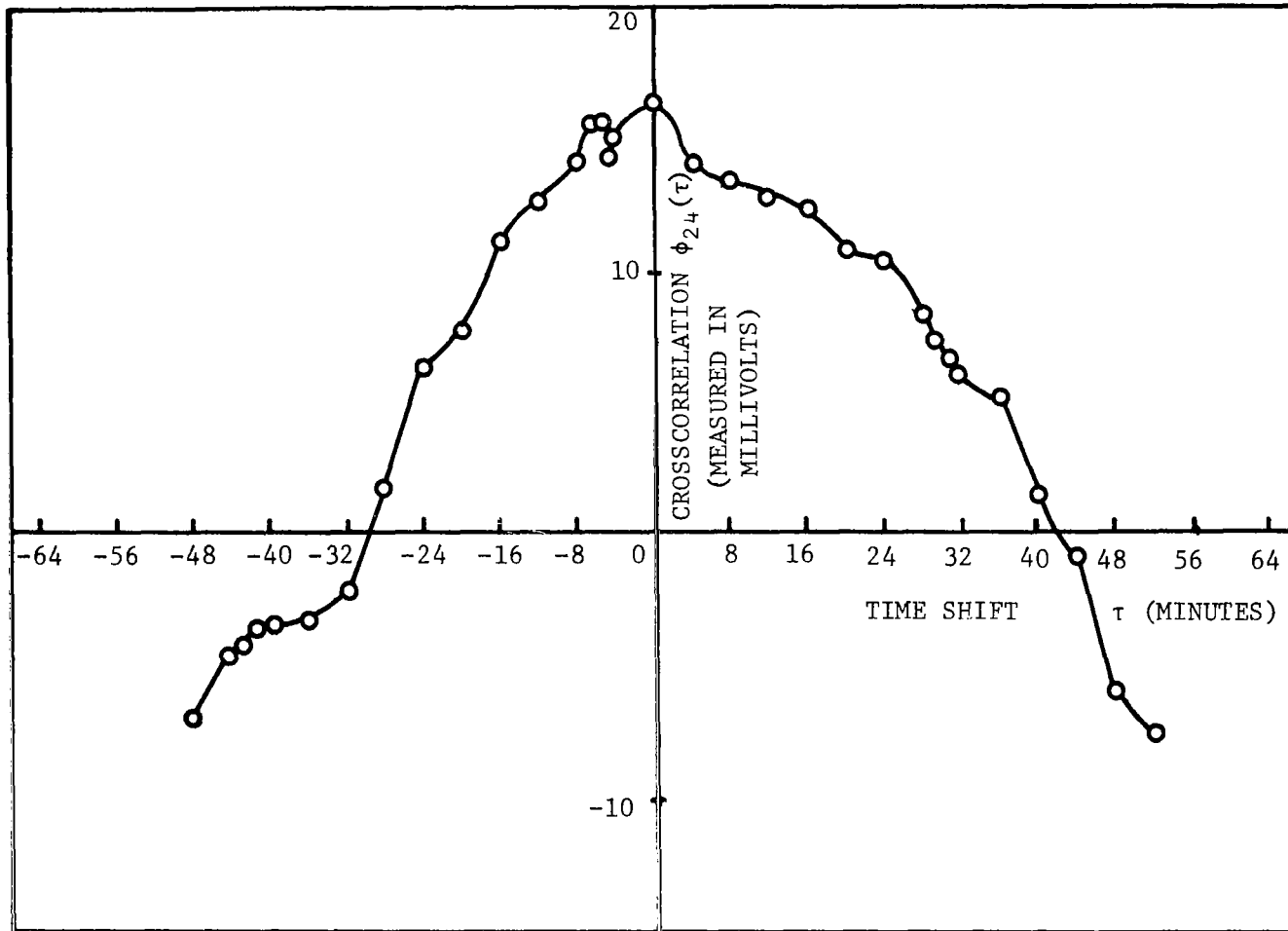


Figure 28. Crosscorrelation curve of channel 2 (Barton-Coker) and channel 4 (Maben-Egypt) with channel 4 delayed.

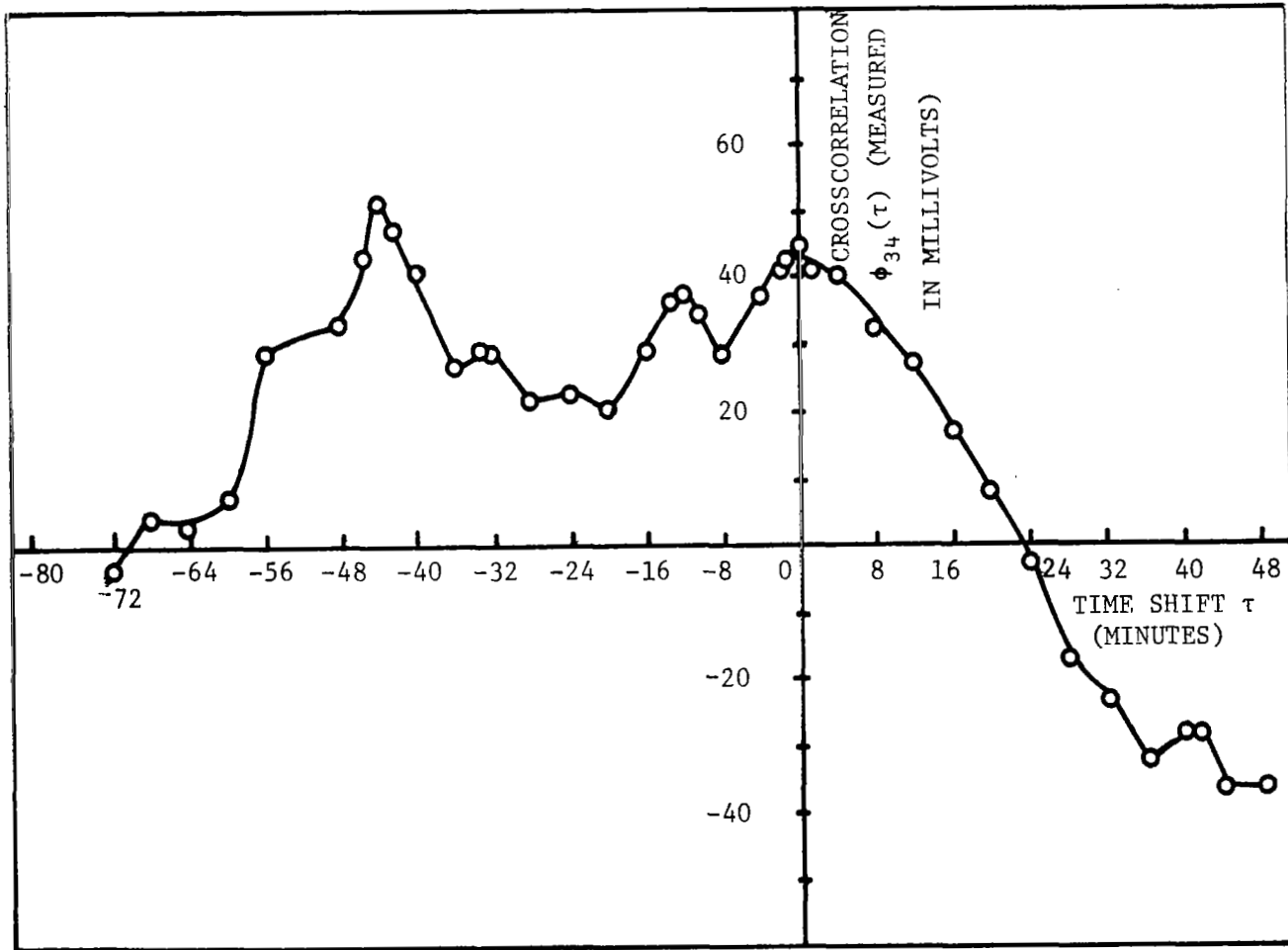


Figure 29. Crosscorrelation curve of channel 3 (Bexar-Egypt) and channel 4 (Maben-Egypt) with channel 4 delayed.

shape or envelope of the curves looks almost alike; however, there are some ripples in the envelopes. The peaks of the $\phi_{23}(\tau)$ appear mostly at positive τ (around 2 minutes), but that of the $\phi_{34}(\tau)$ appears mostly at negative τ . This indicates that there is some correlation between fading over these paths, but that fading occurs along one path at a later time than along the other.

This type information is interesting to communications system designers. The currently accepted theory of microwave propagation over optical paths is that the variations in signal strength are only due to changes in local meteorological conditions along the propagation path. If there is any major degree of correlation between the fluctuations of the signals due to fading activity, as indicated by the present study, the generally held theory should be reconsidered. The performance of the crosscorrelation is based on a statistical basis. If there is an attempt to make a definite and effective conclusion on the assumed theory, more sets of data must be processed. This study just represents the first step of the extensive investigation in this area and gives some introduction and information about performing the crosscorrelation functions between two random continuous signals by the analog computer. A further study is recommended so that more valuable information may be obtained.

PART III

HIGH ELEVATION ANGLE STUDY

CHAPTER XII

RESULTS AND DISCUSSION

In view of the increasing usage and importance of communicating at microwave frequencies between stations located on earth, and those located in satellites, as well as manned space vehicles, it is of the utmost importance to determine what fade margins will be required in order to obtain a given propagation reliability over these paths. The microwave paths will normally be operating at elevation angles ranging from 0° to 90° .

The elevation angle of a microwave path at a receiving or transmitting station is defined as the angle between the path and an imaginary horizontal plane, tangent to the earth at the station under consideration.

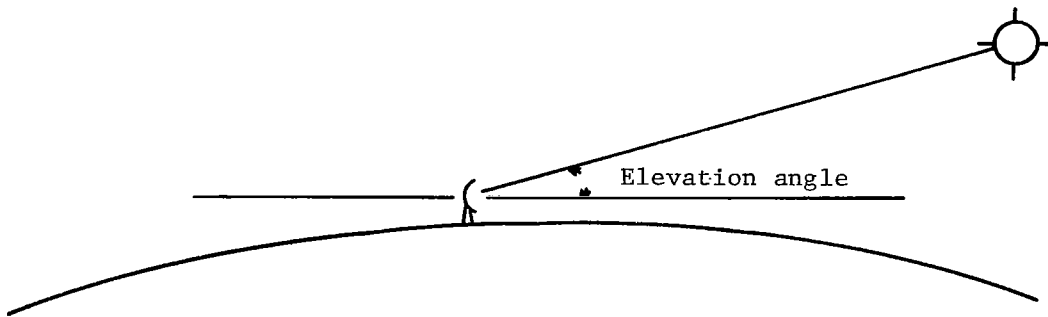


Figure 30. Elevation angle of a microwave path.

In the case of an earth-to-space path, this would have meaning only in the case of the earth station, in which case the minimum useable elevation angle would be zero degrees. There would be exceptions to this, obviously, if the station were surrounded by higher terrain, mountains for example, in which case the minimum useable elevation angle would be greater than zero degrees by whatever amount it took to clear the surrounding obstructions. Another possible exception would be encountered if the earth station were considerably above the surrounding terrain, in which case the elevation angle might possibly lie somewhat below the fictitious plane tangent to the earth's surface at the station's location. In this case, the elevation angle is said to be negative. For most locations on earth, however, the minimum useable elevation angle will be for all practical purposes, zero degrees.

Close examination of the elevation angles used for line-of-sight microwave paths between two stations on earth will show that for all practical purposes, most paths can be assumed to be operating at zero angle. While the actual elevation angles encountered in existing point-to-point systems on earth may be either positive or negative, they are usually so small in magnitude that they may be considered to be zero. Exceptions to this latter statement do exist, however, in the rare case of a short path connecting two stations which have a very marked difference in elevations. A path meeting these conditions was selected and instrumented as a portion of this research. The path studied was a 3.5 mile long path between a station atop a mountain near Siloam, Kentucky,

and a station located in the Ohio River Valley near Wheelersburg, Ohio. This path is designated as the Siloam to Wheelersburg path, with the receiver being located at the Wheelersburg station. The elevation angle at Wheelersburg was approximately 1.5° (the elevation angle at Siloam was approximately -1.5°).

This "high elevation angle" path was chosen to examine what effect having an elevation angle greater than zero would have on the propagation over the path. During the literature search conducted at the beginning of this research, several statements (which were in reality postulates) were encountered saying that paths with elevation angles greater than 1° will not experience fading due to tropospheric changes.

Experience obtained by both the Communications Satellite Corporation* and Bell Telephone Laboratories** indicate that little if any fading is obtained on microwave paths having elevation angles of 20° or greater. Results obtained on zero degree elevation angle paths between stations on earth indicate considerable fading activity which must be taken into account and allowed for by having sufficient fade margin to obtain the required propagation reliability, if a useable microwave communications system is to be had (e.g., see Part I of this report). Since the fading activity, and consequently the propagation reliability, of a path changes markedly between zero degrees elevation angle, and 20° , it should be apparent that for communication between

*Telephone Conversation with Mr. Sidney Metzger, Communications Satellite Corporation, Washington, D. C.

**Telephone Conversation with Dr. P. T. Hutchison, Bell Telephone Laboratories, Holmdel, N. J.

an earth and a space station, the propagation reliability of a given length path in any particular location will be a function of the elevation angle of the path, with the propagation reliability obtained from a given fade margin decreasing as the elevation angle decreases. If the statements encountered in the literature search were correct, and fading was not obtained at elevation angles above 1° , then the problem of determining how propagation reliability varied with elevation angle would be one of academic interest only, having little if any practical value. This would be true since most point-to-point paths on earth have elevation angles which are for all practical purposes, equal to zero degrees. Furthermore, the elevation angles of paths between earth stations and space stations are normally limited to a minimum value of approximately 4° or so, due to the increase in the receiving system temperature at lower elevation angles caused by noise radiation from the earth (which has a high temperature compared with that of the sky) being picked up by the antenna. Consequently, if fading activity ceased at elevation angles greater than 1° , there would be no need to concern one's self with propagation reliability on paths between earth and space stations since no fading would be obtained on any operational links which might be used. With this in mind, a path having as large an elevation angle as possible, was sought for on Texas Eastern Transmission Corporation's 2GHz microwave system. The Siloam to Wheelersburg path which was selected had a 1.5° elevation angle, which was one and a half times the 1° value above which it had been postulated that fading would cease. It should be noted with care, however, that while this path had an elevation angle approaching the minimum values which may be used on earth

to space microwave links, that due to its extremely short length (only 3.5 miles) the depths of fading encountered on this path should be appreciably less than that which would be incurred on an earth to space path having the same elevation angle. The latter type path, due to its much longer length in the earth's atmosphere, would most probably require a much higher fade margin to obtain the same propagation reliability as that obtainable on the 3.5 mile long Siloam to Wheelersburg path for any given fade margin.

Examination of Figure 31, reveals that a 6 dB fade margin is required to obtain a propagation reliability of 90% (which would mean that 10% of the time, the system would be unuseable). While fades as deep as 15 db were obtained during the 10 month period of time the propagation over this path was studied, a 9 db fade margin would be sufficient to give a propagation reliability of 99.99%. Once again though, it should be pointed out that examination of the results obtained in the other nine microwave paths studied in this research revealed that the longer the length of the path (in the earth's atmosphere, of course) the larger the fade margin must be to obtain a given value of propagation reliability. Consequently, a 1.5° elevation angle path between an earth station located at Wheelersburg, Ohio, and a space station above, would require a fade margin considerably greater than 9 db in order to obtain the 99.99% propagation reliability that 9 db of fade margin gave on the 3.5 mile long 1.5° elevation angle Siloam to Wheelersburg path.

In conclusion, it should be pointed out that the results obtained over this path reveal that fading is still present at an elevation

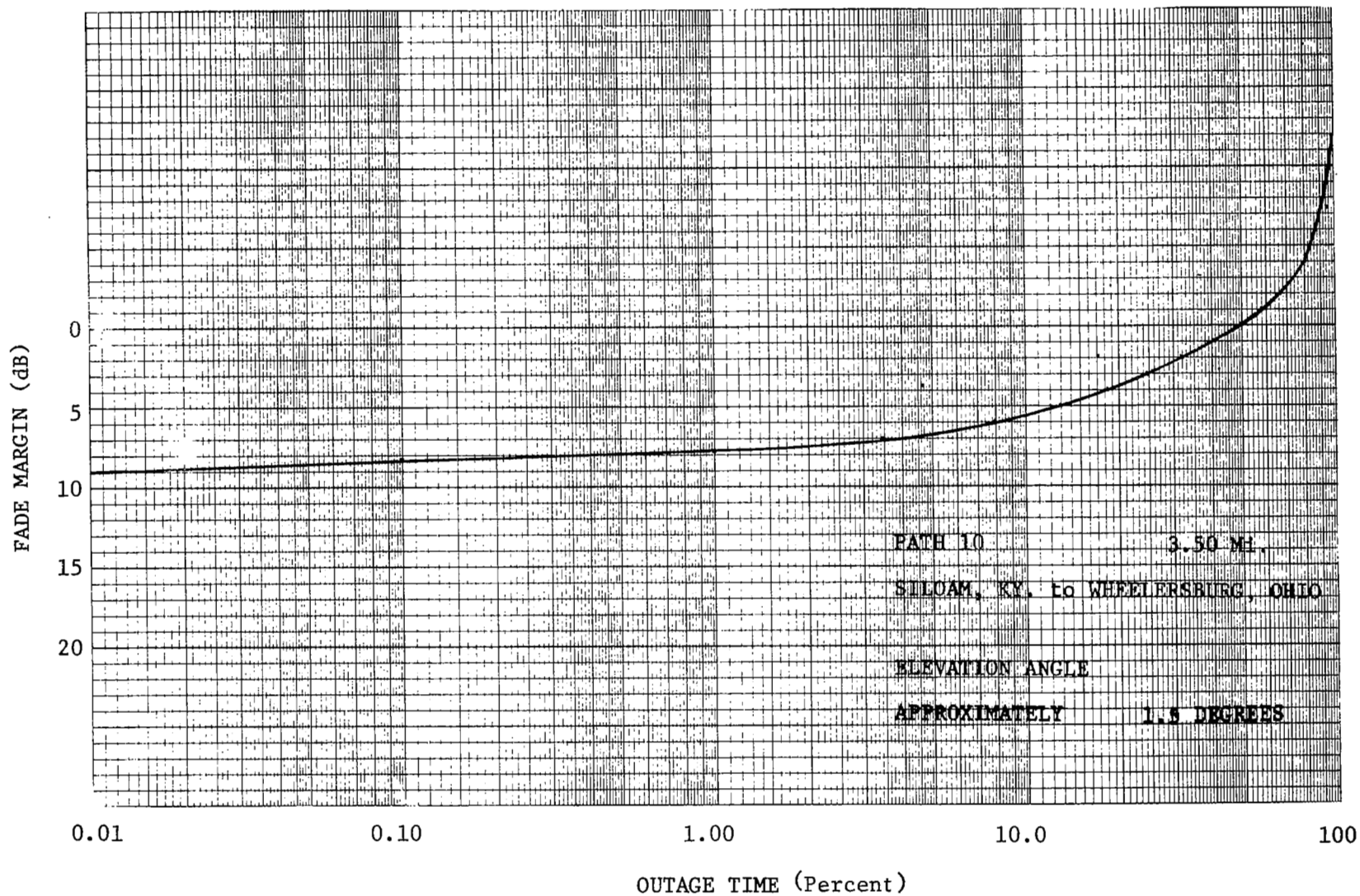


FIGURE 31. STATISTICAL DISTRIBUTION FOR HIGH ANGLE PATH

angle of 1.5° and would definitely have to be considered in the design of any reliable communications system having an elevation angle of this order of magnitude. Consequently, no assurance whatsoever has been obtained as to what fade margins should be allowed to obtain a given propagation reliability for earth to space paths operating with elevation angles lying between 1.5° and 20° . Hopefully, fading will cease for elevation angles two or three times greater than that of the Siloam to Wheelersburg path, but since systems cannot be designed on hope, research should be accomplished to determine exactly how propagation reliability varies as a function of elevation angle so that reliable communication systems can be designed for use at elevation angles of less than 20° .

APPENDIX I

COMPUTER PROGRAMS

Slide rule accuracy is not sufficient when using the equations of Chapter III to calculate fade margin. For this reason a program was written to compute the fade margin on the IBM 1620 digital computer. Figure 32 shows this program.

To meet Forgo program restrictions renaming the variables was necessary as follows:

Latitude	=	VAT
Longitude	=	VON
Path Length	=	PL
Fade Margin	=	FM
Propagation Reliability	=	PR
L_1	=	VONPO
L_2	=	VONP1
K_0	=	VKO
K_1	=	VK1
G	=	VKOP
H	=	VK1P
L_1	=	$G (\text{Long})^2 + B (\text{Long}) + A$
L_2	=	$R (\text{Long})^2 + H (\text{Long}) + G$
G	=	$F (\text{PL})^2 + E (\text{PL}) + D$
H	=	$U (\text{PL})^2 + T (\text{PL}) + S$

```

C   C   INGELS           FADE MARGIN
      READ, A,B,C,D,E,F,G,H,R,S,T,U
8    READ, VAT, VON, PL
      VKOP=F*(PL**2)+E*(PL)+D
      VONPO=C*(VON**2)+B*(VON)+A
      VONPO=VONPO/57.2958
      TO=SINF(VONPO)/COSF(VONPO)
      VAT=VAT/57.2958
      VKO=VKOP*COSF(VAT)*TO
      VK1P=U*(PL**2)+T*(PL)+S
      VONP1=R*(VON**2)+H*(VON)+G
      VONP1=VONP1/57.2958
      T1=SINF(VONP1)/COSF*VONP1)
      VK1=VK1P*COSF(VAT)*T1
      PR=0.01
5    FM=VKO+0.43429*VK1*LOGF(1.+PR*1000.)
      PUNCH, PR, FM, VKO, VK1,
      IF(PR-0.01)          4,3,4
3    PR=0.05
      GO TO 5
4    IF(PR-0.05)          7,6,7
6    PR=0.1
      GO TO 5
7    GO TO 8
      END

```

FIGURE 32. PROGRAM FOR CALCULATION
OF FADE MARGIN

The Forgo format is a floating point type which means that the input data may be typed on a single card with a minimum of five spaces between variables.

For this research the values of A, B, C, D, E, F, G, H, R, S, T, and U were determined from the least squares program, see Figure 33, and are:

A = -1147.4	B = 26.205	C = - .14396
D = 32.097	E = - 4.3311	F = .051425
G = - 847.76	H = 19.411	R = - .10551
S = - 6.6078	T = .96409	U = - .011791

```

C   C   INGELS   LEAST-SQUARES
      DIMENSION A(20,20),X(30),U(300),V(300),S(300),SK(300)
111  READ, M,(U(I),V(I),I=1,M),N
      J=N+1
      DO 10 I=1,K
      S(I)=0.
10   SK(I)=0.
      DO 12 I=1,K
      DO 12 NN=1,M
      IA=I+1
12   S(I)=S(I)+U(NN)**IA
      DO 13 I=1,K
      DO 13 NN=1,M
      IB=I-1
13   SK(I)=SK(I)+V(NN)*U(NN)**IB
      DO 1 NN=1,K
      JA=NN-1
      DO 1 I=1,K
1   A(I,NN)=S(I+JA)
      DO 17 I=1,K
17  A(I,J+1)=SK(I)
      N=N+1
      M=N+1
15  D=1.
      T=1.
      K=1
      KN=K+1
100 IF(A(K,K))6,2,6
     2 DO 3 J=KN,N
       II=J
       IF(A(J,K))4,95,4
95   K=K+1
       IF(N-K)98,98,100
98   D=0.
      GO TO 999

```

FIGURE 33. PROGRAM FOR FITTING
A CURVE WITH A POLYNOMIAL


```

7 A(K,J)=A(K,J)/T
  DO 7 J=1,M
6 T=A(K,K)
5 A(KKK,I)=A(KKK,I)+A(II,I)
  KKK=K
4 DO 5 I=1,M
  NN=K+1
  DO 8 IK=NN,N
  XXX=A(IK,K)
  DO 8 J=1,M
8 A(IK,J)=A(IK,J)-A(K,J)*XXX
  K=K+1
  IF(N-K) 200,200,100
200 CONTINUE
  D=D*A(N,N)
16 X(N)=A(N,M)/A(N,N)
  LLL=N-1
  DO 14 I=1,LLL
  SUMA=0.
  DO 14 J=1,I
  LL=N-1
  KK=N+1-J
  SUMA=SUMA+A(LL,KK)*X(KK)
14 X(LL)=(-SUMA+A(LL,M))/A(LL,LL)
  PUNCH,(X(I),I=1,N)
  GO TO 111
999 STOP
  END

```

FIGURE 33. (continued)

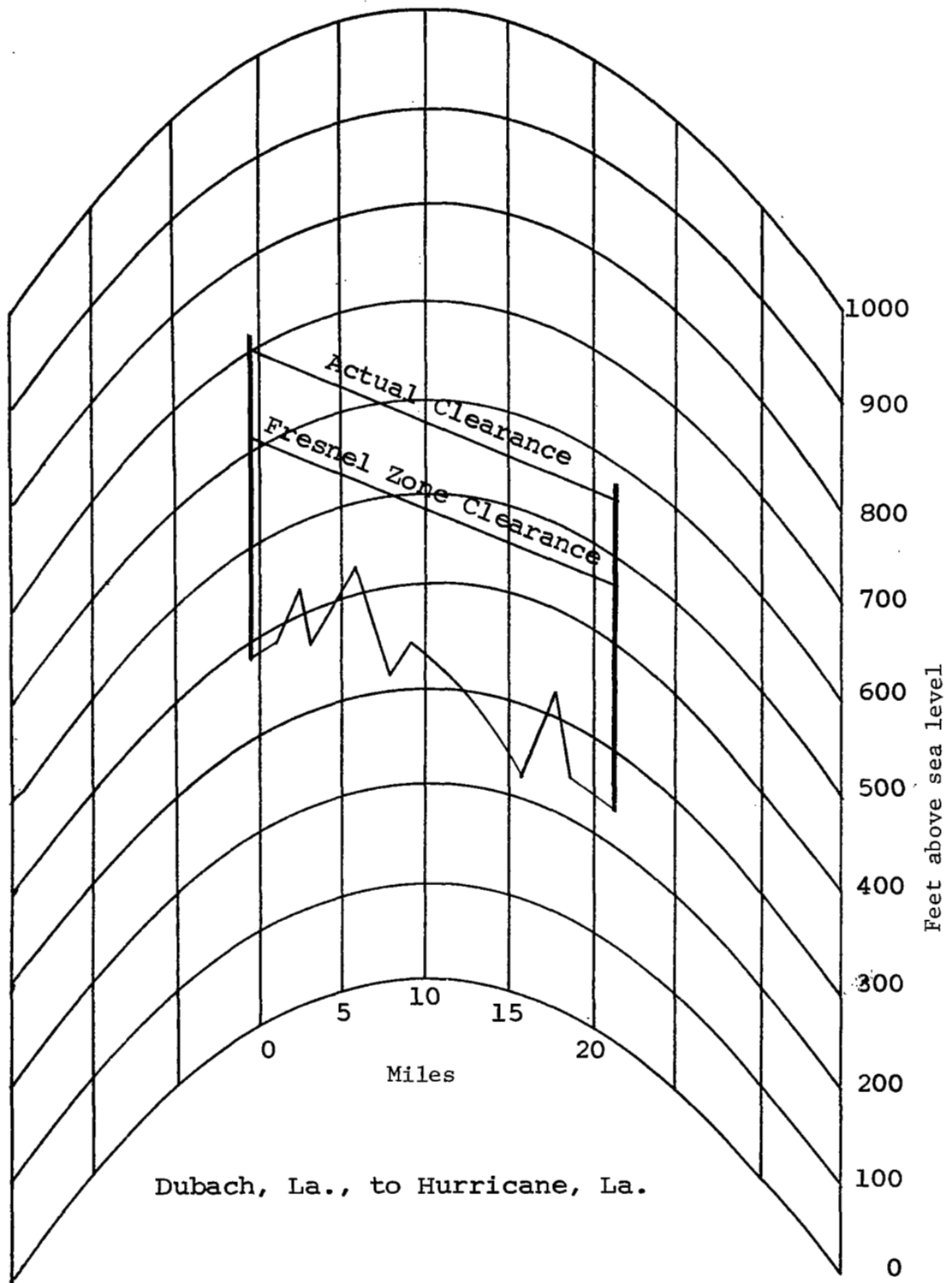
APPENDIX II

PATH PROFILES

A complete path profile of each path has been plotted by the Texas Eastern Transmission Corporation. These plots are included here. The plots are made on profile paper with the earth's horizon drawn with a radius of four-thirds normal earth radius. Thus the path of a ray from transmitter to receiver is drawn as a straight line on these plots for standard atmosphere conditions.

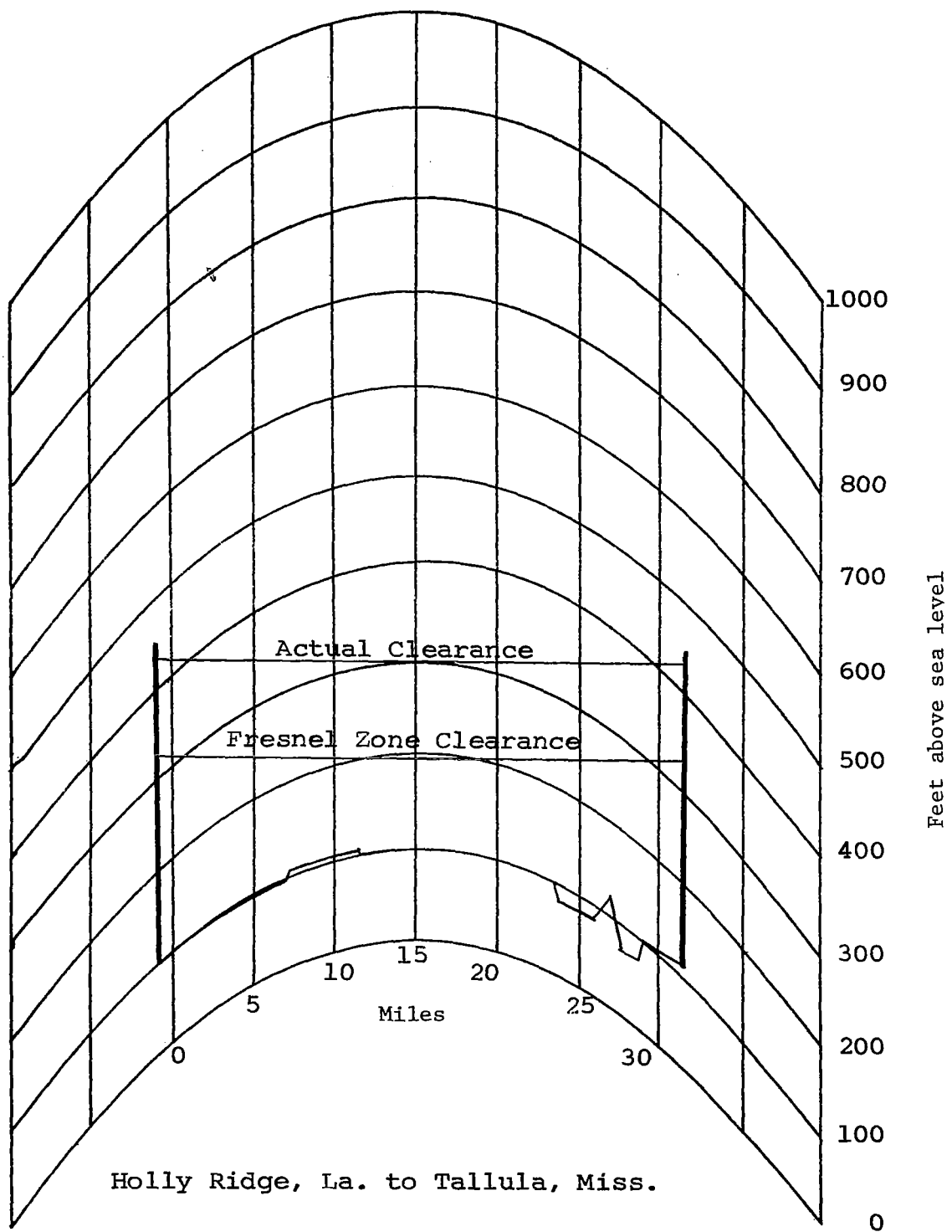
On each plot the first Fresnel zone clearance line is indicated as well as the path of a ray under standard atmosphere conditions.

Each path has sufficient clearance except the Maben to Egypt path which has only a twenty-foot deficiency and then only at one point. This insufficient clearance did not prove to be a difficulty.



Dubach, La., to Hurricane, La.

FIGURE 34. PATH PROFILE FOR PATH 1



Holly Ridge, La. to Tallula, Miss.

FIGURE 35. PATH PROFILE FOR PATH 2

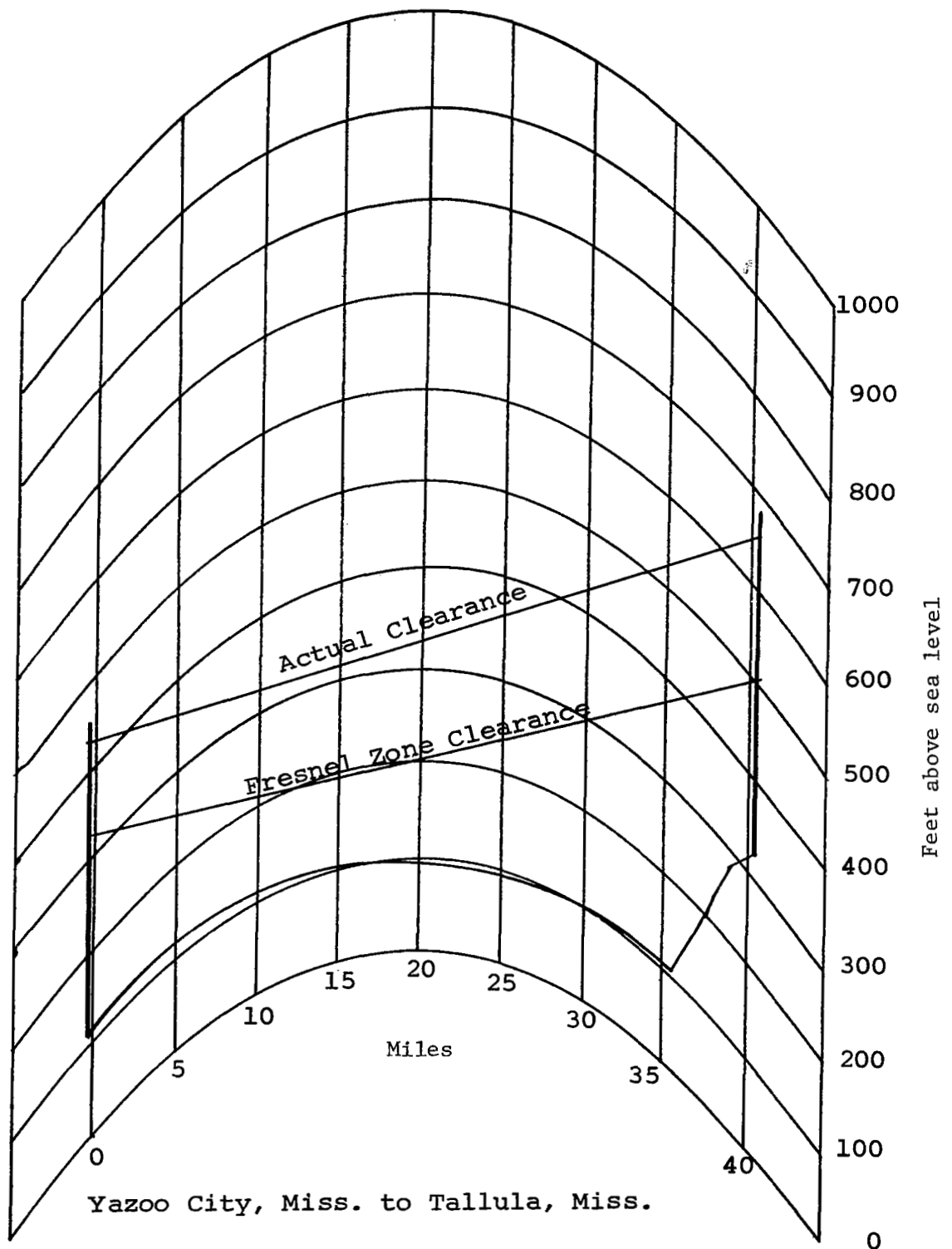


FIGURE 36. PATH PROFILE FOR PATH 3

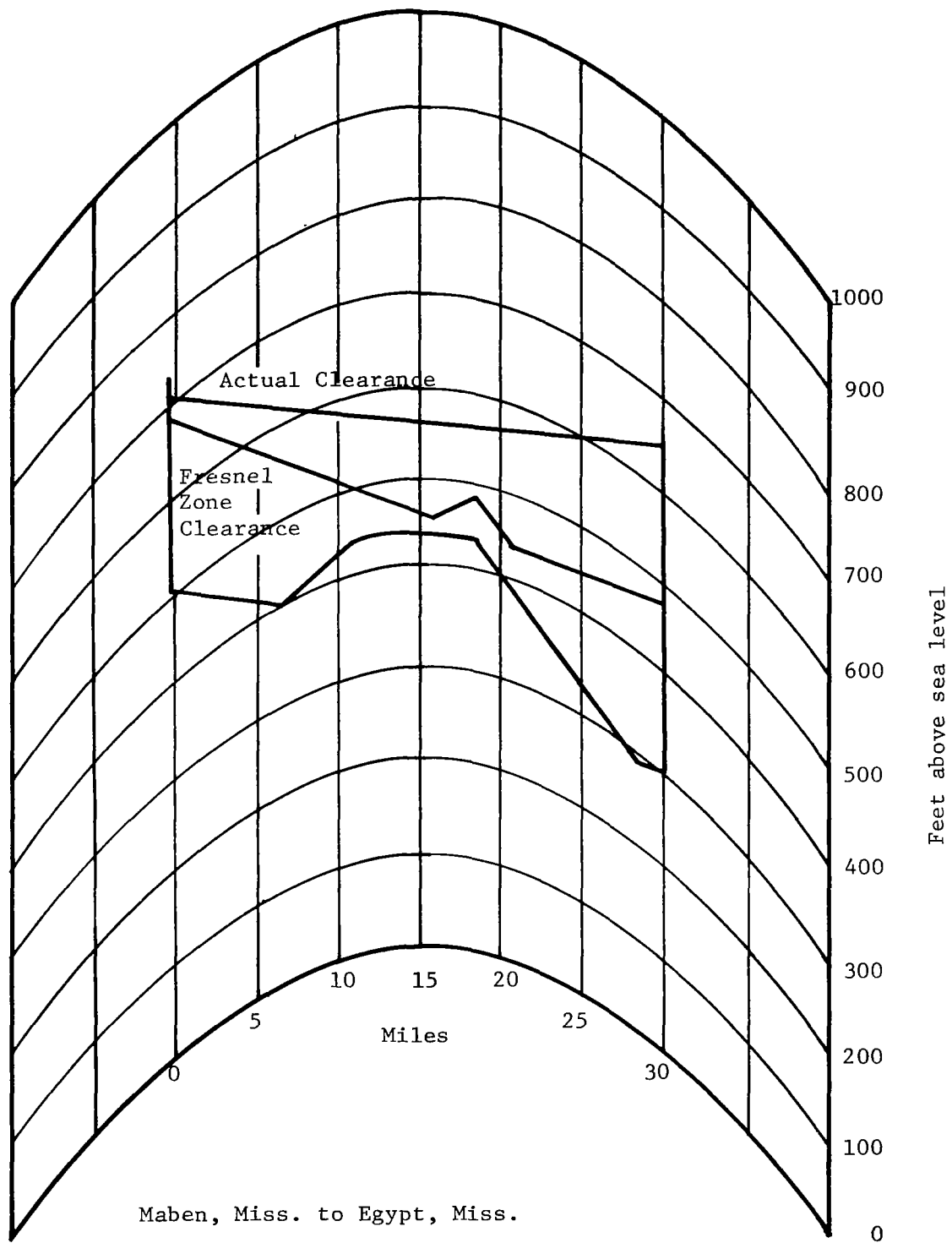
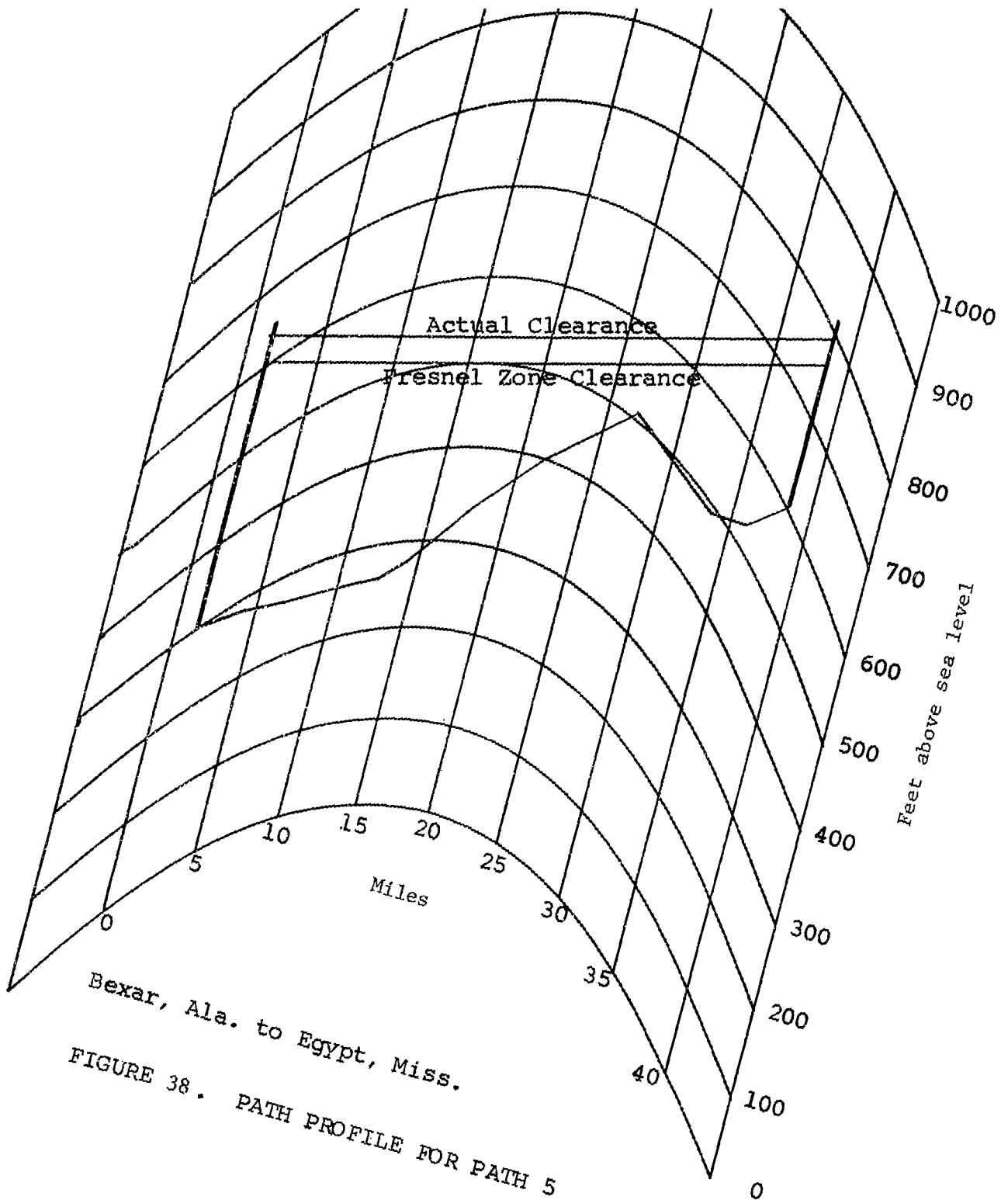
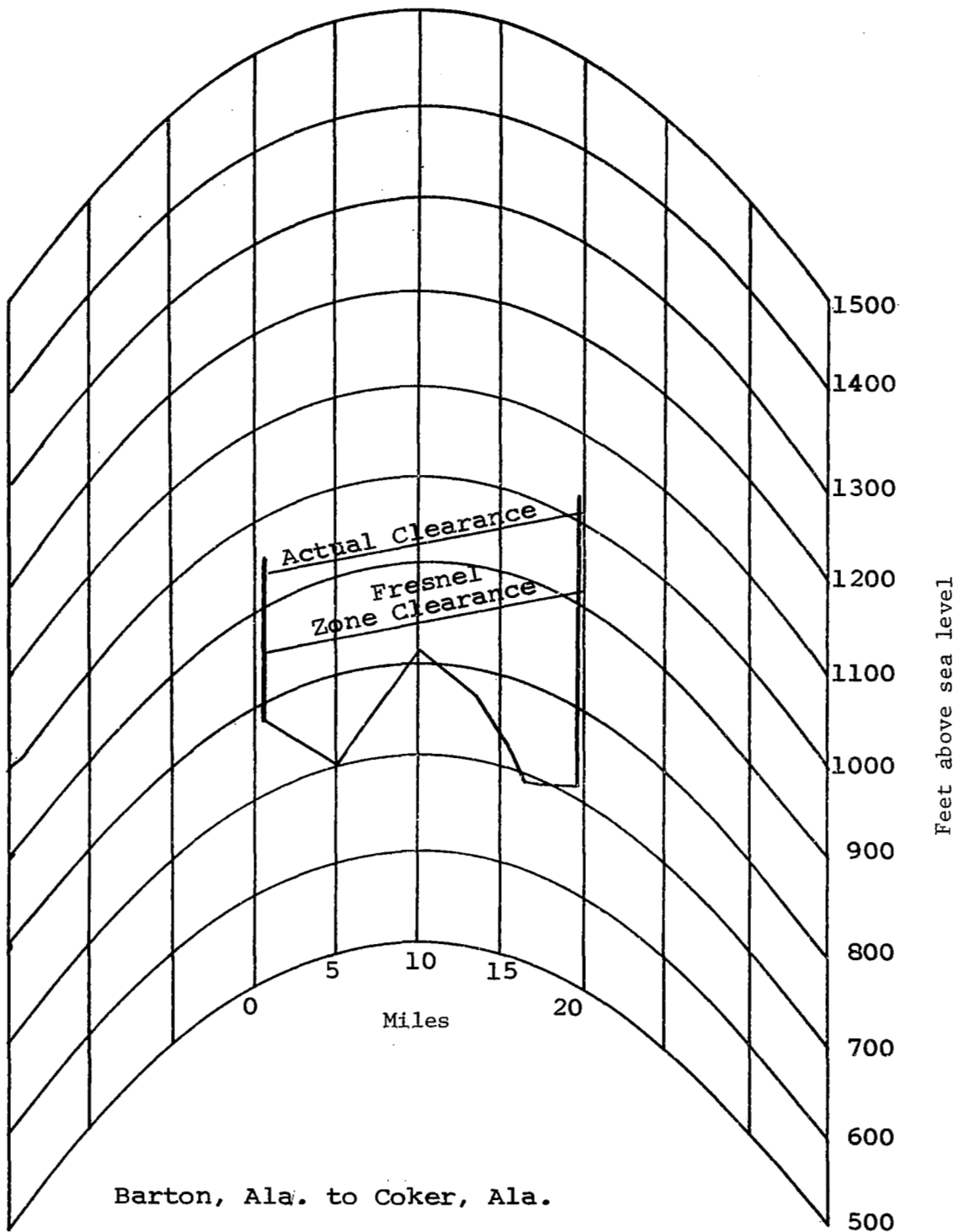


FIGURE 37. PATH PROFILE FOR PATH 4



Bexar, Ala. to Egypt, Miss.

FIGURE 38. PATH PROFILE FOR PATH 5



Barton, Ala. to Coker, Ala.

FIGURE 39 . PATH PROFILE FOR PATH 6

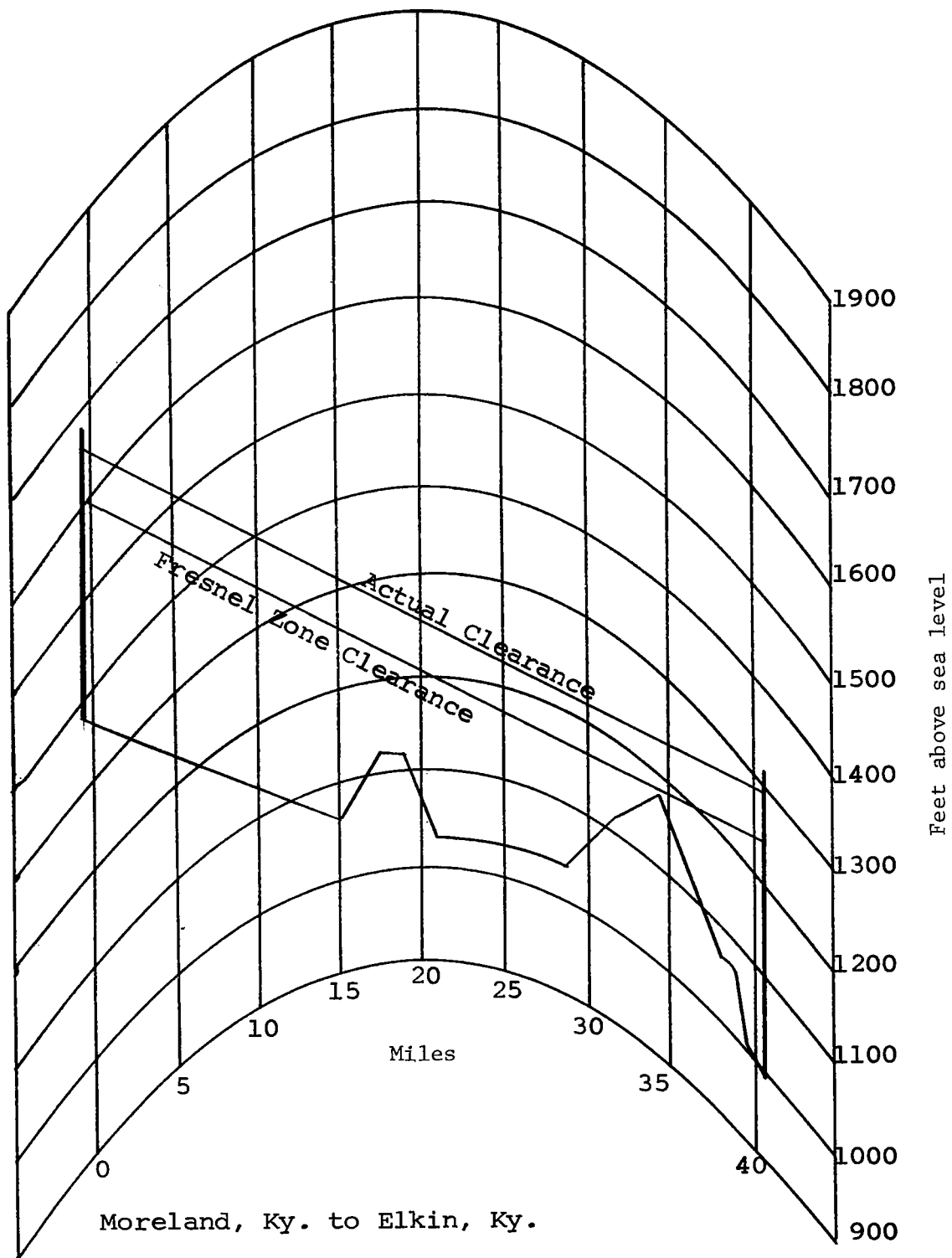
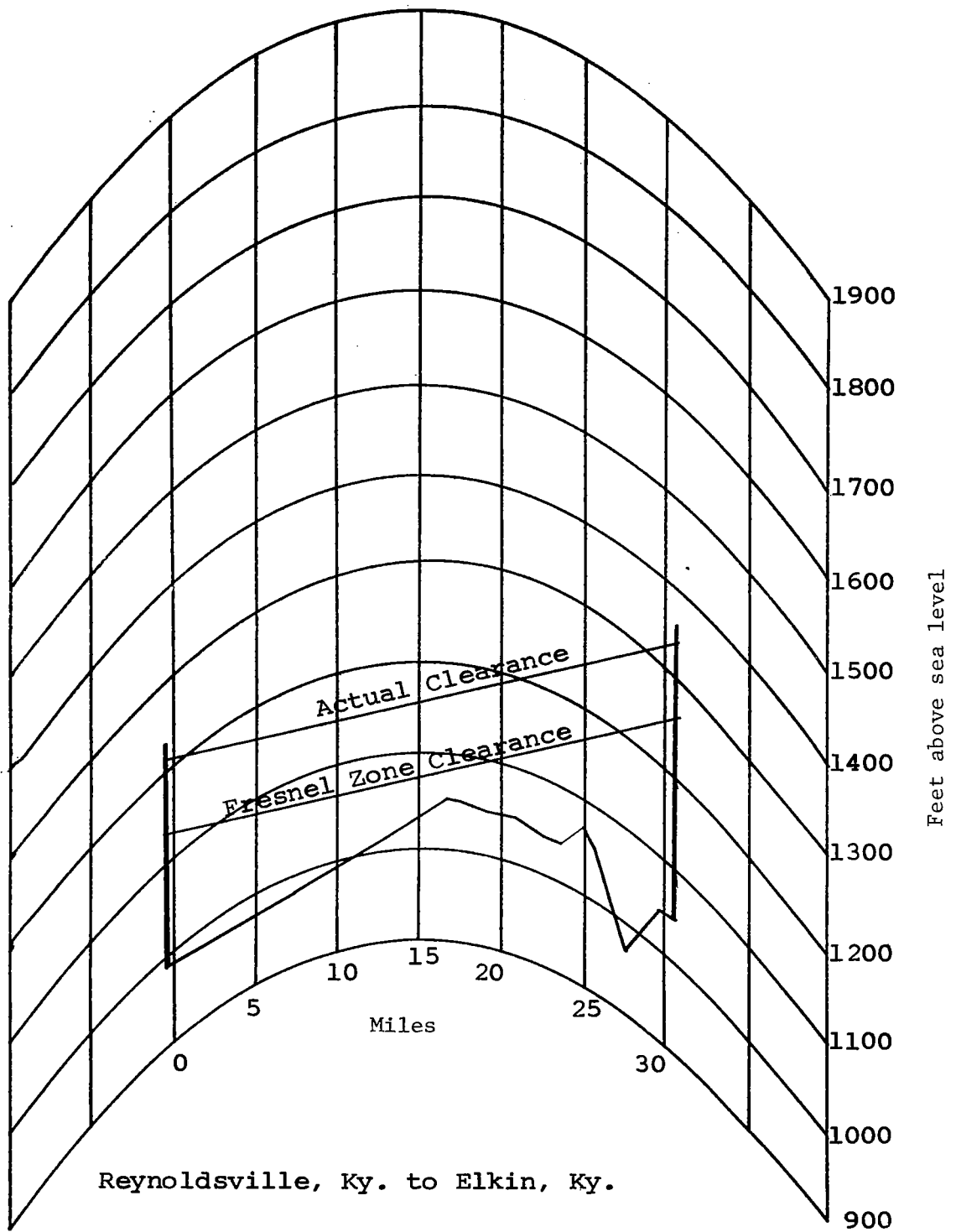
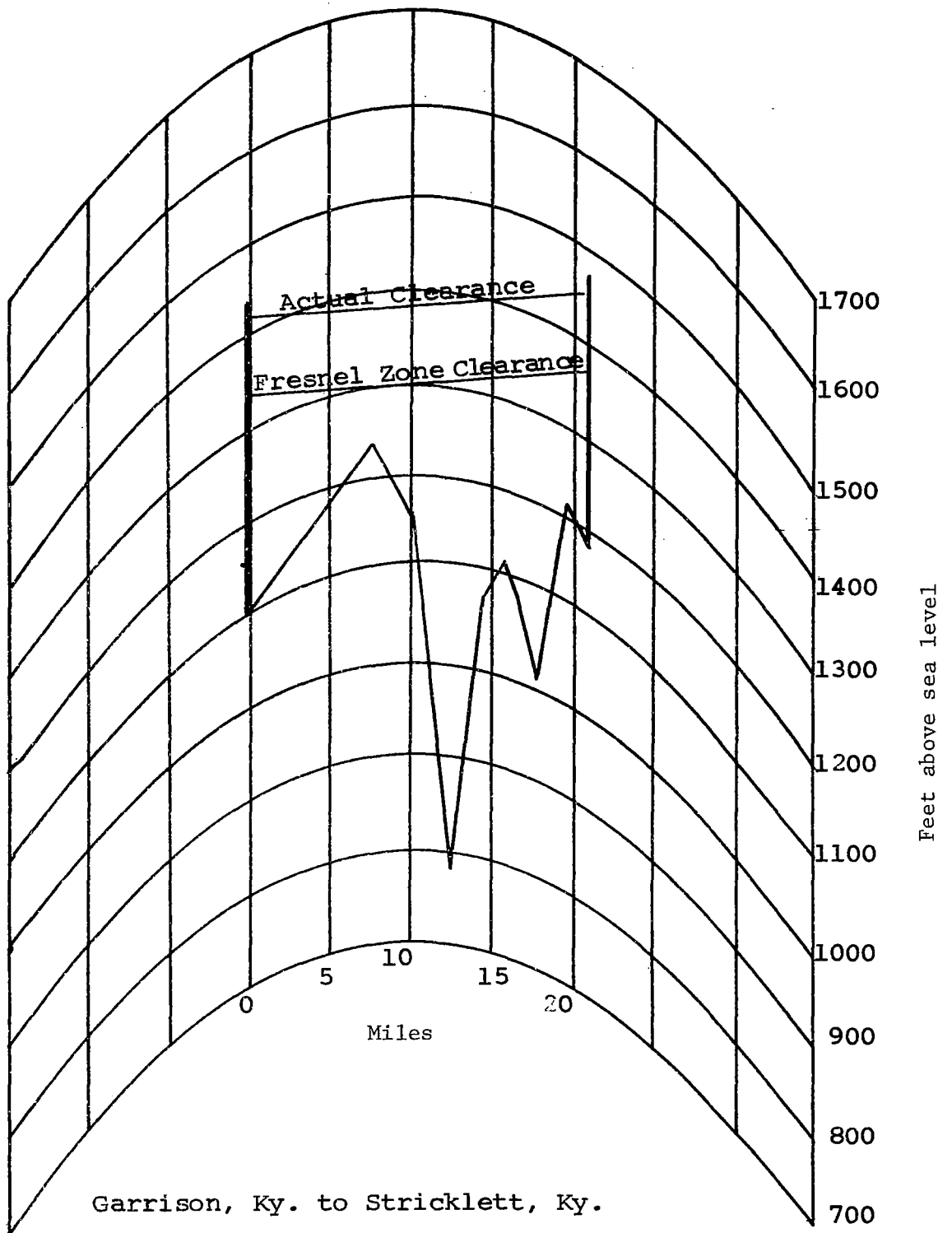


FIGURE 40. PATH PROFILE FOR PATH 7



Reynoldsville, Ky. to Elkin, Ky.

FIGURE 41. PATH PROFILE FOR PATH 8



Garrison, Ky. to Stricklett, Ky.

FIGURE 42. PATH PROFILE FOR PATH 9

APPENDIX III

DISCUSSION OF EQUIPMENT OPERATION

The AGC voltage of the receiver is recorded on a Moseley strip chart recorder (Model 680). As the input signal varies the AGC voltage varies nonlinearly, see Figure 43, causing the pen on the strip chart to vary in position. This variation in position of the pen is used to turn light sensor diodes (T.I. type H 38) on and off, thus providing an electrical indication when the input signal drops below certain preset levels. These preset levels are in 5 dB increments below the maximum input tolerable by the receiver. The large change in resistance of the light sensor diodes is used to turn an elapsed time meter on or off depending upon whether the received signal is above or below that level. A photograph showing the diode units mounted on the Moseley recorder is given in Figure 44.

Calibration of the recorder is accomplished by connecting a Hewlett Packard UHF signal generator (Model 616A) to the input of the receiver and adjusting the recorder sensitivity so that full scale deflection corresponds to a pre-selected input level. This input level is slightly lower than the maximum signal the receiver will tolerate without oscillating but higher than the median received signal level. This level is determined by the characteristics of the receiver at a given station, but is usually approximately -35 dBm.

After the recorder is properly adjusted for full-scale deflection with the pre-selected input level applied, one of the light sensor diodes is then adjusted so that a metal plate mounted on the Moseley

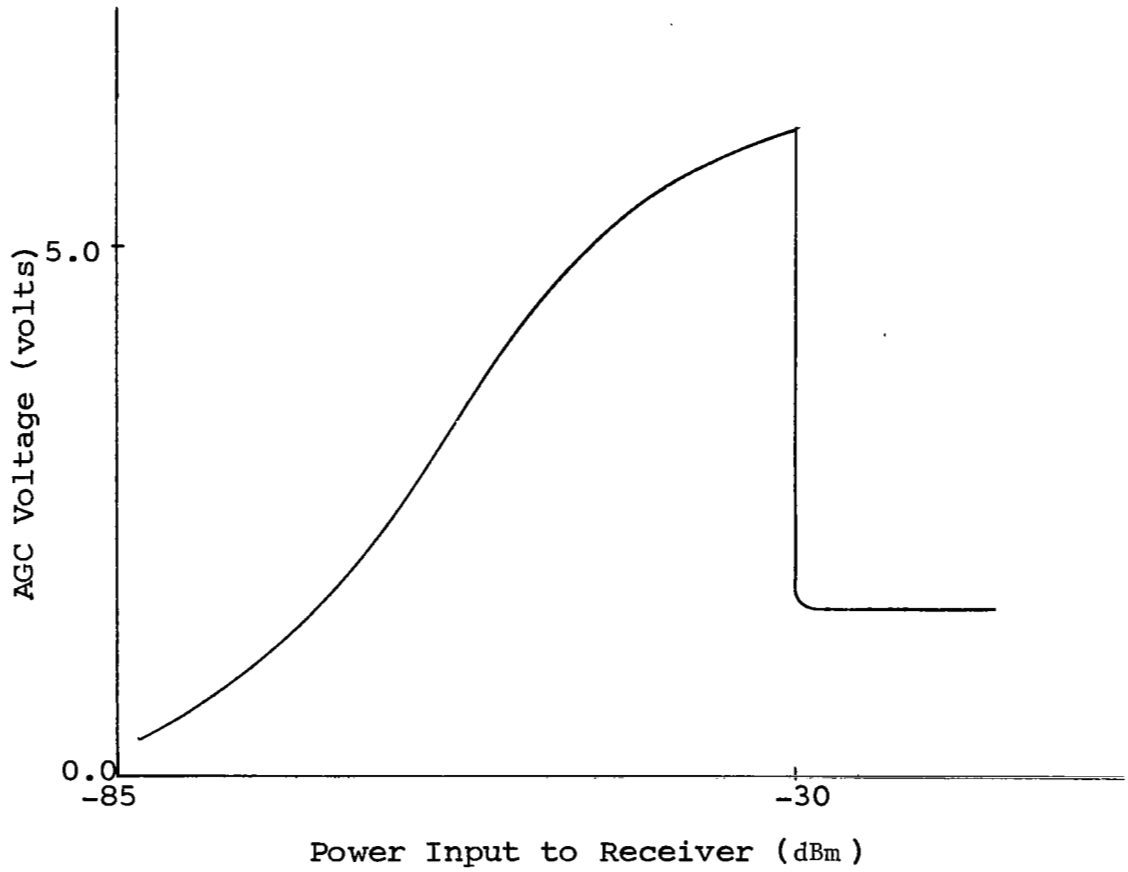


FIGURE 43. A GENERAL AGC VOLTAGE CHARACTERISTIC CURVE

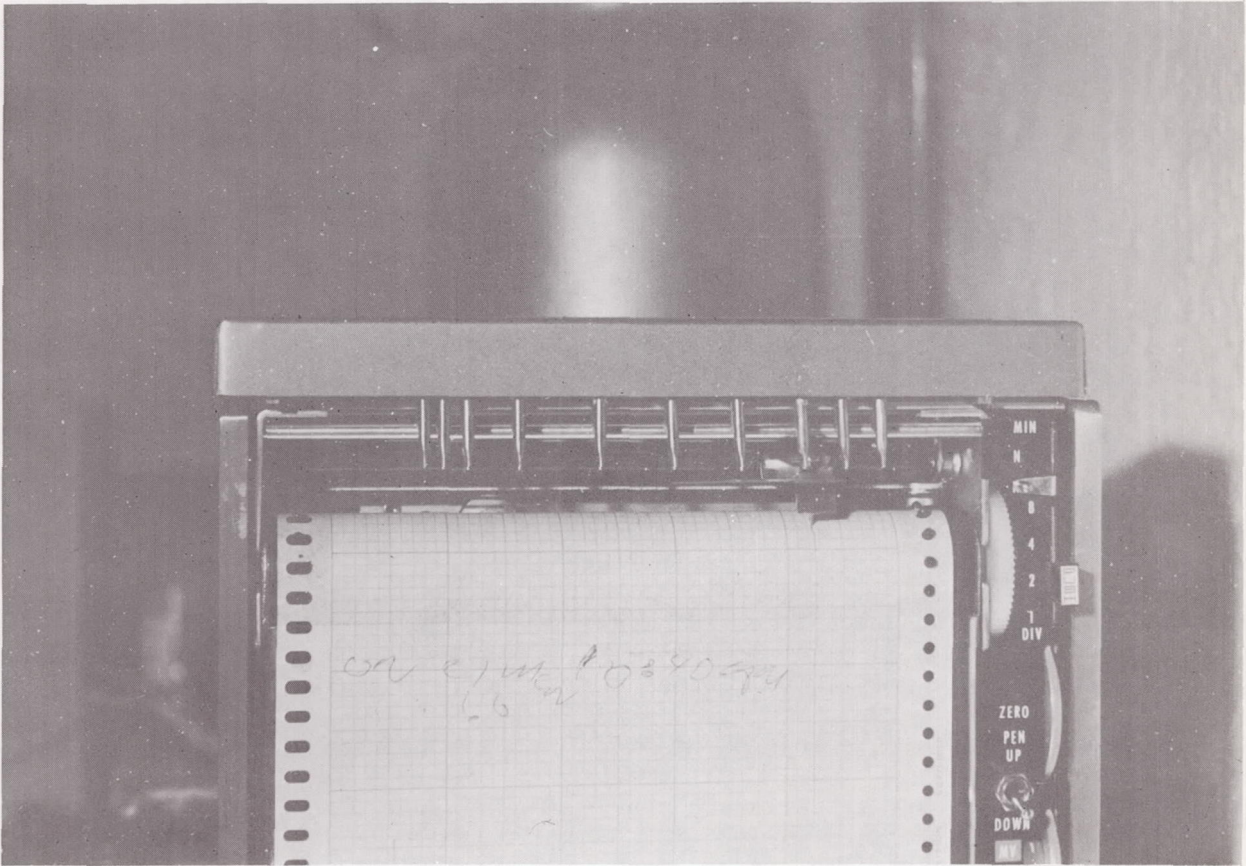


Figure 44. Photograph Showing Diode Units Mounted On Mosely Recorder.

recorder pen will shield the diode from the light source. The diode is set so that it is on the threshold of being on or off. The input signal is now reduced 5 dB from the pre-selected maximum and the second diode is adjusted so that it is on the threshold of being on or off. In this manner the input signal is quantized into ten 5dB increments.

With the recorder pen in a position corresponding to full-scale deflection, ten elapsed time meters (GE type 236) of the signal distribution analyzer will be activated. If the input signal is lowered to a level corresponding to the largest value instrumented, the number one photo diode will be energized and will cause elapsed time meter number one to cease operation. Lowering the receiver input signal an additional 5 dB will cause photo diode number two to be energized and will deactivate clock number two. For each additional 5 dB decrease in the input signal, an additional clock will be deactivated. A logic circuit prevents the photo diodes corresponding to signal levels below that of the instantaneous received signal level from operating and deactivating their respective clocks.

A photograph of the instrumentation for a typical station is shown in Figure 45. Note that there are eleven clocks mounted on the signal distribution analyzer. The extra clock runs continuously to give the total elapsed time, corresponding to the total time of operation. One additional function of the Moseley recorder is to indicate on the strip chart record when the microwave link has an equipment outage, such as power failure at the transmitter. This type of outage time must be subtracted from the total elapsed time meter readings since it

is outage time attributable to equipment failure rather than atmospheric effects.

The elapsed time meters plus an identification data plate are shown mounted on the front panel of the distribution analyzer unit in Figure 45. An automatic camera (Olympus Pen Model EM, 35 mm - 1/2 frame) with an attached timer clock photographs the panel assembly every six hours, starting with midnight.

Each installation was routinely serviced every two weeks. The equipment was checked and calibrated, film and chart paper replaced, etc.

In Figure 46 is shown a detailed schematic of the Signal Distribution Analyzer. If the light sensor diode is turned off by the light blocking shield of the recorder as described on page 111, the amplifier will turn the relay off thus allowing the clock associated with the relay to run. The relay logic is constructed so that no relay associated with a light sensor diode position at a higher signal level than the activated diode may be turned on.

Transistor Q1 of the amplifier, Figure 47, is turned on by exposure to light. When Q1 turns on, it turns Q2 off which turns Q3 on which turns Q4 on. When Q4 turns on, it activates the relay turning it on.

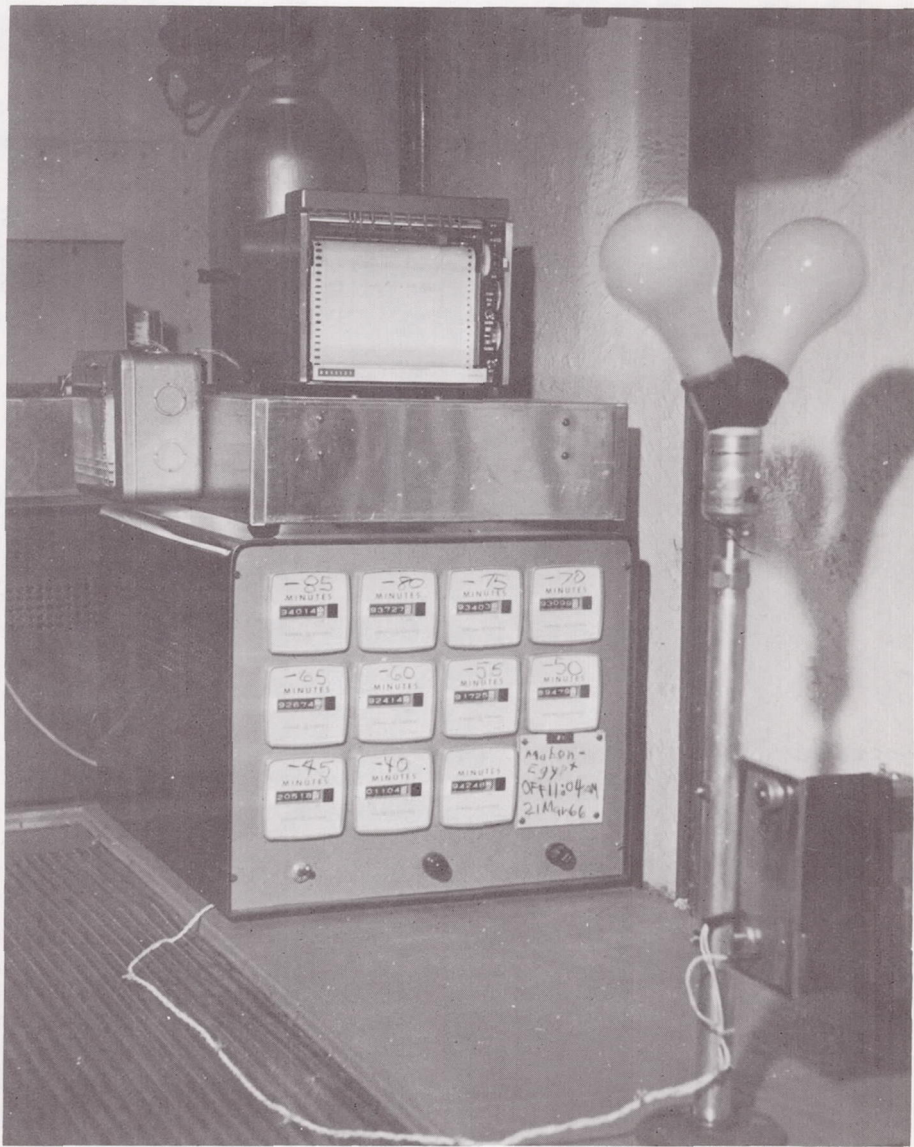


Figure 45. Photograph Showing the Instrumentation for a Typical Station.

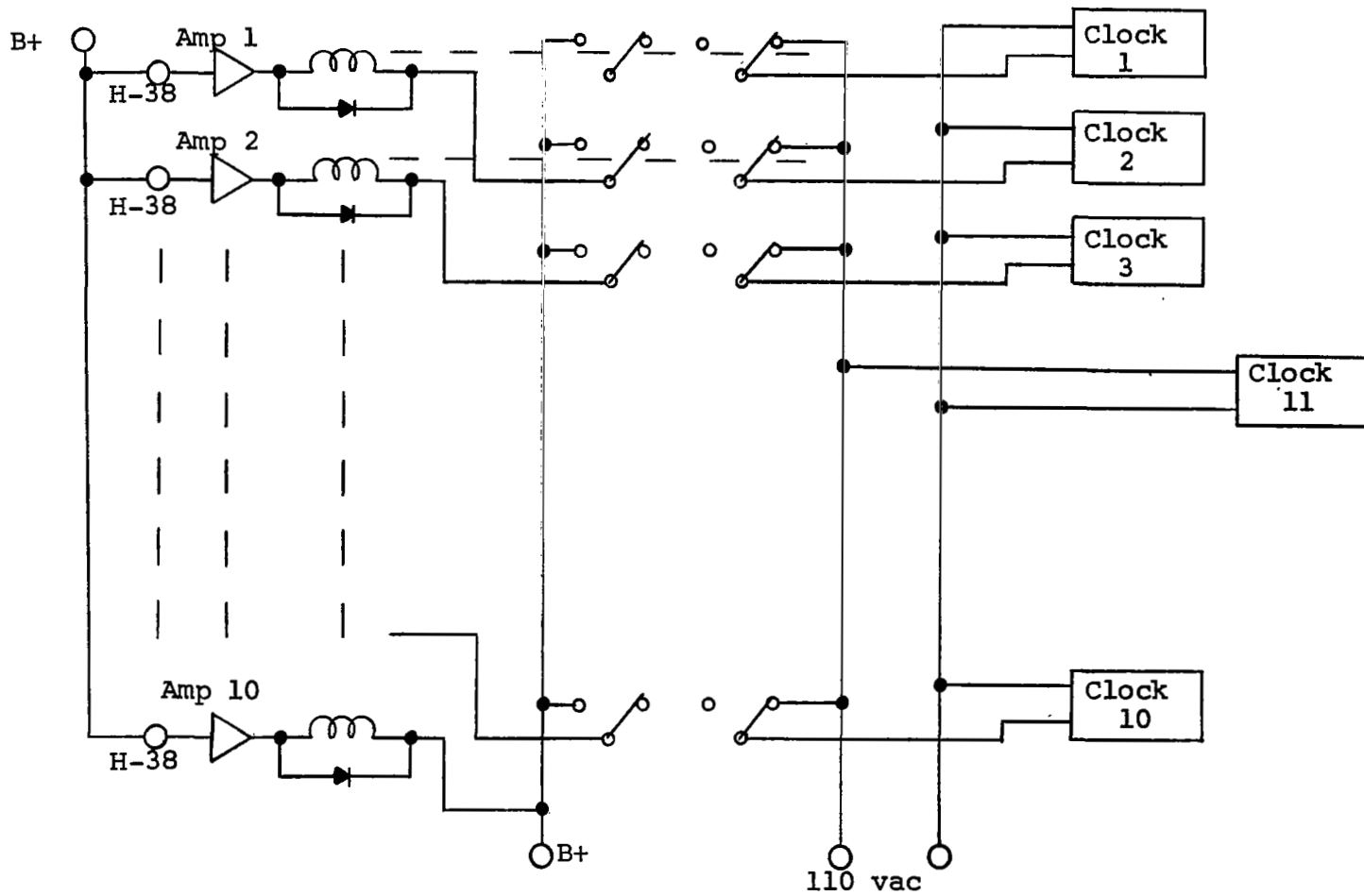


FIGURE 46. SCHEMATIC OF THE SIGNAL DISTRIBUTION ANALYZER

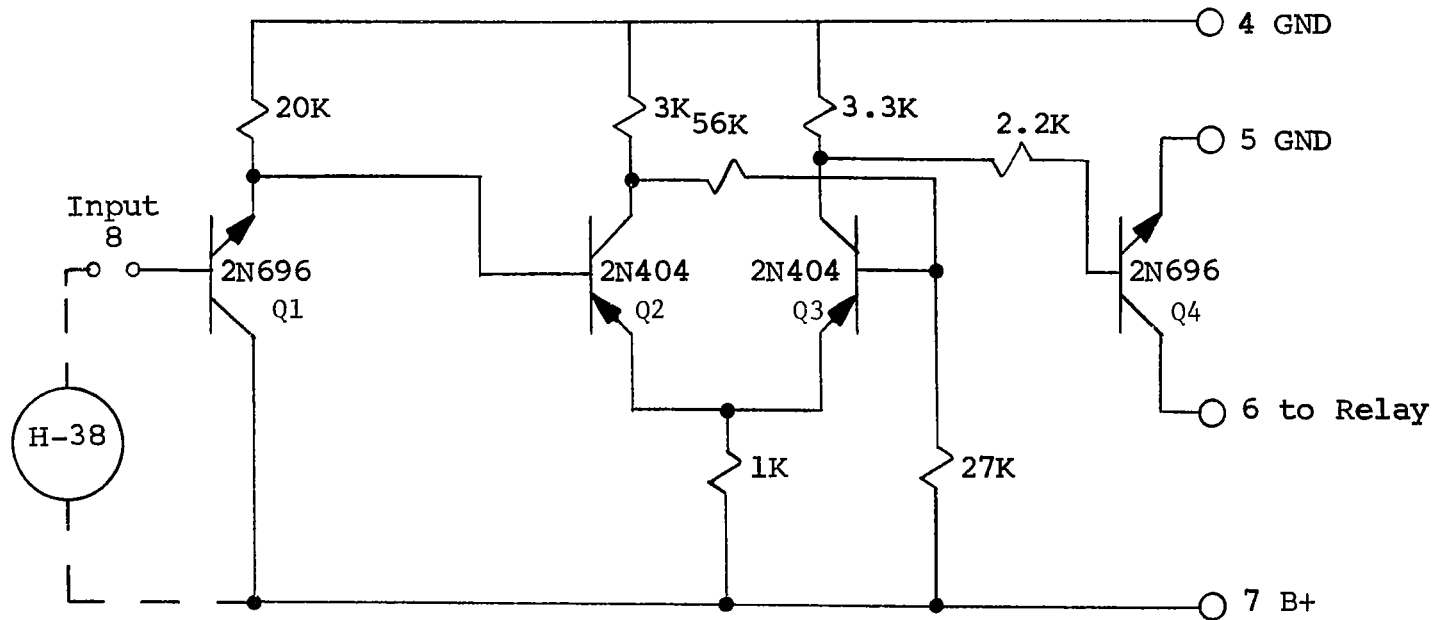


FIGURE 47 . SCHEMATIC OF A TYPICAL AMPLIFIER

REFERENCES

1. De Forest, Lee, "An Early Note on Wave Propagation", IRE-Proc., Vol. 18, No. 9, September 1930, pp. 1600-1601.
2. Boyd, J. E., R. A. Martin, C. Yoe, F. B. Brown, "The Effect of Atmospheric Conditions on the Propagation Characteristics of Electromagnetic Waves in the Microwave Region", Technical Report No. 4, Final Report on Project No. 109-8, Contract No. W28-099-9C-175. Georgia Institute of Technology, State Engineering Station, Atlanta, Georgia, June 30, 1951; pp. 43.
3. Jordan, E. C., Electromagnetic Waves and Radiating Systems, Prentice-Hall, Inc., 1950, pp. 611-618.
4. Egli, J. J., "UHF Radio-Relay System Engineering", IRE-Proc., Vol. 41, 1953, p. 118.
5. Hebert, Jr., J. O., F. M. Ingels, and J. J. Troyka, "A Summary of Experimental Research on Microwave Propagation Over Optical Paths", prepared under NASA Research Grant NGR 25-001-007, Engineering and Industrial Research Station, Mississippi State University, Jan., 1966.
6. Brown, R. G., and J. W. Nilsson, Introduction to Linear System Analysis, Wiley and Sons, 1962, pp. 121-131.
7. Gough, M. W., V.H.F. & U.H.F., "Propagation Within Optical Range", Marconi Rev., Vol. 12, October-December, 1949, pp. 121-139.
8. Stiltz, Harry, Aerospace Telemetry, Prentice-Hall, Inc., Englewood, New Jersey, 1961, p. 249.
9. Simon, Leslie E., An Engineer's Manual of Statistical Methods, John Wiley and Sons, Inc., New York, 1941.
10. Kenney, John F., Mathematics of Statistics, D. Van Nostrand Company, Inc., New York, 1947.
11. Neville, Adam M. and John B. Kennedy, Basic Statistical Methods for Engineers and Scientists, International Textbook Company, Scranton, Pennsylvania.
12. Simon, Leslie E., An Engineer's Manual of Statistical Methods, John Wiley and Sons, p. 145.
13. Lee, Y. W., Statistical Theory of Communication, John Wiley and Sons, Inc., New York, 1960, p. 205.
14. Lee, Y. W., 1960, p. 214.
15. Lee, Y. W., and J. B. Wiesner, "Correlation Functions and Communication Applications", Electronics, Vol. 23, June 1950, pp. 86-92.

16. Lee, Y. W., 1960, p. 54.

17. Lee, Y. W., 1960, p. 78.

BIBLIOGRAPHY

1. Barsis, A. P., J. W. Herbstreit, and K. O. Hornberg, Cheyenne Mountain Tropospheric Propagation Experiments, U. S. Bureau of Standards Circular No. 554, January 3, 1955, 39 pages.
2. Barsis, A. P., and M. E. Johnson, "Prolonged Space-Wave Fadeouts in Tropospheric Propagation", J. Res. of U. S. Bureau of Standards (Radio Propagation), Vol. 66D, No. 6, November-December, 1962, pp. 681-693.
3. Bean, B. R., "Prolonged Space-Wave Fadeouts at 1046 Mc. Observed in Cheyenne Mountain Propagation Program", IRE-Proc., Vol. 42, May 1954, pp. 848-853.
4. Bean, B. R. and B. A. Cahoon, "Correlation of Monthly Median Transmission Loss and Refraction Index Profile Characteristics", J. Res. of U. S. Nat. Bur. Standards (Radio Propagation), Vol. 65D, No. 1, January-February, 1961, pp. 67-74.
5. Bean, B. R., L. Fehlhaber, and J. Grosskopf, "Comparative Study of the Correlation of Seasonal and Diurnal Cycles of Transhorizon Radio Transmission Loss and Surface Refractivity", Journal of Research of the National Bureau of Standards, Vol. 66, Section D, September 1962, pp. 593-599.
6. Bendat, Julius S., Principles and Applications of Random Noise Theory, John Wiley and Sons, Inc., New York, 1958.
7. Bogle, A. G., "Some Aspects of Microwave Fading on an Optical Path Over Sea", Inst. of Elect. Engrs. (Radio and Communications Engr.), Vol. 99, September 1952, pp. 236-240.
8. Boyd, J. E., R. A. Martin, C. Yoe, and F. B. Brown, "The Effect of Atmospheric Conditions on the Propagation Characteristics of Electromagnetic Waves in the Microwave Region", Technical Report No. 4, Final Report on Project No. 109-8, Contract No. W28-099-9C-175. Georgia Institute of Technology, State Engineering Station, Atlanta, Georgia, June 30, 1951.
9. Brennan, D. G., "Smooth Random Functions Need Not have Smooth Correlation Functions", IRE-Proc., Vol. 45, July 1957, pp. 1016-1017.
10. Brown, R. G. and J. W. Nilsson, Introduction to Linear Systems Analysis, Wiley and Sons, 1962, pp. 121-131.
11. Bryant, E. C., Statistical Analysis, McGraw-Hill Book Company, Inc., New York, 1960.
12. Bullington, K. "Radio Propagation at Frequencies Above 30 mcps", IRE-Proc., Vol. 35, October 1947, pp. 1122-1136.

13. Bullington, K., "Reflection Coefficients of Irregular Terrain", IRE-Proc., Vol. 42, August 1954, pp. 1258-1262.
14. Bussey, H. E., "Microwave Attenuation Statistics Estimated from Rainfall and Water Vapor Statistics", IRE-Proc., Vol. 38, July 1950, pp. 781-785.
15. Chavance, Pierre, Lucien Boithias, and Pierred Blassel. "Etude de Propagation D'Ondes Centrimetriques dans la Region Mediterraneene", (Study of Propagation of Centimeter Waves in the Mediterranean Region), Annales Des Telecommunications, Vol. 9, No. 6, June 1954, pp. 158-185.
16. Chavance, Pierre, "Etude de la Propagation des Ondes Centrimetriques dans le Nord de la France", (Study of the Propagation of the Centimeter Waves in Northern France), Annales Des Telecommunications, Vol. 7, No. 6, June 1952, pp. 154-261.
17. Collins, C., "Simple Digital Correlator", Review of Scientific Instruments, Vol. 29, June 1958, pp. 487-490.
18. Crawford, A. B. and W. C. Jakes, Jr., "Selective Fading of Microwaves", Bell System Tech. Journal, Vol. 31, January 1952, pp. 68-90.
19. Davenport, W. B., Jr. and W. L. Root, An Introduction to the Theory of Random Signal and Noise, McGraw-Hill Book Company, Inc., New York, 1958.
20. Day, J. P. and L. C. Trolese, "Propagation of Short Radio Waves Over Desert Terrain", IRE-Proc., Vol. 38, February 1950, pp. 165-175.
21. De Forest, Lee, "An Early Note on Wave Propagation", IRE-Proc., Vol. 18, September 1930, pp. 1600-1601.
22. DeLange, O. E., "Propagation Studies at Microwave Frequencies by Means of Very Short Pulses", Bell System Tech. Journal, Vol. 31, January 1952, pp. 91-103.
23. Diamantides, N. D., "Analog Technique Devices Correlation Functions", Electronics, Vol. 35, April 13, 1962, pp. 65-67.
24. Diamantides, N. D., "Correlational and Spectral Techniques in Modern Communication and Control Systems", Electrical Engineering, Vol. 80, November 1961, pp. 860-965.
25. Durkee, A. L., "Results of Microwave Propagation Tests Over a 40 Mile Overland Path", IRE-Proc., Vol. 36, February 1948, pp. 197-205.
26. Egli, J. J., "UHF Radio-Relay System Engineering", IRE Proc., Vol. 41, January 1953, pp. 115-118.
27. Epstein, J. and D. W. Peterson, "Experimental Study of Wave Propagation at 850 Mc.", IRE-Proc., Vol. 41, May 1953, pp. 595-611.

28. Ezekiel, Mordecai, Methods of Correlation Analysis, John Wiley and Sons, Inc., New York, 1941.
29. Gough, M. W., V.H.F. & U.H.F., "Propagation Within Optical Range", Marconi Rev., Vol. 12, October-December 1949, pp. 121-139.
30. Gray, R. E., "The Refractive Index of the Atmosphere as a Factor in Tropospheric Propagation Far Beyond the Horizon", IRE International Convention Record, Vol. 5, Part IV (Antennas and Propagation), 1957, pp. 3-11.
31. Hamlin, E. W. and W. E. Gordon, "Comparison of Calculated and Measured Phase Difference at 3.2 Cm.", IRE-Proc., Vol. 36, October 1948, pp. 1218-1229.
32. Hancock, John C., An Introduction to the Principles of Communication Theory, McGraw-Hill Book Company, Inc., New York, 1961.
33. Hay, D. R. and G. E. Poaps, "Prolonged Signal Fade-Out on a Short Microwave Path", Canadian J. of Phys., Vol. 37, March 1959, pp. 313-321.
34. Hebert, J. O., Jr., F. M. Ingels, and J. J. Troyka, "A Summary of Experimental Research on Microwave Propagation Over Optical Paths", prepared under NASA Research Grant NGR 25-001-007, Engineering and Industrial Research Station, Mississippi State University, Jan., 1966.
35. Ikegama, F., "Influence of Atmospheric Duct on Microwave Fading", IRE-Transactions on Antennas and Propagation, Vol. AP-7, No. 3, July 1959, pp. 252-257.
36. Jordan, E. C., Electromagnetic Waves and Radiating Systems, Prentice-Hall, Inc., 1950, pp. 611-618.
37. Karplus, E., "Communications on Quasi-optical Frequencies", Electronics, Vol. 2, No. 6, June 1931, pp. 666-667 (one of the first reports).
38. Katzin, Bauchman, Binnian, "3 and 9 cm Propagation in Low Ocean Ducts," IRE-Proc., Vol. 35, September 1947, pp. 891-906.
39. Kaylor, R. L., "Statistical Study of Selective Fading of Super-High Frequency Radio Signals", Bell System Tech. Journal, Vol. 32, September 1953, pp. 1187-1202.
40. Kenney, John F., Mathematics of Statistics, D. Van Nostrand Company, Inc., New York, 1947.
41. Kerr, D. E., Propagation of Short Radio Waves, Vol. 13, Radiation Laboratory Series, McGraw-Hill, 1951.
42. Kiely, G. G., "Some Measurements of Fading at Wavelength of 8 mm Over Very Short Sea Path", Brit. Instn. of Radio Engrs. Journal, Vol. 14, February 1954, pp. 89-92.

43. Kitchen, F. A., W. R. R. Joy, and E. G. Richards, "Some Factors Influencing 3 cm Radio-Wave Propagation Within and Beyond the Radio Horizon", Instn. of Elect. Engrs. Proc. (Radio and Electronic Engr.), Part B, Vol. 109, May 1961, pp. 257-263.
44. LaGrone, A. H., and C. W. Chapman, "Some Propagation Characteristics of High UHF Signals in the Immediate Vicinity of Trees", IRE-Transactions on Antennas and Propagation, Vol. AP-9, September 1961, No. 5, pp. 487-491.
45. Lee, Y. W., Statistical Theory of Communication, John Wiley and Sons, Inc., New York, 1960.
46. Lee, Y. W. and J. B. Wiesner, "Correlation Functions and Communication Applications", Electronics, Vol. 23, June 1950, pp. 86-92.
47. McPetrie, J. S., B. Starnecki, H. Jarkowski, and L. Sincinski, "Oversea Propagation on Wavelength of 3 and 9 Centimeters", IRE-Proc., Vol. 37, March 1949, pp. 243-257.
48. Medhurst, Richard G., "Rainfall Attenuation of Centimeter Waves; Comparison of Theory and Measurement", IEEE-Transactions on Antennas and Propagation, Vol. AP-13, No. 4, July 1965, pp. 550-563.
49. Middleton, D., An Introduction to Statistical Theory, McGraw-Hill Book Company, Inc., New York, 1960.
50. Millar, J. R. and L. A. Byam, Jr., "A Microwave Propagation Test", IRE-Proc., Vol. 38, 6 June 1950, pp. 619-626.
51. Miller, G. A., H. W. Halbert, "Final Report Suffield Tropospheric Project", JCC/WP/TP No. 3, Canadian Radio Wave Propagation Committee, April 1946.
52. Mueller, G. E., "Propagation of 6 mm Waves", IRE-Proc., Vol. 34, April 1946, pp. 181-183.
53. Neville, Adam M. and John B. Kennedy, Basic Statistical Methods for Engineers and Scientists, International Textbook Company, Scranton, Pennsylvania.
54. Norton, K. A., "Transmission Loss of Space Waves Propagated Over Irregular Terrain", IRE-Trans. on Antennas and Propagation, No. AP-3, August 1952, pp. 152-166.
55. Pearson, Frank A., and Kenneth R. Bennett, Statistical Methods, John Wiley and Sons, Inc., New York, 1942.
56. Phillips, W. E., "Permittivity of Air at a Wavelength of 10 Centimeters", IRE-Proc., Vol. 38, July 1950, pp. 786-790.
57. Robertson, S. D. and A. P. King, "Effect of Rain Upon Propagation of Waves in 1 and 3 cm Regions", IRE-Proc., Vol. 34, April 1946, pp. 178-180.

58. Saxton, J. A. and H. G. Hopkins, "Some Adverse Influences of Meteorological Factors on Marine Navigational Radar", Instn. of Elect. Engrs. Proc. (Radio and Communications Engr.), Vol. 98, Part III, January 1951, pp. 26-36.
59. Schetzen, M., "Measurement of Correlation Functions", Proceedings of the IEE, Vol. 111, December 1964, pp. 2100-2104.
60. Schulkin, M., "Average Radio-Ray Refraction in the Lower Atmosphere", IRE-Proc., May 1952, pp. 554-561.
61. Schwartz, Mischa, Information Transmission, Modulation, and Noise, McGraw-Hill Book Company, Inc., New York, 1959.
62. Sharpless, W. M., "Measurements of the Angle of Arrival of Microwaves", IRE-Proc., Vol. 34, November 1946, pp. 837-848.
63. Simon, Leslie E., An Engineer's Manual of Statistical Methods, John Wiley and Sons, Inc., New York, 1941.
64. Smith-Rose, R. L., and (Miss) A. C. Strickland, "An Experimental Study of the Effect of Meteorological Conditions Upon the Propagation of Centimetric Radio Waves", Meteorological Factors in Radio-Wave Propagation, Physical Society (London, 1946), pp. 18-37.
65. Stiltz, Harry, Aerospace Telemetry, Prentice-Hall, Inc., Englewood, New Jersey, 1961, p. 249.
66. Straighton, A. W., D. F. Metcalf, and C. W. Tolbert, "Study of Tropospheric Scattering of Radio Waves", IRE-Proc., Vol. 39, June 1951, pp. 643-648.
67. Straighton, A. W., "Microwave Radio Reflection from Ground and Water Surfaces", IRE-Transactions on Antennas and Propagation, Vol. PGAP-4, December 1952, pp. 37-45.
68. Stratton, J. A., "The Effect of Rain and Fog on the Propagation of Very Short Radio Waves", IRE-Proc., Vol. 18, June 1930, pp. 1064-1074.
69. Strickland, A. C. (Miss), "Refraction in the Lower Atmosphere and its Applications to the Propagation of Radio Waves", Meteorological Factors in Radio-Wave Propagation, Physical Society (London, 1946), pp. 253-267.
70. Terman, F. E., Electronic and Radio Engineering, McGraw-Hill, 1955.
71. Thompson, L. E., "Microwave Propagation Experiments", IRE-Proc., Vol. 36, May 1948, pp. 671-676.
72. Tolbert, C. W., and Straighton, A. W., "Attenuation and Fluctuation of Millimeter Radio Waves", IRE International Convention Record, Vol. 5, Part IV (Antennas and Propagation), 1957, pp. 12-18.

73. Trolese, L. G., J. P. Day, and R. U. F. Hopkins, "Propagation Characteristics of Microwave Optical Links", IRE-Trans. on Antennas and Propagation, Vol. PG AP-4, December 1952, pp. 31-36.
74. Trolese, L. G., "Foreground Effects on Overland Microwave Transmissions", IRE-International Convention Record, Vol. 5, Part IV (Antennas and Propagation), 1957, p. 31.
75. Wexler, R. and J. Weinstein, "Rainfall Intensities and Attenuation of Centimeter Electromagnetic Waves", IRE-Proc., Vol. 36, March 1948, pp. 353-355.
76. Wenstrom, W. H., "Historical Review of Ultra-Short Wave Progress", IRE-Proc., Vol. 20, January 1932, pp. 95-112.
77. Wickizer, G. S. and A. M. Braaten, "Propagation Studies on 45.1, 474, 2800 mcps Within and Beyond Horizon", IRE-Proc., Vol. 35, July 1947,
78. Wielis, J. B., "A B C's of Regression and Correlation Analysis", The Oil and Gas Journal, Vol. 59, January 23, 1961, pp. 97-98, 101, 104.